Imperial College London

Necroptosis and Necroinflammation: Implication from Acute Kidney Injury to Chronic Kidney Disease

A thesis submitted to Imperial College London for the degree of Doctor of Philosophy

Qizhe Sun
CID: 01369569

February 2023

Division of Anaesthetics, Pain Medicine, and Intensive Care
Department of Surgery and Cancer
Faculty of Medicine
Chelsea & Westminster Hospital Campus
Imperial College London
United Kingdom

Statement of Originality

I, Qizhe Sun, affirm that the work presented in this document is my own original creation and does not contain any unauthorised material or plagiarised content. All sources used in the creation of this work have been fully and properly cited, and any ideas or information obtained from external sources have been thoroughly summarised and integrated into my own words and understanding. Some experiments in Chapter 5 and Chapter 6 were performed together with students, Min Liang and Priyanka Kamath, under my day-to-day supervision.

Copyright Declaration

Abstract

Background: Acute kidney injury (AKI) is a common medical condition that significantly increases the risk of developing chronic kidney disease (CKD), involving epithelial-mesenchymal transition (EMT), fibrosis and impaired kidney function. Necroinflammation and necroptosis play key roles in AKI. My project evaluates their impact in AKI to CKD/renal fibrosis progression across AKI models, identifying potential therapeutics to mitigate AKI and CKD/renal fibrosis risk.

Methods: Nephrotoxic agents (cisplatin [CDDP], pemetrexed [PEM], gentamicin [GM], and aristolochic acid-I [AA-I]) were used on HK2 cells for nephrotoxicity-AKI simulation. Ischaemia-reperfusion injury (IRI) induced-AKI was created in mice through renal clamping and in HK2 cells using oxygen-glucose deprivation (OGD). Sepsis associated-AKI (S-AKI) was induced by lipopolysaccharide (LPS). To demonstrate the participation of necroptosis, toll-like receptor (TLR), receptor for advanced glycation end products (RAGE), and c-Jun N-terminal Kinase (JNK), respective inhibitors or antagonists were applied to *in vitro* and *in vivo* experiments. The anti-EMT properties of Dexmedetomidine (Dex), an α2-adrenoceptor (α_2-AR) agonist with renal-protective properties, were also investigated.

Results: CDDP, PEM, and AA-I significantly inducing necroptosis and EMT through TLR-4. The necroptosis inhibitor Necrostatin-1 (Nec-1) was able to alleviate these effects. GM, in contrast, induced apoptosis without significant EMT induction.

IRI triggered necroptosis and EMT both *in vitro* and *in vivo*, with Nec-1 showing protection. High mobility group box-1 protein (HMGB-1) was found to trigger EMT via TLR/JNK signalling.

In the S-AKI model, Dex attenuated LPS-induced renal injury and EMT via α2-adrenoceptor activation, inhibited necroinflammation, and showed protective effects against transforming growth factor-β1 (TGF-β1)-induced EMT, associated with JNK inhibition.

Conclusion: Necroptosis-associated necroinflammation is involved in AKI and subsequent EMT through TLR4/JNK cellular signalling pathways. These can be therapeutic targets for further development and potentially translate into clinical practice. Dex prevented necroinflammation and EMT, indicating its great value for clinical use but subjected further clinical studies.

Acknowledgement

I would like to give my heartfelt thanks to my supervisor, Professor Daqing Ma, a Full Professor of Anaesthesia, Macintosh Professor of Royal College of Anaesthetists, BOC Chair, and the Head of Anaesthesia of the Division of Anaesthetics, Pain Medicine & Intensive Care at Imperial College London, for his knowledge, insightful comments, and constructive criticism. I also express my sincere gratitude to my co-supervisor, Dr. Hailin Zhao, a research associate in the Division of Anaesthetics, Pain Medicine & Intensive Care, for his support, encouragement, and guidance.

I would like to extend our appreciation to Professor Dongxin Wang and Dr. Yi Bing of Peking University First Hospital, Beijing, China, for their collaborations in establishing the *in vivo* mice model in Chapter Seven. I also appreciate the camaraderie and support from Ms. Lingzhi Wu, Dr. Jiang Cui, Dr. Cong Hu, Dr. Masae Iwasaki, Dr. Chen Kien Pac-Soo, Dr. Enqiang Chang, Dr. Qian Chen, Ms. Xiaomeng Li, and Ms. Priyanka Kamath throughout my studies at Imperial College London.

I acknowledge the financial support provided by the China Scholarship Council and Imperial College, and the illustrations in this thesis were created with BioRender.com.

Finally, I would like to acknowledge my family and loved ones for their constant love, support, and encouragement. Their unwavering belief in me has been a source of strength throughout my academic journey.

List of Abbreviations

A-SMA	α-SMA
A2-AR	α2-adrenoceptor
AA-I	aristolochic acid-I
AAs	aristolochic acids
ACR	albumin-to-creatinine ratio
AKD	acute kidney disease
AKI	acute kidney injury
ATM	Ataxia-Telangiectasia mutated
ATP	adenosine triphosphate
ATR	ATM- and Rad3-related
BAK1	Bcl-2 Antagonist/Killer 1
BAX	Bcl-2-associated X protein
BCL2	B-cell lymphoma 2
CCK-8	Cell Counting Kit-8
CDDP	cisplatin
CHOP	C/EBP Homologous Protein
CKD	chronic kidney disease
CoQ10	coenzyme Q10
CVD	cardiovascular disease
CXCR4	C-X-C chemokine receptor type 4
DAMPs	damage-associated molecular patterns
DAPI	diamidino-2-phenylindole
DEX	dexmedetomidine

DMSO	dimethyl sulfoxide
ECM	extracellular matrix
EMT	epithelial-mesenchymal transition
EndoMT	endothelial-mesenchymal transition
ER	endoplasmic reticulum
ERK	extracellular signal–regulated kinase
ESRD	end-stage renal disease
FADD	fas-associated death domain
FLIP	FADD-like interleukin 1β-converting enzyme-like inhibitory protein
GAPDH	glyceraldehyde 3-phosphate dehydrogenase
GSDMD	gasdermin D
GFR	glomerular filtration rate
GIS	glomerular injury score
GM	gentamicin
GSDME	gasdermin E
HK-2	Human kidney-2
HMGB-1	high mobility group box-1 protein
HPV-16	human papilloma virus type 16
HSPs	heat shock proteins
ICC	immunocytochemistry
IHC	immunohistochemistry
IL-1	interleukin-1
IRI	ischaemia-reperfusion injury
JNK	jun N-terminal kinase

KDIGO	Kidney Disease Improving Global Outcomes
LDS	lithium dodecyl sulphate
LPS	lipopolysaccharide
MAPKs	mitogen-activated protein kinases
MLKL	mixed lineage kinase domain-like protein
MMPs	matrix metalloproteinases
MOMP	mitochondrial outer membrane permeabilisation
NC	naive control
NDS	normal donkey serum
NLRP3	NLR family pyrin domain containing 3
NSCLC	non-small cell lung cancer
OD	optical density
OGD	oxygen-glucose deprivation
PAMPs	pathogen-associated molecule patterns
PBS	phosphate-buffered saline
PEM	pemetrexed
PI	propidium Iodide
PRRs	pattern recognition receptors
PS	phosphatidylserine
QOL	quality of life
RAGE	receptor for advanced glycation end products
RAP	RAGE antagonist peptide
RCD	regulated cell death
RIP	ratio of phosphorylated-receptor-interacting protein kinase

RIP1	receptor-interacting protein kinase 1
RIP3	receptor-interacting protein kinase 3
ROS	reactive oxygen species
RRT	renal replacement therapy
S-AKI	sepsis-associated AKI
SASP	senescence-associated secretory phenotype
SCr	serum creatinine
SD	standard deviation
SH	sham surgery group
SPF	specific pathogen-free
TAK1	transforming growth factor-β-activated kinase 1
TBM	tubular basement membrane
TECs	tubular epithelial cells
TGF	transforming growth factor
TIM-3	T cell immunoglobulin mucin-3
TIR	toll-interleukin 1 receptor domain
TIS	tubular injury score
TLR	toll-like receptor
TLR4	toll like receptor-4
TNF	tumour necrosis factor
TNFR	TNF receptor
TP53	trigger the tumour suppressor protein P53
TRADD	tumour necrosis factor receptor associated death domain
TRIF	TIR-domain-containing adapter-inducing interferon-β

UO	urine output
UUO	unilateral ureteral ligation
UV	ultraviolet
WST-8	water-soluble tetrazolium salt-8

Table of Contents

Index of Figures

Index of Table

Chapter One

Introduction

Chronic kidney disease (CKD), a condition in which a gradual loss of kidney function occurs over time, has become a heavy health burden worldwide. Recently, a strong association between acute kidney injury (AKI) and chronic kidney disease (CKD) has been demonstrated (1). Many patients develop CKD towards renal fibrosis despite a complete clinical recovery of AKI. However, the precise mechanisms underlying remains to be elucidated and hence there is a no treatment strategy available to prevent or slow down the transition from AKI to CKD.

Renal fibrosis, characterised by excessive extracellular matrix (ECM) accumulation, is the most typical manifestation of CKD (2). ECM is predominantly synthesised and released from myofibroblasts, an activated form of fibroblasts (3). Upon persistent inflammation, tubular epithelial cells (TECs) can dedifferentiate into myofibroblasts via epithelial-mesenchymal transition (EMT) which is an important mechanism contributing to the production of ECM and subsequent CKD.

Necroinflammation, an auto-amplification loop caused by mutually enhanced necrosis and danger-associated molecular patterns (DAMPs)-associated inflammation (4), is believed to be a key element of sustained inflammation. Necroptosis, a type of programmed necrosis, involves in various types of AKI. The present study aims to evaluate the role of necroptosis and necroinflammation in AKI to CKD and/or kidney fibrosis progression and uncover potential therapeutics in attenuating acute injury and hence decreasing the risk for CKD or renal fibrosis development.

Surgical bilateral renal pedicle clamping, or intraperitoneal lipopolysaccharide (LPS) injection was performed on C57BL/6 mice to establish an ischemia-reperfusion injury (IRI) or sepsis model, respectively. In vitro, human renal proximal tubular cells (HK2) were cultured and treated with nephrotoxic agents (Cisplatin [CDDP], Pemetrexed [PEM], Gentamicin [GM] or Aristolochic acid-I [AA-I]), oxygen-glucose deprivation (OGD), LPS, to mimic nephrotoxicity-, IRI-, or sepsis-induced AKI, respectively. To investigate the underlying molecular mechanisms, respective pharmacological inhibitors or antagonists of necroptosis, toll-like receptor-4 (TLR-4), receptor for advanced glycation end products (RAGE), α_2-adrenoceptor (α_2-AR), and c-Jun N-terminal Kinase (JNK), were applied to *in vitro* and *in vivo* experiments. An overview of this study is illustrated in **Figure 1.1**.

First, we investigated the role of necroptosis on EMT in response to nephrotoxic agents (CDDP, PEM, GM or AA-I). CDDP, PEM and AA-I induced necroptosis and EMT via TLR-4, which was alleviated by necrostatin-1 (Nec-1, an inhibitor of necroptosis).

Next, we investigate the role of necroptosis on EMT in IRI models. We found that IRI promoted necroptosis and EMT. Inhibition of necroptosis suppressed EMT. Necroptosis-released molecules induced further necroptosis and EMT, as evidenced by conditioned medium collected from OGD-treated cells caused necroptosis and EMT. We then evaluated the effects of DAMPs on EMT, including high mobility group box 1

(HMGB-1) and histones. It was found that HMGB-1 induced EMT via TLR4/JNK signalling pathways.

Finally, we examined that if Dexmedetomidine (Dex) reduces necroinflammation and EMT in an LPS-induced sepsis model. Our data showed Dex significantly alleviated LPS-induced AKI, myofibroblast activation, NLRP3 inflammasome activation, and necroptosis in mice. Atipamezole, an antagonist of α_2-AR, counteracted its protective effects. Dex attenuated LPS or TGF-β1-induced EMT and prevented necroinflammation in response to LPS stimulation *in vitro*. The anti-EMT effects of Dex were associated with JNK inhibition.

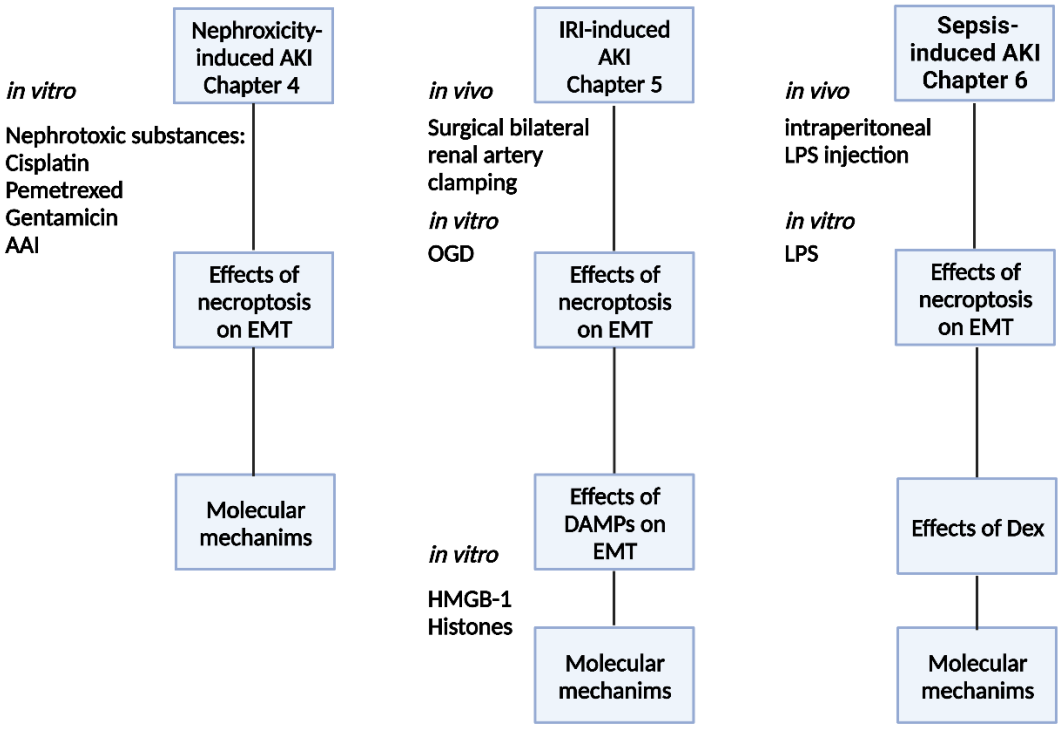

Figure 1. 1 Study overview

The effects of necroptosis-associated necroinflammation were examined in different AKI models, including nephrotoxicity (chapter 4)-, IRI (chapter 5)-, and sepsis-induced AKI models (chapter 6), as well as the underlying molecular mechanisms. The protective effect of Dex and its mechanisms were also evaluated in LPS-induced sepsis models (chapter 6).

AKI: acute kidney injury; EMT: epithelial-mesenchymal transition; IRI: ischaemia-reperfusion injury; DAMPs: danger-associated molecular patterns; Dex: Dexmedetomidine; AAI: aristolochic acid I; OGD: oxygen-glucose deprivation; HMGB-1: high mobility group box 1

Chapter Two

Background

2.1 Chronic kidney disease

2.1.1 The disease and its impact

Chronic kidney disease (CKD) is a medical condition characterised by a gradual decrease in kidney function over time (5). It has become a significant global public health concern due to its increasing prevalence and unfavourable outcome, affecting more than 9% of the world's population and leading to over 1 million deaths annually (6). According to a simulation model based on 1999 to 2010 US National Health and Nutrition Examination Surveys, CKD prevalence in adults over 30 is estimated to increase from 13.2% in 2010 to 16.7% in 2030 (7). CKD-associated mortality has also climbed dramatically (increased by 41.5% between 1990 and 2017) and now accounts for 4.6% of all-cause death (8).

Individually, CKD significantly impairs patients' quality of life (QOL). CKD patients suffer from risks of premature death and high medical costs, and as the disease progresses, many unpleasant symptoms often manifest, such as fatigue and weakness, nausea and vomiting, mental illness, and pain (9), where pain is the most frequent complaint (10), with a prevalence of over 60% (11, 12). Besides, QOL can be substantially reduced when patients experience mental disorders, such as anxiety and depression, which are common among CKD patients (13, 14). Some studies showed that 38-54% of CKD patients had anxiety and depression (15, 16). CKD is associated with many complications, including fluid and electrolyte abnormalities, cardiovascular disease

(CVD), mineral bone disorder, and anaemia, which also contribute to reduced QOL and even cause death (10, 17, 18). The incidence and severity of symptoms and complications are substantially increased when the disease progresses to end-stage renal disease (ESRD) (19-21), at which stage kidney cease functioning and patients need renal replacement therapy (RRT) to support their life.

In addition to the impact on individuals, the financial impact is also significant. CKD costs over £1.4 billion in England and $110 billion in the USA annually and is continually increasing alongside its prevalence(22, 23). Most of the expenditure is for RRT and CVD complications, accounting for more than half of the total costs (22). Given the impact of ESRD on QOL and the high expenditure on RRT, it is important to uncover effective therapeutic methods to prevent CKD progression.

2.1.2 Definition and diagnosis

The latest clinical guideline from The Kidney Disease: Improving Global Outcomes (KDIGO) defines CKD as "abnormalities of kidney function present for > 3 months with health implications" (24). A diagnosis of CKD can be made when at least one of the following criteria is present for more than three months: decreased glomerular filtration rate (GFR), with a value less than 60 ml/min/1.73 m^2; the presence of albuminuria, defined as a urine albumin level of 30 mg or more per 24 hours or a urine albumin-to-creatinine ratio (ACR) of 30 mg/g or higher; evidence of kidney damage, as demonstrated by imaging or histological findings, abnormalities in urine sediment,

electrolyte imbalances due to renal tubular disorders, or a history of kidney transplantation (24). Patients with CKD can be classified according to their GFR, ACR and cause, which confirms the CKD staging and determines disease management and prognosis (24) (**Table 2.1**).

Categories of CKD based on GFR, ACR, and cause

GFR (ml/min/1.73 m^2)	G1	G2	G3a	G3b	G4	G5
	>90	60-89	45-59	30-44	15-29	<15
ACR (mg/g)	A1		A2		A3	
	<3		3-29		>30	
Cause	Systematic disease		Genetic disorders		History of kidney injury	
	• Diabetes • Hypertension • Obesity • Autoimmune disease • Systemic infections (e.g., HIV infection) • Maglinant tumors		• APOL1-mediated kidney disease • Polycystic kidney disease • Congenital anomalies of the kidney and urinary tract • Others		• Pre-renal (e.g., trauma, cardiac failure) • Renal (e.g., nephrotoxins, glomerulonephritis, endotoxemia) • Post-renal (e.g., urinary tract obstruction)	

Table 1. Categories of CKD based on GFR, ACR, and cause

CKD: chronic kidney disease; GFR: glomerular filtration rate; ACR: urine albumin-to-creatinine ratio; HIV: human immunodeficiency virus; APOL1: Apolipoprotein L1

2.1.3 Prognosis and treatment

CKD is often asymptomatic at early-stage until the disease progresses to G4 and above (25). Progression to ESRD takes between months to decades (26), and the rate of CKD progression varies by cause, age, and interventions. Some life-threatening complications, including cardiovascular disease, volume and electrolyte disorders, kidney failure, infections, and uraemia, may occur during the development. A meta-analysis based on categorical data showed that GFR and ACR are strong predictors of various clinical outcomes, including kidney failure, progressive CKD, mortality from cardiovascular disease, acute kidney injury, and death. Based on these findings, a heat map was created to reflect the prognosis of CKD (27) (**Figure 2.1**).

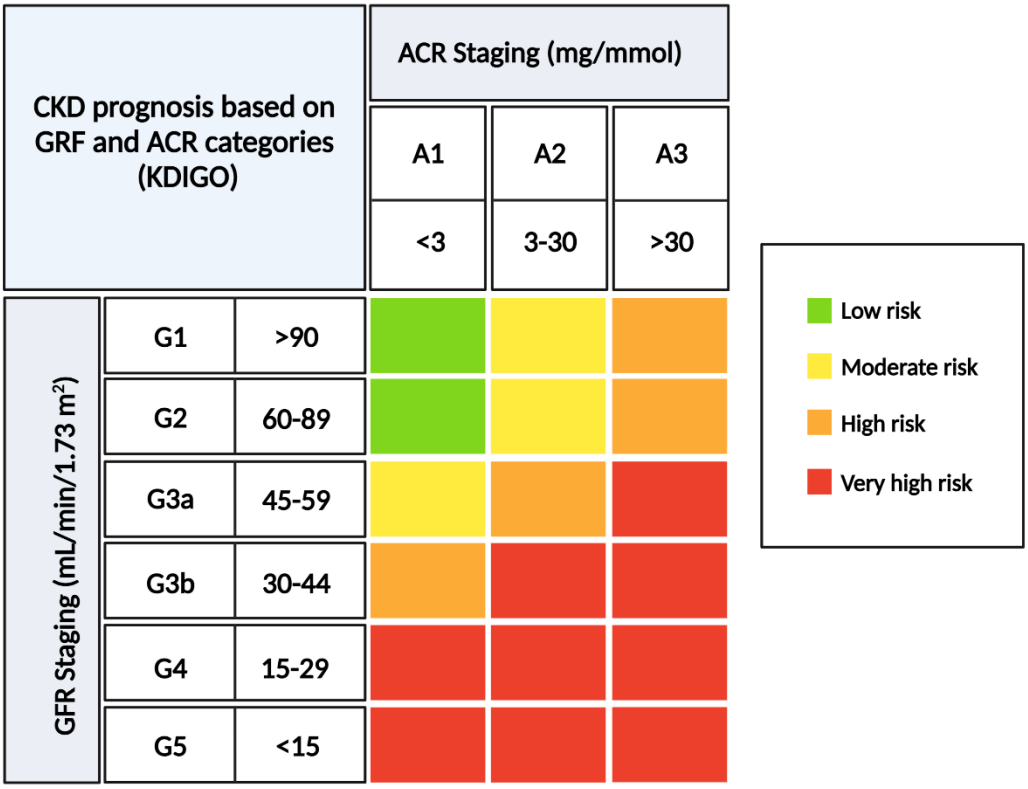

Figure 2. 1 CKD prognosis based on GRF and ACR categories (KDIGO)

Prognosis here refers to clinical outcomes including cardiovascular mortality, kidney failure, AKI, progressive CKD, and death. Colours reflect the ranking relative risk. Green: low risk; yellow: moderate risk; orange: High risk; red: very high risk. The figure is reproduced with permission from KDIGO.
GFR: glomerular filtration rates; ACR: albumin-to-creatinine ratio; CKD: chronic kidney disease; KDIGO: the Kidney Disease Improving Global Outcomes organisation

Conservative management is the primary and preferable treatment for CKD (10), that includes interventions on lifestyle and dietary, root causes, complications and comorbidities (24). Physical activity, smoking cessation, and weight reduction (for overweight and obese individuals) are recommended as they can improve cardiovascular health and potentially slower the decline of renal function (28-30). Protein and sodium intake restrictions are associated with benefits on GFR and

albuminuria, therefore have been adapted clinically (31-33). For CKD caused by systematic diseases and genetic disorders, interventions targeting on the root cause is often effective. For example, the treatment for diabetic CKD and hypertension, mostly through glycaemic and blood pressure control, has been shown to slower CKD development (24, 34, 35). However, for CKD patients caused by a history of AKI, effective medication is still not available, which is due to an incomplete understanding of the AKI-CKD transition.

2.1.4 Renal Fibrosis

Renal fibrosis, characterised by glomerulosclerosis, vascular sclerosis, and tubulointerstitial fibrosis, is the ultimate pathological manifestation of CKD (36). The signature histological appearance of it is the excessive accumulation of extracellular matrix (ECM) (37). Regardless of the cause, the development of renal fibrosis is a dynamic process that encompasses four interrelated phases: initiation, activation, execution, and advancement (38).

Following a prolonged injury, inflammation acts as a primer, establishing the fibrogenic stage and initiating tissue fibrogenesis. Inflammation is a crucial component of the repairing processes; excessive inflammation, however, can be detrimental and result in further damage (39). Tissue injuries trigger inflammation by creating proinflammatory environments where gradient chemokines attract immune cells to the site of injury (40). Once the immune cells have infiltrated the site of injury, they

become activated and produce proinflammatory molecule, which leads to an increase in fibrogenic cytokines, resulting in the activation and proliferation of ECM-producing cells, such as fibroblasts, pericytes, tubular epithelial cells, endothelial cells, and circulating fibrocytes (41-43). These cells then assemble a multicomponent, integrin-linked protein complex that manages the formation of ECM via interpreting fibrogenic signals, eventually leading to development of renal fibrosis (44, 45).

2.2 Acute kidney injury

2.2.1 The disease

Acute kidney injury is a condition charactesized by a sudden decrease in renal function, as indicated by elevated levels of creatinine in the blood and decreased urine output (46). The currently clinical guideline by KDIGO diagnoses AKI as “an increase in the serum creatinine (SCr) level to at least 0.3 mg/dL within 48 hrs, an increase of SCr to more than 1.5 times of the baseline (which is known or presumed to have occurred within the prior 7 days), or a urine output (UO) is decreased to less than 0.5 mL/kg/h for 6 hrs” (47). AKI is a prevalent condition, occurring in 5-7% of hospitalised patients and 50-60% of critically ill patients (48-50), leading to prolonged hospital stays, high medical costs, and increased in-hospital mortality, as well as elevated risks of cardiovascular disease, CKD development, and long-term mortality (51).

AKI can be classified into three categories based on the underlying causes, including pre-renal, post-renal, and intra-renal. Pre-renal causes are typically related to

decreased blood flow to the kidneys, such as in the case of cardiac failure. Post-renal causes can result from a blockage in the urinary tract, while intra-renal causes are related to direct damage to the kidneys, such as nephrotoxicity caused by certain medications (47).

2.2.2 Nephrotoxicity induced AKI

2.2.2.1 Mechanisms of nephrotoxicity

Nephrotoxic medications are common causes for AKI, especially in hospitalised patients (52). Due to their continuous exposure to medications and their byproducts, glomerular, interstitial, and tubular cells are vulnerable to the effects of various drugs. (53). In addition, due to their ability to concentrate and reabsorb glomerular filtrate, which is linked to high levels of circulating toxins, renal tubular cells are especially susceptible to nephrotoxicity (54).

Kellum et.al summarised and categorised nephrotoxic medicines into six broad classes (55). First, certain medications exhibit direct chemical nephrotoxicity, including chemotherapeutics (e.g., cisplatin and pemetrexed) and antimicrobials (e.g., gentamicin and amphotericin). These drugs, which are eliminated through the kidneys, can become particularly harmful if renal function decreases, leading to accumulation of drugs and their metabolites (56). The second category encompasses substances that cause harm to the kidneys through immune-mediated mechanisms, leading to allergic tubulointerstitial nephritis, a condition that can be challenging to identify because of

its subtle symptoms (57). Another category involves medications, such as angiotensin receptor blockers, that affect the intrarenal haemodynamic and reduce GFR (58). The fourth category involves drugs that crystallize within the kidney tubules, causing intrarenal blockage of urine flow and kidney damage, referred to as crystal-induced kidney injury (59). Another category involves drugs that cause AKI through their pharmacological effects, such as uricosuric pharmaceuticals that can cause acute urate nephropathy. Lastly, the elimination of certain drugs or their by-products can compete with creatinine transporters, giving the appearance of AKI, even though other kidney functions remain unaffected.(60).

2.2.2.2 Chemotherapy drug nephrotoxicity

Chemotherapy drugs have the potential to cause kidney damage and negatively impact cancer treatment outcomes and patient survival (61). These drugs can harm various components of the kidney, such as the glomerulus, tubules, interstitium, and microvasculature, leading to a variety of clinical manifestations, including electrolyte imbalance, AKI, and potentially CKD (62). Chemotherapeutic agents can cause nephrotoxicity in many different ways, which are all listed in **Table 2.2**.

Class	Drugs	Adverse outcomes on the kidney
Alkylating agents	Cisplatin; Bendamustine; Cyclophosphamide; Ifosfamide	AKI; Tubulointerstitial nephritis; Fanconi syndrome; CKD
Antimetabolites	Pemetrexed; Chlopharabine; Methotrexate; Gemcitabine	AKI; Tubulointerstitial nephritis; Tubular acidosis; CKD
Antitumor antibiotics	Daunorubicin; Doxorubicin; Mitomycin	AKI; Nephrotic syndrome; Glomerular sclerosis; TMA
Plant alkaloids	Irinotecan; Topotecan; Etoposide; Teniposide	AKI; Tubulointerstitial disease; Rhabdomyolysis-induced AKI
Targeted agents	Bosutinib; Dasatinib; Imatinib; Bevacizumab; Ramucirumab; Ipilimumab; Pembrolizumab	AKI; Tubulointerstitial nephritis; Glomerulonephritis; TMA; CKD

Table 2. Major classes of chemotherapy drugs and their nephrotoxicity

AKI: acute kidney injury; CKD: chronic kidney disease; TMA: Thrombotic Microangiopathy

2.2.2.3 Antimicrobials

Among hospital patients, nephrotoxicity caused by antimicrobials is one of the leading causes of AKI (63). Antimicrobials can lead to both structural and functional damage to the kidney, resulting in varying degrees of kidney injury, from minor tubular injury to the need for renal replacement therapy. The most prevalent mechanisms are direct nephrotoxicity on tubular cells and crystallisations (64). The most frequent causes of antibiotic-associated AKI are aminoglycosides, such as gentamicin, and beta-lactams, such as cephaloridine (65-67).

2.2.2.4 Herbal ingredients

Herbal medicines and nutrient supplements have been used widely across the world, with an increasing number of people turning to these products to treat a variety of healthy issues in various national healthcare settings (68-70). Although some herbal medicines have promising potential and are widely used, most of them have not been tested and their use is not monitored. In fact, many of them have negative side effects, such as nephrotoxicity. Herbal ingredient nephrotoxicity can cause acute kidney injury, nephrolithiasis, chronic interstitial fibrosis, and other kidney pathological syndromes, namely herbal nephropathy (71). Herbal nephropathy can be caused by multiple ways, including direct nephrotoxicity on renal cells, toxicity of additive compounds (e.g., heavy metals), crystal deposition within the kidney, interaction with co-administrated medications, and alterations on homeostasis that result in nephrotoxic circumstances, such as nephrolithiasis (70).

2.2.3 Ischaemic-reperfusion injury (IRI)-induced AKI

2.2.3.1 Pathophysiology of IRI-AKI

Ischemia-reperfusion injury (IRI) a condition where blood flow to a particular area is temporarily reduced and then restored, is a major cause of AKI in clinical practice (72). The underlying mechanisms behind the development of AKI caused by IRI are intricate and involve a range of interactions between various cell types (Figure 2.2). In brief, IRI triggers ATP depletion and hypoxia, leading to damage in the endothelial and epithelial cells, as well as the recruitment and activation of immune cells (73). The injury to the endothelial cells results in vasoconstriction, increased permeability, infiltration of leukocytes, release of cytokines, endoplasmic reticulum stress (ER stress), and production of reactive oxygen species (ROS) (74). The epithelial cells, on the other hand, experience loss of cell polarity, disruption of cellular junctions, disarray of the cytoskeleton, accumulation of cellular debris, and increased ROS production, along with the release of damage-associated molecular patterns (DAMPs) and cytokines (75). These ROS, cytokines, and DAMPs further activate immune cells, creating an ongoing cycle of injury and inflammation (76).

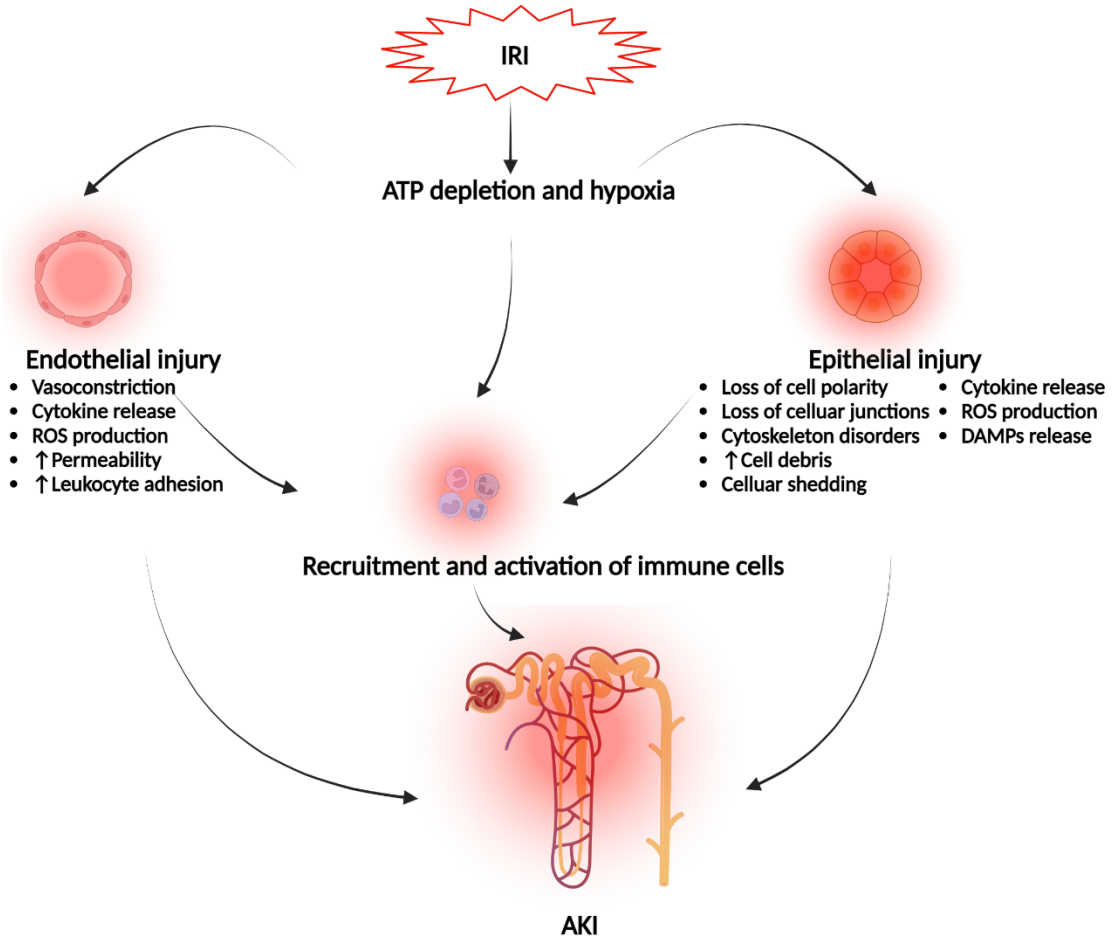

Figure 2. 2 Pathophysiology of IRI-AKI

IRI causes ATP depletion and hypoxia, which lead to endothelial injury, epithelial injury, and recruitment and activation of immune cells. Endothelial injury is characterised of vasoconstriction, increased permeability, leukocyte infiltration, cytokine release and ROS production. Epithelial injury can cause loss of cell polarity and cellular junctions, cytoskeleton disorders, increased cell debris, cellular shedding, ROS production, and release of DAMPs and cytokines. ROS, cytokines, and DAMPs can further activate immune cells. Injured endothelial and epithelial cells and activated immune cells together cause inflammation and AKI.

IRI: ischaemia-reperfusion injury; ATP: adenosine triphosphate; ROS: reactive oxygen species; DAMPs: danger-associated molecular patterns

2.2.3.2 Energy depletion

The initial metabolic change of ischaemic AKI is energy depletion. Blood blow is reduced or disrupted during ischaemic period, leading to inadequate supply of glucose and oxygen, which greatly suppress adenosine triphosphate (ATP) production (77). Insufficient oxygen supply shifts glucose metabolism from oxidative phosphorylation to anaerobic glycolysis, which declines the efficiency of ATP synthesis and causes intracellular lactic acidosis (78). The depletion of ATP can result in the ineffectiveness of important ion pumps on the cell membrane, causing imbalances in sodium and potassium levels (79). An increase in intracellular sodium disrupts the functioning of Na^{+}-H^{+} exchangers. Additionally, the inactivity of the Ca2+-ATPase pumps located in the endoplasmic reticulum results in a decreased capacity of reabsorbing calcium ions. (80). These lead to an imbalance in ion and fluid levels, which causes cellular swelling (81). Deficient Oxygen can also cause malfunctions of mitochondrial electron transport chain, leading to activation of caspase cascades, oxidative stress, membrane permeabilization, and subsequent cell death (82).

2.2.3.3 Oxidative stress

Oxidative stress refers to a state where there is an imbalance between the generation and removal of reactive oxygen species (ROS), leading to both non-regulated or regulated cell death (73). This can worsen the harm caused by IRI and is often a result of mitochondrial dysfunction (83). There are various forms of ROS, such as peroxides

and superoxide. (84). These reactive species react with biological macromolecules, such as lipids and DNA, leading to cellular dysfunction or death. ROS can attack cell membranes and blood vessels, causing lipid peroxidation and affecting membrane permeability and ion transport (85). Besides, ROS can cause the production of cytokines, which stimulates inflammation and immune response (86).

2.2.3.4 Structural Alterations

During IRI, the brush border of proximal tubular cells undergoes structural changes (87). This brush border, made up of microvilli, plays a role in the reabsorption of small molecules (e.g., peptides) (88). During IRI, a lack of ATP leads to a breakdown in microfilaments, altering the structure of microvilli and disrupting the orientation of cells, resulting in the creation of protuberances and irregularities on the plasma membrane, which eventually break off and are discharged into the tubular lumen (89). Additionally, in response to IRI, integrins, which are transmembrane receptors that mediate cellular adhesion, may move to the apical side of epithelial cell membrane and cause cell detachment, leading to obstruction within tubules and kidney damage (90, 91).

2.2.3.5 Apoptosis

Apoptosis is a form of cell death that involves shrinkage of cells, fragmentation, nuclear condensation, and rapid phagocytosis by phagocytes (92). It is a critical component in homeostasis and facilitates quick removal of the dying or injured cells without causing significant damage to the surrounding tissue (93, 94). Apoptosis can be initiated either by the damaged cell itself through the intrinsic pathway or by interaction with extracellular pro-apoptotic molecules via the extrinsic pathway (94, 95). Apoptosis is initiated via a group of cysteine-aspartic proteases termed caspases, which can be divided into two categories: the initiator caspases, which include caspases 8 and 9, and the executioner caspases consisting of caspases 3, 6, and 7 (95). Once apoptotic signals are detected, the initiator caspases become active, triggering the activation of executioner caspases, leading to a series of events, including DNA fragmentation, nuclear condensation, and the release of phagocytotic signals (96, 97).

2.2.3.6 Necrosis and programmed necrosis

Necrosis is a different type of cell death that is characterised by disorganised chromatin clustering and cell membrane disruption. The release of cytoplasmic content into extracellular space can cause an immune response and trigger inflammation, leading to further tissue damage and potentially exacerbating the underlying injury (98). The understanding of necrosis has been greatly evolved recently. In the past, necrosis was perceived as an uncontrolled, energy-independent cell death

that is induced by severe and sudden damage, such as hypoxia or inflammation (99). Recently, genetic evidence (100-102) and the identification of necrosis inhibitors (103, 104) have uncovered various types of regulated necrosis, a form of cell death that involves disruption of cell membrane in a controlled manner (105). Multiple modes of cell death have been demonstrated to share the concept, including necroptosis, pyroptosis, ferroptosis, and NETosis (106).

2. 3 The transition from AKI to CKD

2.3.1 The involvement of AKI in CKD development

In the past, it was commonly held that patients who survived AKI would experience a full recovery of kidney function to normal levels without any long-term consequences. Recently, however, this has been proven to be false. A meta-analysis by Coca et al. showed that the risk of developing CKD or ESRD was significantly high for AKI patients, with a 9-fold higher risk of CKD and a 3-fold higher risk of ESRD than normal population (107). This increased risk was found to be related to the severity, duration, and frequency of the AKI episode (108-110). Animal and *in vitro* experiments also observed that following an episode of AKI, maladaptive repair processes can occur (111-116). These processes are characterised by the development of fibrosis, reduction in the number of tubules, and chronic inflammation within the interstitial space, ultimately leading to the acceleration of aging in the kidneys and a decline in renal function (117).

The potential underlying mechanisms are shown in **Figure 2.3** and discussed in the following sections.

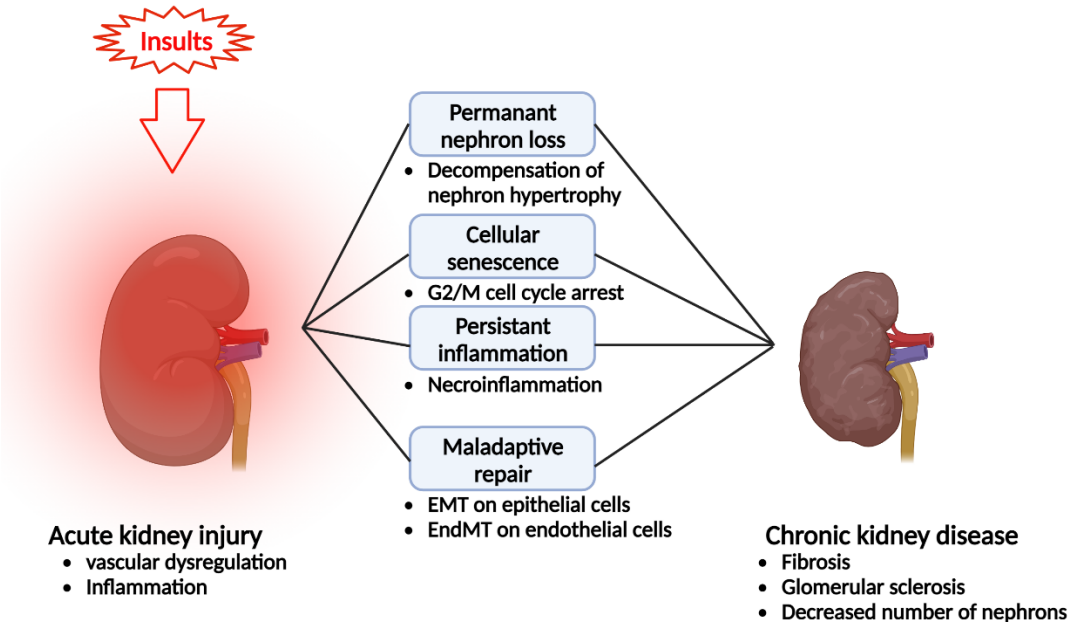

Figure 2. 3 Potential mechanisms of AKI-CKD transition

Acute kidney, featured inflammation and vascular dysregulation, can cause chronic kidney disease via multiple mechanisms. AKI can direct damage nephrons and cause decompensation of nephron hypertrophy, leading to irreversible nephron loss. It can also cause cellular senescence, persistent inflammation, and maladaptive repair. Epithelial and endothelial cells can be supplementary resources of fibrogenic cells via EMT and EndMT, respectively.

EMT: epithelial-mesenchymal transition; EndMT: endothelial-mesenchymal transition; AKI: cute kidney injury; CKD: chronic kidney disease

2.3.2 Nephron loss and hypertrophy

In humans, nephrons are generated between weeks 12 and 36 of gestation, with an average of 950,000 nephrons per kidney ranging from 200,000 to >2.5 million (118). After this time, new nephrons cannot be generated, and their number decreases with age (10). During growth, nephrons expand their size to meet increased demands. Physiologically, nephrons can resist increased filtration load via increasing the single-nephron GFR temporarily without undergoing any structural changes as a reserve mechanism (119, 120). Besides, the kidney has regeneration capacity, but this is limited to a small group of immature tubular cells that can replace single epithelial cells (121). If these immature tubular cells are lost, the ability of tubule segment regeneration is disrupted, causing irreversible nephron loss (122).

Nephron hypertrophy is a compensation mechanism to contend glomerular hyperfiltration by increase the filtration surface (123). A characteristic feature of it is the enlargement of key structures, including the glomerular tuft, Bowman's capsule, and the proximal tubule (124). Glomerular hyperfiltration induces the production of various growth factors, most notably transforming growth factor-α (TGF-α), which cause nephron hypertrophy (125). As a compensation mechanism, nephron hypertrophy can maintain a relatively renal function despite a significant loss of nephrons (123). However, when nephron hypertrophy reaches a certain threshold, the increased shear stress on podocytes can lead to damage to the glomerular filtration

barrier, causing glomerulosclerosis and subsequent deterioration on renal function (124).

2.3.3 Cell cycle, cell cycle arrest, and cellular senescence

Cell division is a highly controlled process that leads to the formation of two new cells. Cell division involves five distinct phases: G0, G1, S, G2, and M. G0 is a quiescent phase in which the cell has exited the cell cycle and is no longer dividing (126). The G1 phase, which occurs after cells leave the G0 phase and begin the process of cell division, is characterised by cell size growth and the production of the mRNA and proteins needed for DNA duplication. Then, in the S phase, DNA replication takes place. Following the S phase, the cell advances to the G2 phase, a preparatory stage prior to the M phase. The G2 phase is marked by an acceleration of cell growth and an increased protein production. Cell growth ceases during the M phase, and cell division proceeds in an orderly fashion. Data has shown that tubular epithelial cells are in the G0 phase and poised to G1 under normal circumstances (127, 128).

Cell cycle arrest is a point in the cycle where the cell is no longer engaged in the procedures of cell duplication and division. Irreversible cell cycle arrest at G1 or G2 indicates cellular senescence, a condition where cells stop dividing and growth, with changes in transcription, metabolism, and secretion, along with altered cellular morphology and chromatin organization (129). Cellular senescence, a phenomenon in which cells cease to divide and function properly, can occur both during embryonic

development and aging, as well as in response to cellular damage (130). The dysregulation of the cell cycle in tubular epithelial cells following AKI has been demonstrated by many pre-clinical research (130).

Senescence is a condition where the cell cycle stop cell dividing and growth, with changes in transcription, metabolism, and secretion. Owing to AKI, both cortex and medulla tissues can be senescent, and renal tubular epithelial cells (TECs) are the most frequently senescent cells (131). In fact, senescence of TECs is a key mechanism that accumulates senescent cells and causes progression of kidney damage (132). It has been demonstrated that TECs can exhibit a G2/M cell cycle arrest following severe or persistent injury, instead of the typical G1/0 arrest under normal circumstances (133). Through the activation of c-jun N-terminal kinase (JNK) signalling, this cellular senescence increases the production of pro-fibrotic factors, such as transforming growth factor-β (TGF-β), which leads to renal fibrosis and CKD (133). Pharmacological interventions that reverse G2/M arrest slowed down the development from AKI to CKD, indicating the vital role of senescence in AKI-CKD transition (116). Besides, it has been shown that severe AKI can activate tubular epithelial cells (TECs) to a senescence-associated secretory phenotype (SASP) where TECs have intensive signalling activities on multiple profibrotic pathways that leads to overproduction of pro-fibrotic factors, resulting in activation of fibroblasts, accumulation of ECM, and ultimately CKD (126, 133).

2.3.4 Maladaptive repair

At the tissue level, the outcome of AKI is determined by the interplay between adaptive and maladaptive repair processes. Maladaptive repair is characterised by accumulation of extracellular matrix (ECM), increased level of profibrotic factors, and persistent inflammation. ECM is predominantly synthesised by myofibroblasts, an activated form of fibroblasts (134, 135). Myofibroblasts can arise from residential fibroblasts, bone marrow-derived fibroblasts, tubular endothelial cells via endothelial-mesenchymal transition (EndoMT), and tubular epithelial cells (TECs) via epithelial-mesenchymal transition (EMT) (136).

EndoMT is a genetic controlled activity where the distinctive properties of endothelial cells are lost and a mesenchymal-like phenotype is acquired (137). Endothelial cells are one of the major targets in AKI, leading to decreased nitric oxide synthesis, dysregulation of blood flow, impaired vascular permeability, and subsequent renal hypoxia (138). various animal studies have revealed that EndoMT has a role in maladaptive repair following AKI (74, 139, 140). After AKI, endothelial cells may change their features and migrate into the interstitial space where they dedifferentiate into myofibroblast and contribute to the progression of CKD.

Similarly, EMT refers to a process where tubule epithelial cells lose their phenotype and acquire features of mesenchymal cells (141). The plasticity of epithelial cells is essential during embryonic development, since it allows reestablishment in anchored

epithelial cells during a developing organism (142). In adults, EMT enables epithelial cells to be an additional source of fibroblasts, which are crucial for repair processes. However, enhanced EMT during renal fibrosis is an unfavourable process, since it leads to overproduced fibrotic scars which breaks the polarised renal tubular epithelial layers (143) and results in reduced renal function. Under normal circumstances, tubular epithelial are tightly connected to each other by intracellular adhesion molecules like E-cadherin, and they attach to the tubular basement membrane (TBM) on their basal side (143). During EMT, tubular epithelial cells lose their connections because of reduced E-cadherin. Meanwhile, activated matrix metalloproteinases (MMPs) disrupt the TBM via enzymatic degradation (144). The loss of intercellular connections and the disruption of TBM enable epithelial cells to migrate into the interstitial space where epithelial cells transform to fibroblasts (2), leading to elevated quantity of myofibroblasts and the overproduction of extracellular matrix which eventually cause fibrosis on kidneys.

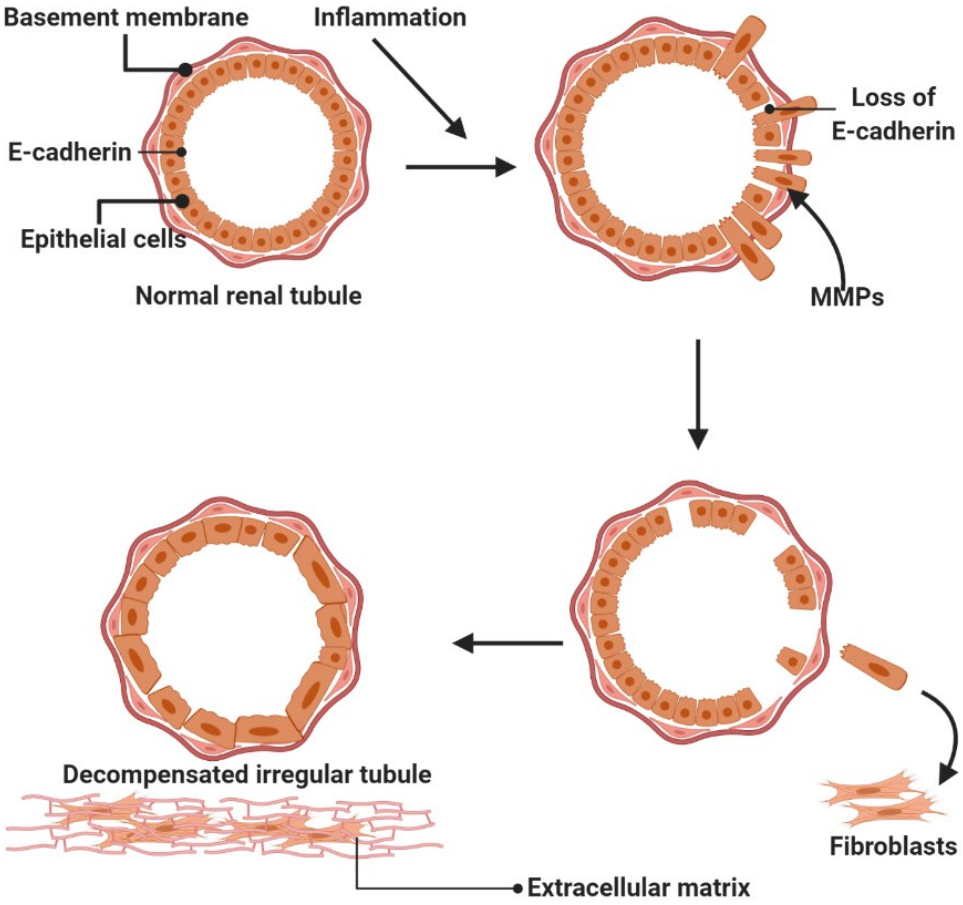

Figure 2. 4 The process of EMT in renal tubules and its contribution to ECM

In a normal renal tubule, TECs are tightly connected to each other by intracellular adhesion molecules like E-cadherin, and they attach to the TBM on their basal side. Upon the stimulation of inflammation, TECs lose their connections because of the loss of E-cadherin via the regulation of profibrotic factors. Meanwhile, activated matrix MMPs disrupt the TBM via enzymatic degradation. These allow TECs to migrate into the interstitial space where epithelial cells transform to fibroblasts resulting in decompensated, irregular tubules that cause a decline in renal function. On the other hand, elevated counts of fibroblasts overproduce ECM that result in renal fibrosis.
EMT: epithelial-mesenchymal transition; TEC: tubular epithelial cells; TBM: tubular basement membrane; MMP: metalloproteinases; ECM: extracellular matrix.

2.3.5 The transforming growth factor-beta 1 signalling pathways

Transforming growth factor-beta 1 (TGF-β1), a member of the TGF-β superfamily, has been identified as a potent inducer of the EMT process (145). TGF-β1 interacts with two types of serine/threonine kinase receptors, known as TGF-β receptor I and II (TβR1 and TβR2). Upon binding of TGF-β1 to TβR2, it generates a heteromeric complex with TβR1, which then proceeds to transmit the TGF-β1 signal via smad-independent or smad-dependent TGF-β signalling pathways (146). Smad-independent TGF-β signalling pathways signal through the mitogen-activated protein kinases (MAPKs) pathways, and the effects of these pathways have not been well elucidated (147). On the other hand, smad-dependent TGF-β signalling pathways have been well studied and are considered as major pathways mediating EMT and fibrosis (148). Smads are a group of structural similar proteins functioning as intracellular signal transducers (149, 150). They can be categorised into three groups, the receptor regulatory group (including smad1, 2, 3, 5 and 8), the common smad (smad4) and the inhibitory group (smad6 and 7). Upon the stimulation of TGF-β1, the TβR2 recruits the TβR1, forming a heteromeric complex which subsequently phosphorylated smad2 and/or smad3. The Phosphorylated smad2/3 bind to smad4 and form a DNA-binding smad complex. The smad complex then translocate into the nucleus targeting genes including profibrotic genes such as snail, α-SMA and twist. The smad complex also induces the transcription of smad7 which can inhibit the phosphorylation of smad2 and 3 (151). Besides, the angiotensin II receptors and the receptor for advanced glycation end products (RAGE)

can activate smad2/3 via extracellular signal–regulated kinase (ERK)/p38 mitogen-activated protein kinase independent of TGF-β (152) (**Figure 2.5**).

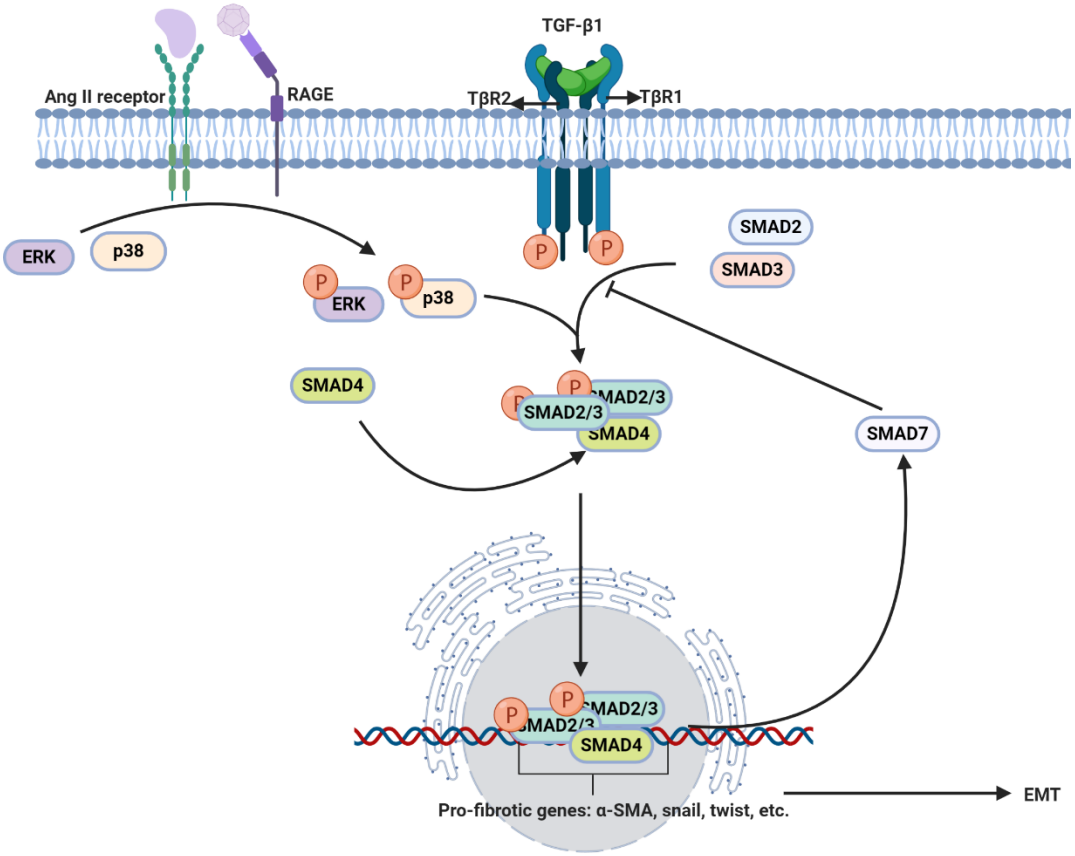

Figure 2. 5 Smad-dependent signalling pathways

Upon the stimulation of TGF-β1, the TβR2 recruits the TβR1, forming a heteromeric complex which subsequently phosphorylated smad2 and/or smad3. The Phosphorylated smad2/3 bind to smad4 and form a DNA-binding smad complex. The smad complex then translocate into the nucleus targeting genes including profibrotic genes such as snail, α-SMA and twist. The smad complex also induces the transcription of smad7 which can inhibit the phosphorylation of smad2 and 3. Besides, the angiotensin II receptors and the receptor for RAGE can activate smad2/3 via ERK/p38 independent of TGF-β.

TGF- β1: transforming growth factor- β1; TβR: TGF-β receptor; α-SMA: α-smooth muscle actin; RAGE: receptor for advanced glycation end products; ERK: extracellular signal–regulated kinase

2.3.6 Persistent inflammation and necroinflammation

Despite a clinical recovery from AKI, chronic inflammation persists in the kidney after AKI, as evidenced by persistent elevations of pro-inflammatory cytokines and biomarkers of renal injury (153), indicating that chronic inflammation caused by AKI may have an important role to promote CKD. Inflammation is a physiological defensive response of immune system to harmful stimuli. In fact, inflammation is a key physio-pathological hallmark of both AKI and CKD. During AKI, the occurrence of inflammation is characterised by massive release of cytokine, increased vascular permeability, and immune cell infiltration. Increased level of inflammation markers, including C-reactive protein, interleukins, and tumour necrosis factor-α (TNF-α) can be detected in the plasma and renal biopsy of patients with CKD and are clinically used to indicate prognosis (154).

Necroinflammation, an auto-amplification loop caused by mutually enhanced necrosis and inflammation (155), may be responsible for the persist inflammation after AKI (**Figure 2.6**). Upon the stimulation of insults, normal cells develop necrosis which causes massive release of danger-associated molecular patterns (DAMPs) including ATP, HMGB-1, HSP, and DNA (156). By interacting with pattern recognition receptors (PRRs), DAMPs not only induce necrosis on neighbouring cells but also recruit and activate immune cells that amplify the inflammation and drive further necrosis (157).

This vicious cycle is termed necroinflammation, and under certain circumstances, it may persist despite the recovery of renal function, leading to the development of CKD.

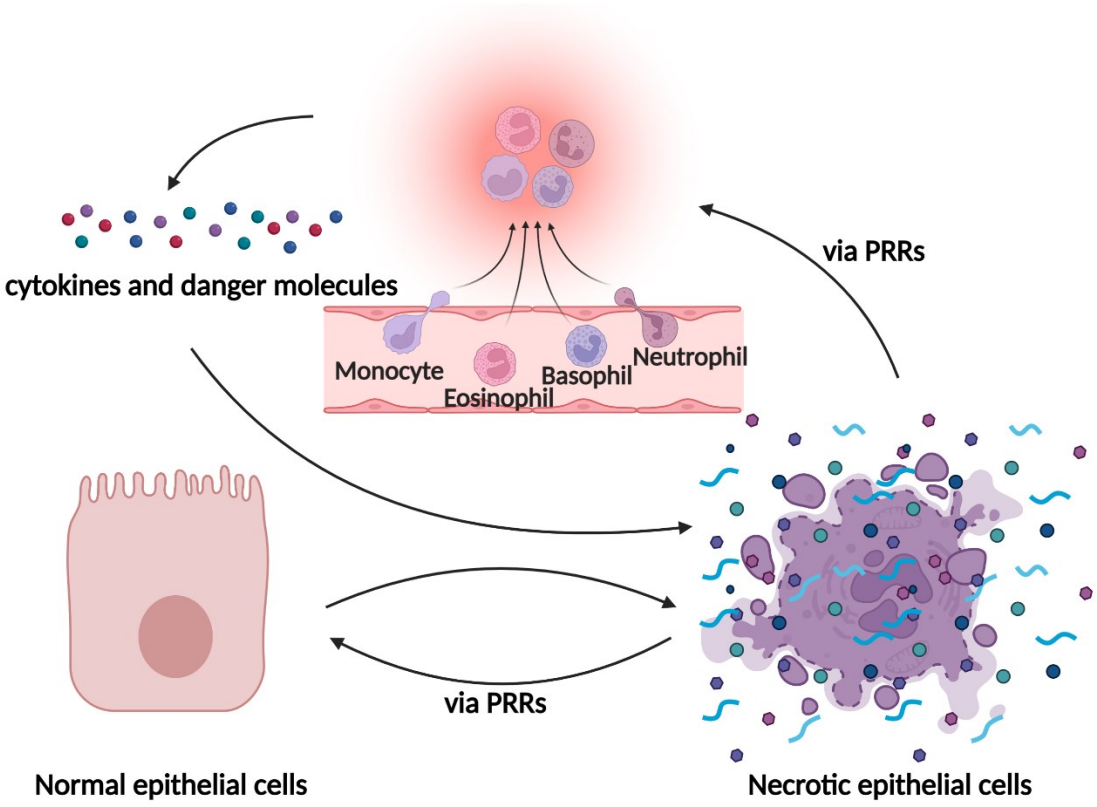

Figure 2. 6 Conceptual model of necroinflammation

Upon the stimulation of insults, normal cells develop necrosis which causes massive release of DAMPs. DAMPs not only induce necrosis on surrounding cells but also recruit and activate immune cells that amplify the inflammation and drive further necrosis on normal cells.
PRRs: pattern recognition receptors; DAMPs: danger-associated molecular patterns

2.3.7 Damage-associated molecular patterns (DAMPs)

DAMPs are endogenous danger molecules within cells that are released from injured or necrotic cells and promote sterile inflammatory response by interacting with pattern PRRs. Despite DAMPs are component of defensive mechanism, they are responsible of many pathological conditions. A considerable number of DAMPs are proteins that naturally occur in the nucleus or cytosol and have a specific intracellular role. When they are released to the extracellular space, they shift from a reducing to an oxidizing environment, resulting in the loss of their biological functions (158). In addition to nuclear and cytosolic DAMPs, other sources of DAMPs include mitochondria, endoplasmic reticulum, and plasma membrane (156).

A variety of DAMPs, such as histones, high-mobility group box 1 (HMGB1), and heat shock proteins (HSPs), have association with renal fibrosis, and their receptors and roles of development of CKD are summarised in **Table 2.3** (159-161).

	DAMPs	Receptors	Reported effects
Nucleus	Histones	TLR2, 4 and 9	Aggravating kidney injury, promoting pro-inflammatory cytokine pathways
Nucleus	HMGB-1	RAGE, TLR2 and TLR 4	Recruiting and activating macrophages, nertrophils and Th2 cells, promoting cell death, and activatiing RAGE/Smad signialing pathway
Cytosol	ATP	P2X7 and P2Y2	Promoting recruitment of macrophages and production of profibrotic factors
Mitochondia	mDNA	TLR9	Promoting recruitment of macrophages and IL-1β production
Endoplasmic reticulum	Calreticulin	CD91	promoting cell migration/proliferation and extracellular matix production

Table 3. Role of DAMPs in the development of CKD

DAMPs: danger-associated molecular patterns; CKD: chronic kidney disease; TLR: toll-like receptor; HMGB-1: high mobility group box 1; RAGE: receptor for advanced glycation end products; ATP: adenosine triphosphate; IL-1β: interleukin-1β

2.3.8 Necroptosis

Necroptosis is a type of programmed cell death with a necrotic death-like appearance (162). Factors that can induce necroptosis include toll-like receptor ligands, tumour necrosis factor-α (TNF-α), DNA-damaging agents and T-cell receptor ligation (163). Signalling pathways of necroptosis remain partially understood. However, the major steps of TNF-α-induced necroptosis has been clarified (**Figure 2.7**). Following the interaction with TNF-α, the TNF receptor (TNFR) gets activated and then recruits receptor-interacting protein kinase 1 (RIP1), transforming growth factor-β-activated

kinase 1 (TAK1), and tumour necrosis factor receptor associated death domain (TRADD) , which binds to the Fas-associated death domain (FADD) (164-166). Normally, when FADD binds to FADD-like interleukin 1β-converting enzyme-like inhibitory protein (FLIP), cells initiate an inflammatory pathway induced by nuclear factor of kappa-light-chain-enhancer of activated B cells (NF-κB) (167). However, if FLIP is degraded, FADD binds to caspase 8, which sets off the apoptotic pathway. If both FLIP and caspase 8 are lost, cells undergo necroptosis, a process that involves the recruitment of RIP3 by RIP1 and subsequent phosphorylation of both proteins. Then the high-energy phosphate bonds are transferred to mixed lineage kinase domain-like protein (MLKL), which subsequently causes cell membrane permeabilization (168, 169). It has been demonstrated that necroptosis have vital roles in various AKI models (170-173), and necroptosis is related to an increase of profibrotic factors, such as TGF-β (174) and IL-1β (175), suggesting that necroptosis may implicate in the development of renal fibrosis.

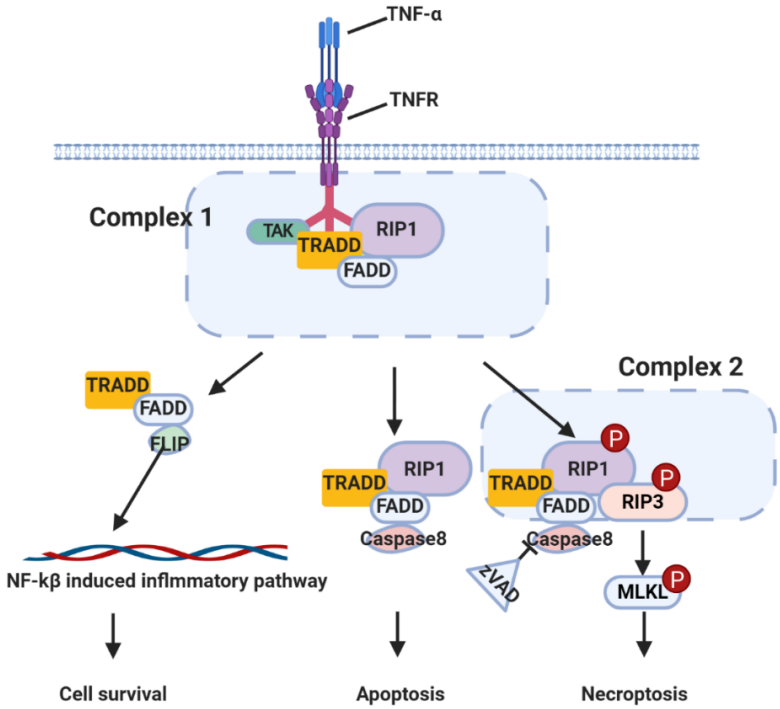

Figure 2. 7 TNF-α induced necroptosis pathway

Upon the stimulation of TNF-α, TNFR forms complex 1, containing RIP1, TAK1 and TRADD, binding with FADD. FADD preferentially binds with FLIP, which causes cells to undergo NF-κB induced inflammation. FADD binds to caspase 8 when FLIP is absent which results in apoptosis. If both FLIP and caspase 8 are lost, MLKL is phosphorylated by the complex 2, causing necroptosis.

TNF-α: tumour necrosis factor-α; TNFR: tumour necrosis factor receptor; RIP1: receptor-interacting serine/threonine-protein kinase 1; TAK1: transforming growth factor-β (TGF-β)-activated kinase 1; TRADD: tumour necrosis factor receptor type 1-associated DEATH domain; FADD: Fas-associated via death domain; FLIP: FADD-like interleukin 1β-converting enzyme-like inhibitory protein; NF-κB: nuclear factor kappa B; RIP3: receptor-interacting serine/threonine-protein kinase 3; MLKL: mixed lineage kinase domain-like protein; zVAD: z-VAD-FMK

2. 4 Hypothesis

It is currently unclear why acute inflammation progresses into chronic, persistent inflammation. Due to the persistent, cyclic nature of necroinflammation, where necrosis and inflammation promote each other, we pose that necroinflammation would be a contributing factor to the progression of acute inflammation into chronic inflammation. Moreover, since necroptosis has been proven to play a key pathogenic role in many models of acute kidney injury (176-179), this form of programmed necrosis is the focus of our research. We hypothesed that in response to various damage, TECs develop necroptosis. These dead cells release DAMPs, resulting in persistent necroinflammation, which leads to nephron loss, maladaptive repair processes such as EMT, and eventually a fibrotic kidney. Therefore, inhibiting necroptosis may attenuate the development of renal fibrosis resulting from AKI. Furthermore, Dexmedetomidine (Dex), a potent cytoprotective anaesthetic, may have the potential to suppress fibrosis development after AKI.

The study aims to investigate the roles of necroptosis, DAMPs, and necroinflammation in EMT and fibrogenesis across various AKI models (nephrotoxicity, IRI, and sepsis), as well as the underlying mechanisms, such as signaling pathways. The ultimate goal is to identify treatments that can prevent the progression of AKI to renal fibrosis by targeting specific molecular pathways.

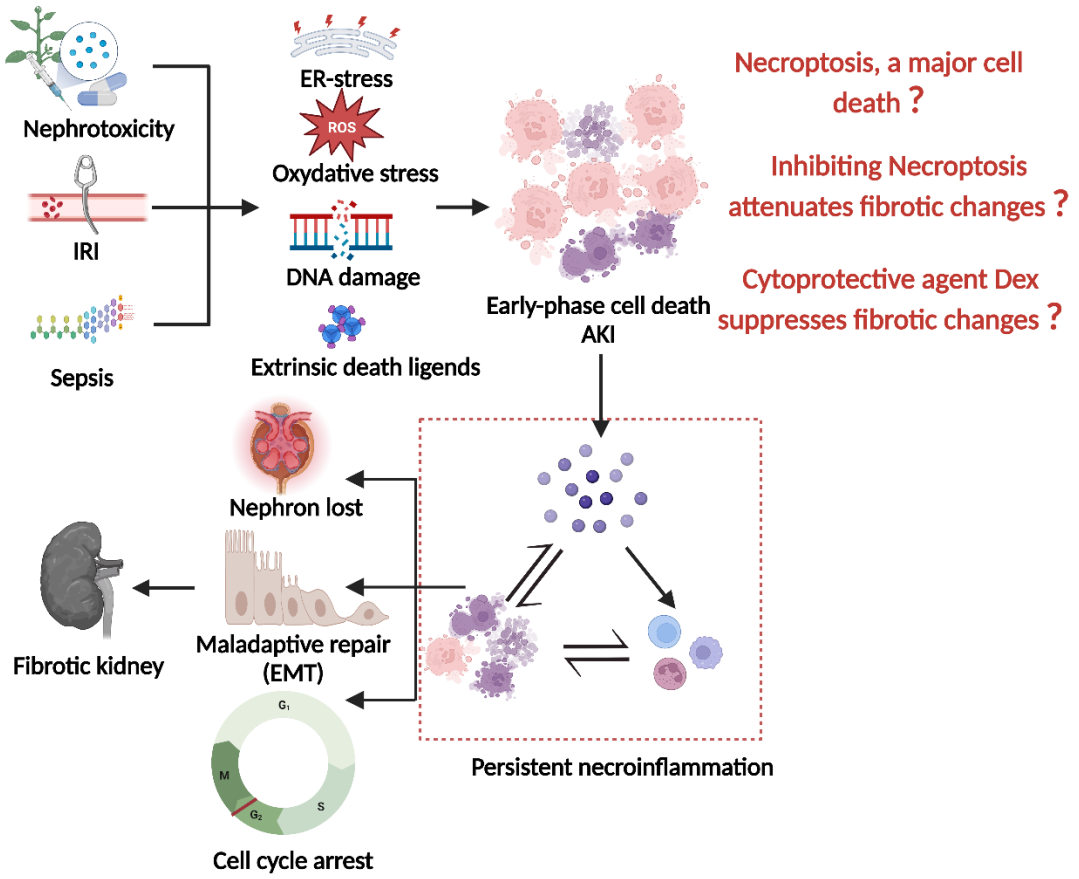

Figure 2. 8 A hypothetical model of the progression of AKI towards CKD

Following injury, TECs are stimulated and experience a variety of stressors, including ER stress, oxidative stress, DNA damage, and/or extrinsic death ligands like TNF-α, leading to necrosis (necroptosis) during the early phase of injury. These dead cells release DAMPs, resulting in persistent necroinflammation, which leads to nephron loss, maladaptive repair processes such as EMT, cell cycle arrest, and eventually a fibrotic kidney.

IRI: ischaemia-reperfusion injury; ER stress: endoplasmic reticulum stress; AKI: acute kidney injury; Dex: Dexmedetomidine; EMT; epithelial-mesenchymal transition

Chapter Three

Methodology

3.1 Cell culture

Human kidney 2 (HK2) cells were purchased from the European Collection of Authenticated Cell Cultures (ECACC, Salisbury, UK). It is a renal proximal tubular epithelial cell line derived from normal adult kidney, and human papilloma virus type 16 (HPV-16) E6/E7 genes were transduced to immortalised the cells. HK2 cells were cultured in Roswell Park Memorial Institute 1640 medium (RPMI 1640 medium; Gibco, Billings, USA) (180-182), supplemented with 10% foetal bovine serum (Invitrogen, Paisley, UK) and 1% penicillin-streptomycin (Invitrogen) and incubated in a humidified incubator at 37 °C with air balanced with 5% CO_2. The medium was changed every three days. After cells reached 70% confluency, they were dissociated with Trypsin (Thermo Fisher Scientific, Waltham, USA) and then centrifuged for subculturing. Biological replicates were conducted for data analysis.

3.2 Nephrotoxicity treatment

The following nephrotoxic substances were used in the present study.

Cisplatin: Cisplatin (CDDP) is a platinum-based alkylating chemotherapy agent. In our study, CDDP (Sigma-Aldrich, Poole, UK) was dissolved in 0.9% NaCl. For the toxicity study, cells were treated with cisplatin at 3μM, 20μM and 100μM respectively. The first concentration is an expected clinical plasma concentration (183), the other two are referred from the research use of cisplatin (184).

Pemetrexed: Pemetrexed (PEM) is a new generation antifolate agent used to treat mesothelioma and non-small cell lung cancer (NSCLC) (185). PEM (Sigma-Aldrich) was dissolved phosphate-buffered saline (PBS) and diluted at 3µM, 20µM and 100µM. Similarly, the first concentration relates to clinical use of pemetrexed (186), while the other two pertain to the usage of pemetrexed in research (187).

Gentamicin: Gentamicin (GM) is an aminoglycoside class of bactericidal antibiotic (188). GM solution (10mg/ml; Gibco) was diluted to 10µM, 20µM and 100µM with distilled water. The first two are therapeutic concentrations of gentamicin (189). The last one is referred from gentamicin *in vitro* studies (190, 191).

AA-I: AA-I are compounds found in plants from the Aristolochiaceae family (192) and have been used for therapeutic purposes. It was dissolved in dimethyl sulfoxide (DMSO). In *in vitro* studies, AAI mainly ranges from 1 to 200µM (193-196), and thus AA-I was diluted to 1µM, 10µM and 100µM for the toxicity study.

3.3 Oxygen-glucose deprivation (OGD) and reperfusion

OGD is the most common method to induce ischaemic injury *in vitro* (197). The OGD medium used in this study was RPMI 1640 without glucose (Gibco) supplemented with 10% foetal bovine serum and 1% penicillin-streptomycin. After the confluency of cells was confirmed, cells were washed with pre-warmed sterile PBS for twice. Then cells were incubated with pre-warmed OGD medium bubbled with 95% N_2 and 5% CO_2 and moved into a chamber flushed with the same gas combination. The chamber was then

quickly sealed and transferred into an incubator at 37 °C for 1 hour. Cells were then incubated in RPMI 1640 medium supplemented with 10% foetal bovine serum and 1% penicillin-streptomycin at 37 °C with air balanced with 5% CO_2 to mimic the reperfusion state (**Figure 3.1**).

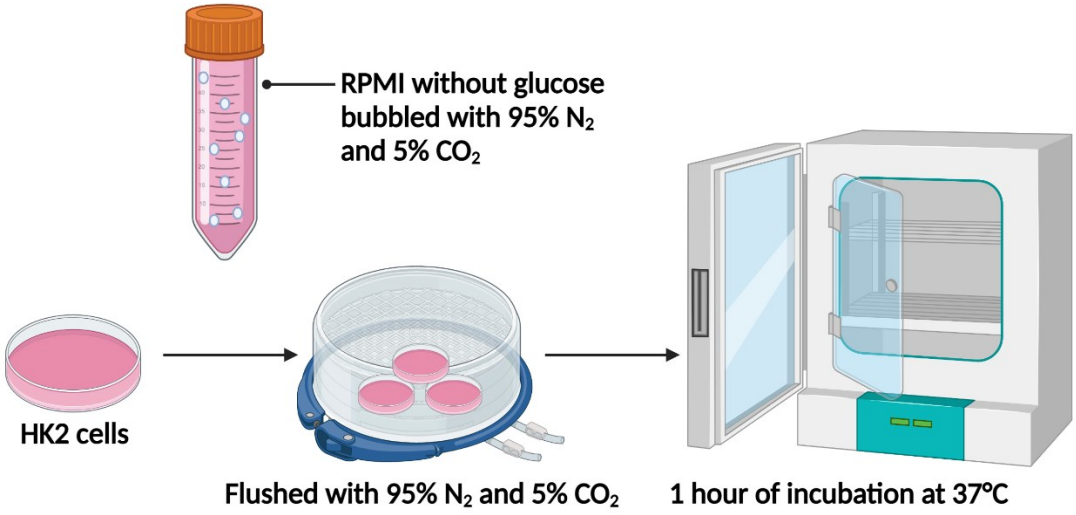

Figure 3. 1 Procedures of OGD

Cells were incubated with pre-warmed OGD medium bubbled with 95% N_2 and 5% CO_2 and moved into a chamber flushed with the same gas combination. The chamber was then quickly sealed and transferred into an incubator at 37 °C for 1 hour.
OGD: oxygen-glucose deprivation; HK2 cells: human kidney 2 cells; RPMI: Roswell Park Memorial Institute 1640 medium

3.4 Cell Counting Kit-8 (CCK-8) assay

CCK-8 assay is a highly sensitive colorimetric test for determining cell viability. The kit employs water-soluble tetrazolium salt-8 (WST-8). WST-8 produces an orange formazan dye upon bio-reduction through cellular dehydrogenases. The amount of the

orange formazan is directly proportional to the number of live cells. Its optical density (OD) can be measured at 460nm (**Figure 3.2**).

Cell suspension was seeded in a 96-well plate and received treatment when reaching confluency. After treatment, cell medium was replaced (90µl/well), and 10µl of CCK-8 kit (Sigma-Aldrich) was added into each well. Wells with 90µl medium and 10µl CCK-8 kit without cells were set as blank. After 4 hours of incubation, the OD value of each well was measured at 460nm using a microplate reader. The survival rate was calculated as (OD_{sample}-OD_{blank}) / ($OD_{naive\ control}$-OD_{blank}) *100%.

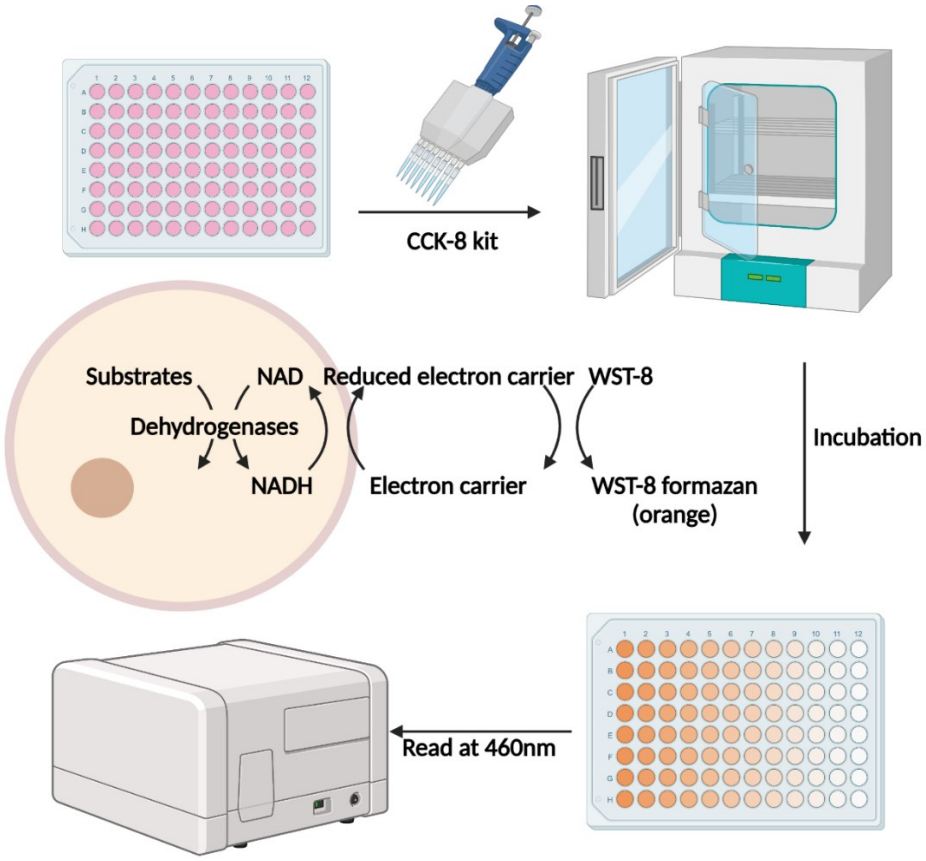

Figure 3. 2 Illustration of CCK8 assay

WST-8 produces an orange formazan via reaction of cellular dehydrogenases. After applying CCK-8 kit into each well, cells were incubated in a humidified incubator at 37 °C with air balanced with 5% CO_2 for 4 hours. Then the OD values were examined by a microplate reader at 460nm.

CCK-8: Cell Counting Kit-8; WST-8: water-soluble tetrazolium salt-8; NAD: nicotinamide adenine dinucleotide; NADH: NAD + hydrogen

3.5 Annexin V/Propidium Iodide (PI) flow cytometry

Annexin V/PI flow cytometry was used to distinguish apoptotic and necrotic cells. Annexin V has a high affinity for phosphatidylserine (PS), which is located on the inner side of cell membrane in normal cells. During apoptosis, cells lose membrane asymmetry that leads to exposure of PS. Therefore, fluorescence labelled Annexin V

can be used to determine apoptosis. PI is a fluorescent agent that attachs to double stranded DNA. PI cannot permeant into healthy live cells, thus PI is utilised to label dead cells. The principle of Annexin V/PI flow cytometry is illustrated in **Figure 3.3**.

In practice, HK-2 cells were cultured in 35mm cell Petri dishes (Costar, Washington, D.C., USA) with 2ml of culture medium in each dish. Following treatment, cells were washed with ice-cold PBS for twice and then dissociated by cell dissociation buffer (Gibco) for 10 minutes at room temperature. Cells were then carefully transferred into 5ml test tubes and washed with Annexin V binding buffer (BioLegend, San Diego, USA) by centrifuging at 1,500rpm for 5 minutes. Then, Cells were resuspension at a concentration of 1 x 10^6 cells/ml with 400µl Annexin V binding buffer. Samples were incubated with FITC Annexin V (BioLegend) for 15 minutes at room temperature. After washing with Annexin V binding buffer via centrifuging, cells were incubated with PI solution (BioLegend) for 5 minutes. Samples were then tested on a flow cytometer (**Figure 3.4**). Data were analysed by a flow cytometry data analysis software, FlowJo (Ashland, USA).

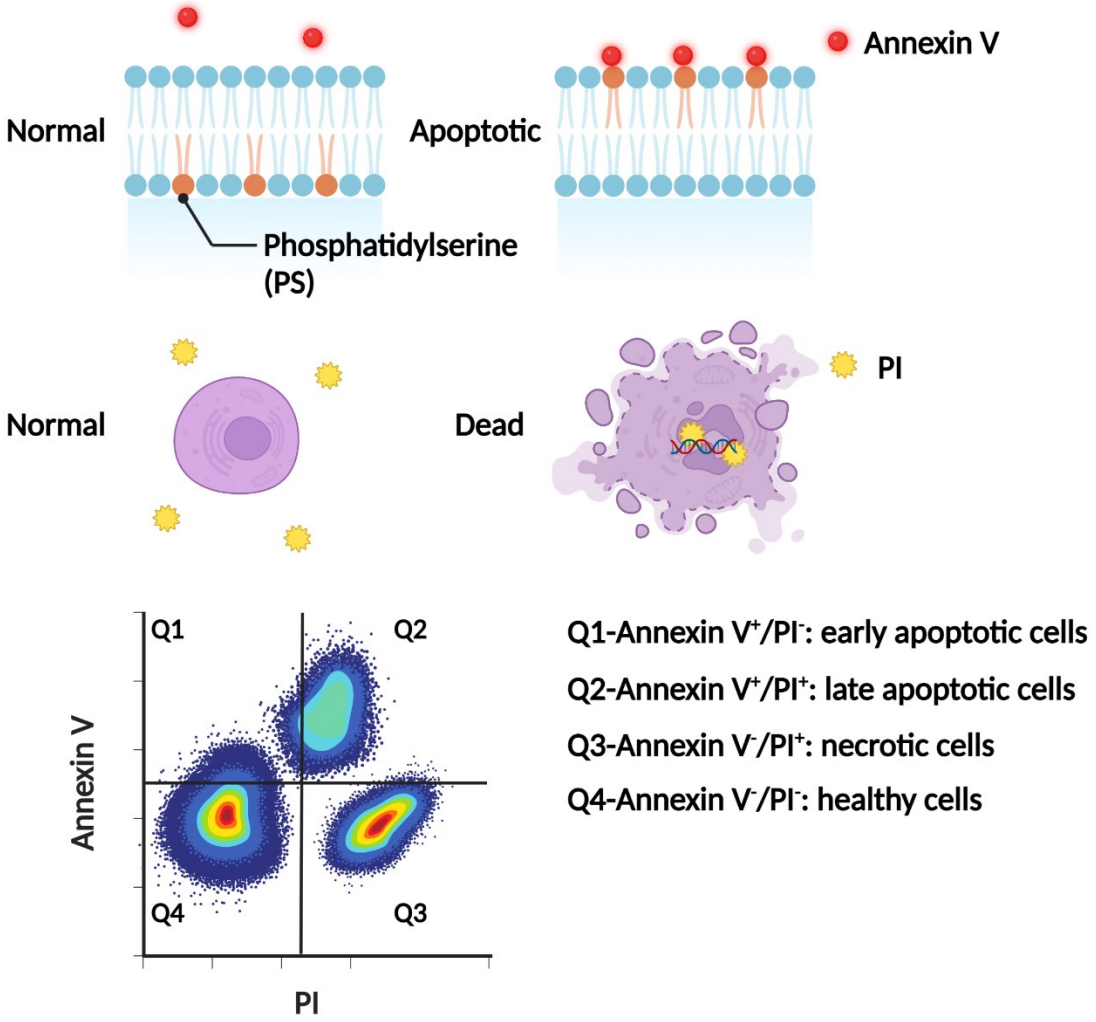

Figure 3. 3 Principle of Annexin V/Propidium Iodide (PI) flow cytometry

Annexin V has high affinity for PS. PS may translocate from cytoplasmic to extracellular side. PI is a fluorescent agent that binds to double stranded DNA. PI cannot permeant into healthy live cells, thus PI can be used to stain dead cells. Ideally, Annexin V^-/PI^- cells are healthy cells, Annexin V^+/PI^- cells are cells undergoing early apoptotic cells, Annexin V^+/PI^+ cells are late apoptotic cells, and Annexin V^-/PI^+ cells are necrotic cells. PS: phosphatidylserine; PI: propidium iodide; Q: quadrant.

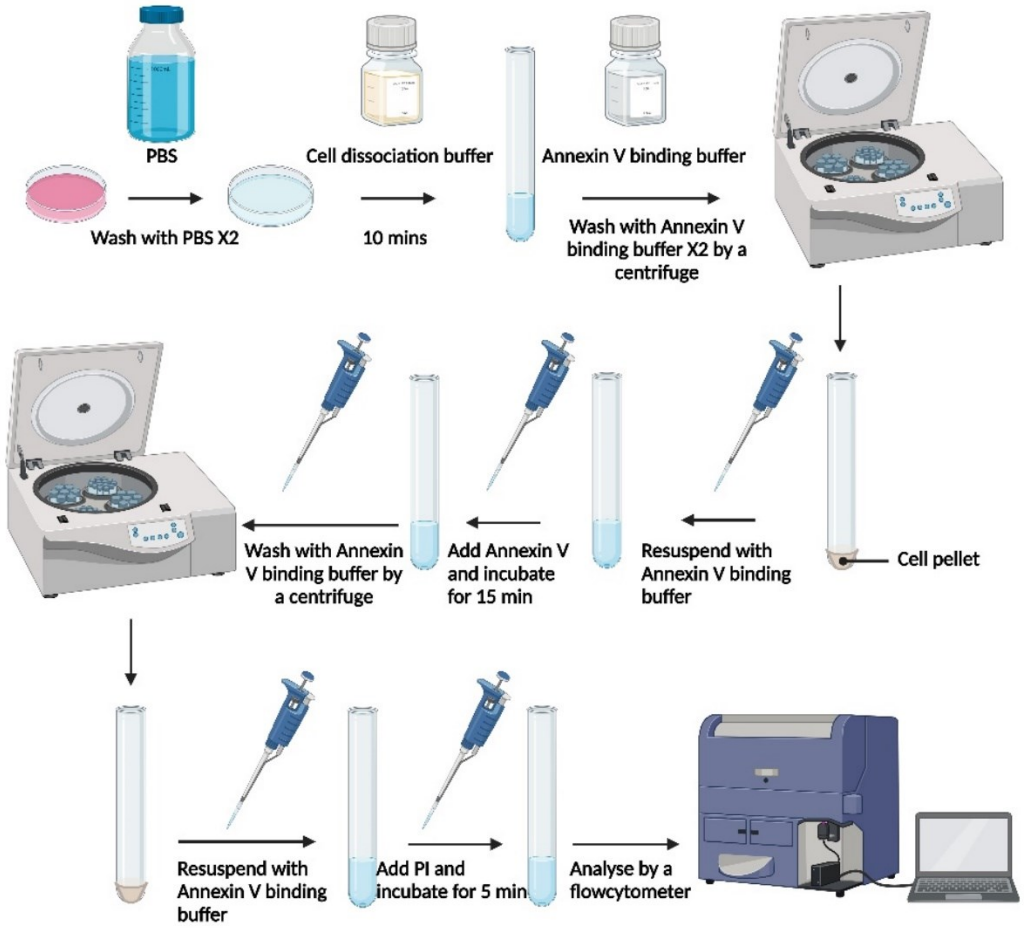

Figure 3. 4 Procedures of flow cytometry

Following treatment, cells were washed with ice-cold PBS for twice and then dissociated by cell dissociation buffer for 10min at room temperature. Cells were then carefully transferred into 5ml test tubes and washed with Annexin V binding buffer by centrifuging at 1,500rpm for 5 minutes. Then, Cells were resuspension at a concentration of 1 x 10^6 cells/ml with 400µl Annexin V binding buffer. Samples were incubated with FITC Annexin V for 15 minutes at room temperature. After washing with Annexin V binding buffer via centrifuging, cells were incubated with PI solution for 5 minutes. Samples were then analysed by a flow cytometer.
PBS: phosphate buffered solution

3.6 Animals and treatment

C57BL/6J mice were purchased from Charles River Laboratories (Wilmington, USA). Mice were kept in temperature and humidity-controlled cages in a specific pathogen-free (SPF) animal research facility at Chelsea & Westminster Hospital, Imperial College London. All experimental procedures in the current study strictly followed the United Kingdom Animals Act 1986.

3.7 Ischaemia-reperfusion injury model *in vivo*

Mice (n=3) were randomly assigned in untreated group, sham control group, ischemia-reperfusion group, and necrostatin-1 (Nec-1, an inhibitor of necroptosis; Calbiochem, Darmstadt, Germany) treated IRI group. Mice were anaesthetised by 1.5% isoflurane (Sigma-Aldrich). In the IRI and NEC group, mice received bilateral renal pedicle clamping for 30 minutes. In the NEC group, mice were injected 1.65 mg Nec-1/kg body weight intraperitoneally at 15 minutes before the onset of ischemia. A temperature controller (Omega Engineering Inc., Stamford, USA) was utilized to maintain the intra-abdominal temperature at 36.0 ± 0.1 °C for the duration of the experiment. All mice were sacrificed 24 hours after treatment with an overdose pentobarbitone i.p. injection (P010, Sigma-Aldrich) and their kidneys were then harvested (**Figure 3.5**). The *in vivo* experiments were conducted by Dr. Hailin Zhao, a research associate in Imperial College London.

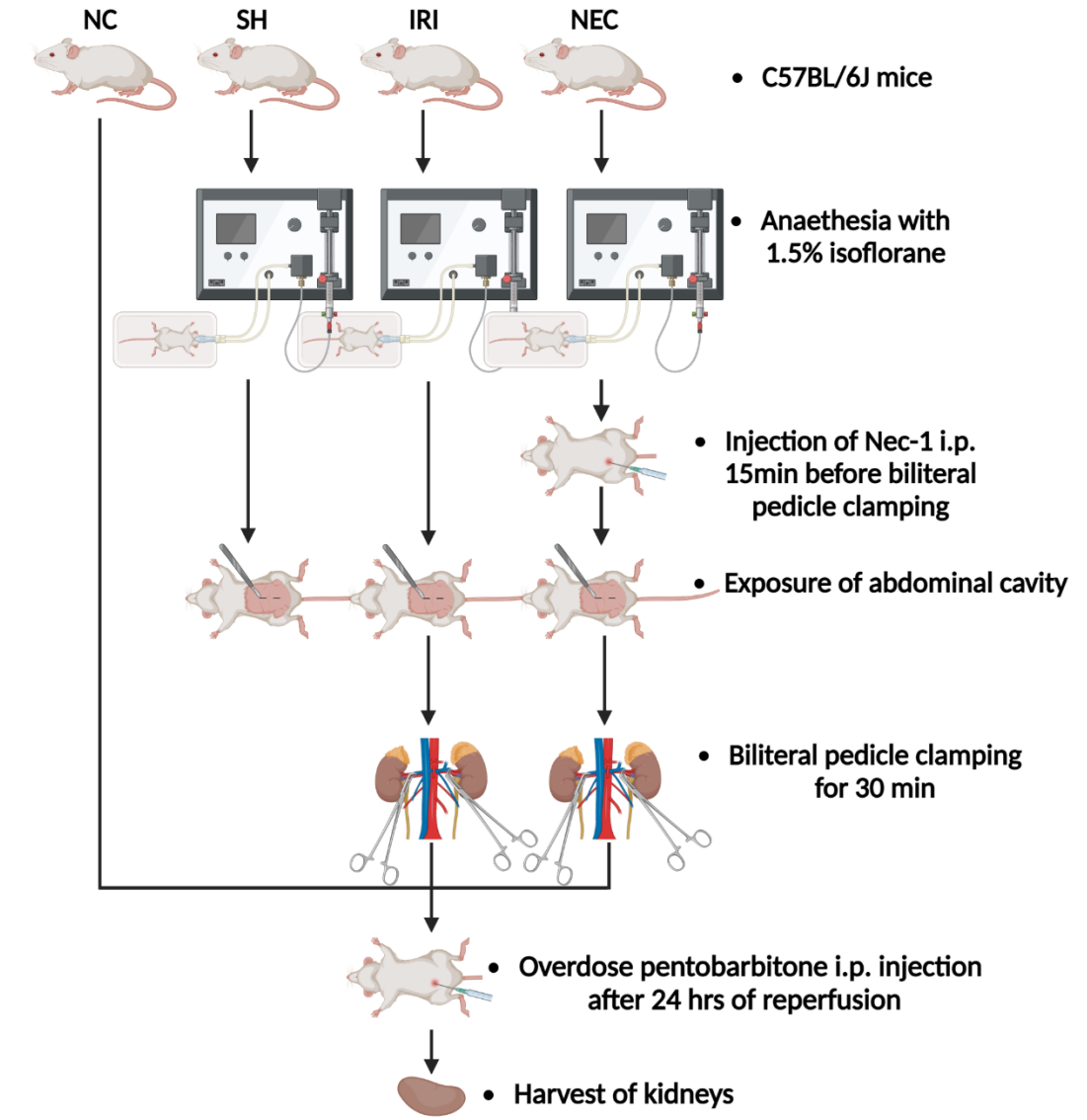

Figure 3. 5 Procedure of ischaemia-reperfusion in vivo model

Adult C57BL/6J mice weighing 20 to 25g were randomly assigned in four groups. NC: untreated; SH: laparotomy without biliteral pedicle; IRI: biliteral pedicle clamping for 30min; NEC: biliteral pedicle clamping for 30min and i.p. injection of Nec-1 15min before ischaemia. Mice were anaesthetised by 1.5% isoflurane. All mice were sacrificed 24 hours after treatment with an overdose pentobarbitone i.p. injection and their kidneys were harvested.

NC: naïve control; SH: sham control; IRI: ischaemic-reperfusion injury; Nec-1: necrostatin-1; i.p.: intraperitoneally.

3.8 Sepsis model *in vivo*

This part study was collaborated with Prof. Dongxin Wang and Dr. Yibing Sun, Peking University First Hospital, Beijing, China. The research protocol was approved by the Ethics Committee of Animal Use for Scientific Research of Peking University First Hospital, and the *in vivo* experiments were conducted by Dr. Yibing Sun. Adult male C57BL/6J mice (aged 10 weeks and weighing 20 to 25g), were randomly administered intraperitoneally with lipopolysaccharides (LPS) alone, LPS with Dexmedetomidine (Dex) or LPS, Dex and α_2-adrenoreceptor (α_2-AR) antagonist Atipamezole (Atip, n=5/group). Mice of the LPS alone group received 10mg/kg LPS from Escherichia Coli-O111:B4 (L2630, Sigma-Aldrich). Mice in the LPS+DEX groups received 25g/kg Dex (SML0956, Sigma-Aldrich) intraperitoneally every two hours for a total of three times immediately after LPS administration whilst mice in the LPS+DEX+ATIP group, after LPS administration, ATIP mice were given Atip (A9611, Sigma-Aldrich) intraperitoneally at a dose of 500 g/kg every two hours for a total of three times followed by Dex as above. Mice in the control group received comparable volumes of saline (n=5). All mice were sacrificed 24 hours after treatment with an overdose pentobarbitone i.p. injection and their kidneys were then harvested.

3.9 Haematoxylin and eosin (H&E) staining

H&E staining is one of the principal methods to study histology. Cell nuclei are stained purple-blue by haematoxylin, while the cytoplasmatic substances are stained pink by

eosin, and other structures are stained different mixtures of these colours (198). Thus, H&E staining can be used to study cell nuclei, cytoplasm, and an overview of histological structure.

In our study, the kidney sections were fixed with 5% formalin (Sigma-Aldrich) and imbedded in wax, and then sectioned (5µm) and subsequently stained with haematoxylin and eosin (Sigma-Aldrich). For each sample, 5 fields (20x magnification) were evaluated under an Olympus BX4 microscope (Watford, UK). The level of cell necrosis and loss of epithelial brush border were blindly assessed and scored by a <20% (0), 20% (1), 50% (2) and ≥80% (3) loss of nuclei and brush border to generate a glomerular injury score (GIS) and a tubular injury score (TIS) respectively (199).

3.10 Immunofluorescent staining

Immunofluorescent staining is a technique that uses fluorophore-conjugated antibodies to label a specific antigen. It can be classified as direct IF and indirect IF. Direct IF employs antibodies directly labelled with a fluorophore; indirect IF uses a primary antibody that targets the antigen of interest, and a fluorophore-conjugated secondary antibody that binds to the primary antibody. IF can be used to stain both tissues (immunohistochemistry; IHC) and cells (immunocytochemistry; ICC).

3.10.1 IHC preparation

Paraffin Wax Embedding and Sectioning: Kidneys were fixed in 4% paraformaldehyde (Santa Cruz, Dallas, USA) for 24 hours. Then kidneys were dehydrated by graded ethanol (Sigma-Aldrich) and xylene (Sigma-Aldrich). After embedding in paraffin at 56 °C for 1 hour, kidneys were sectioned into 10μm slices and mounted onto slides (Sigma-Aldrich) (**Figure 3.6**). Being dried overnight, slides were stored in a slide storage box and ready for use.

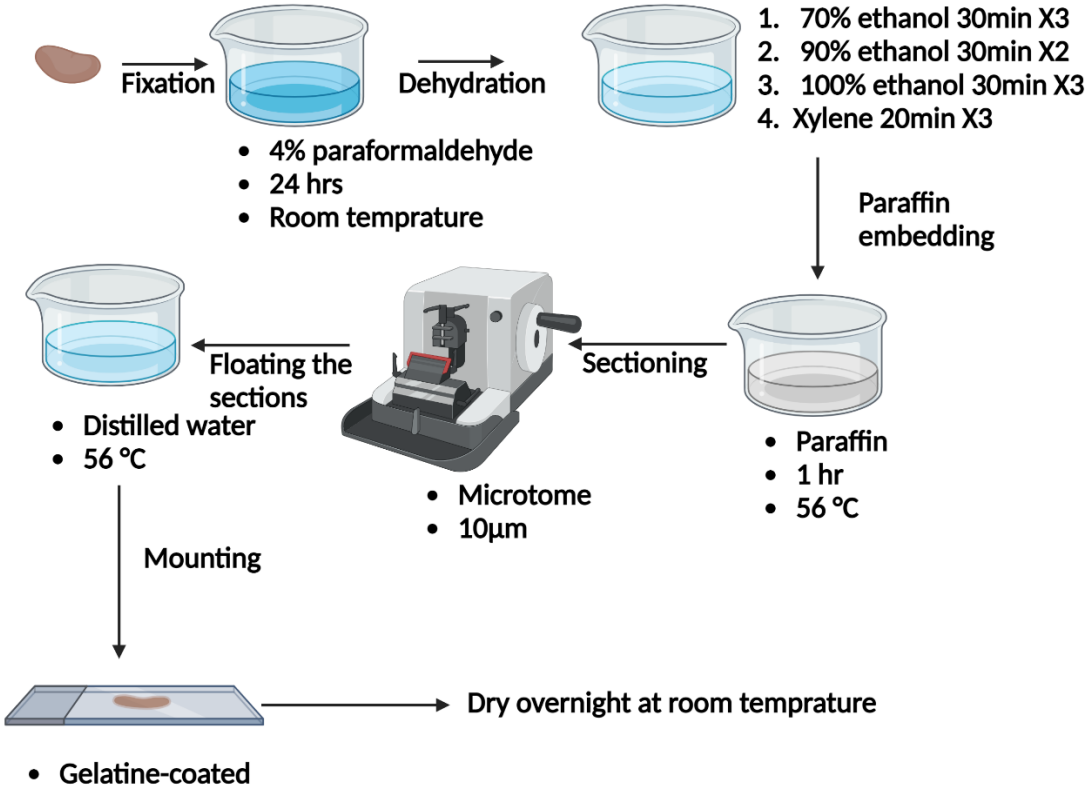

Figure 3. 6 Procedures of tissue paraffin embedding and sectioning

Kidneys were fixed in 4% paraformaldehyde for 24 hours at room temperature. Then they were dehydrated in graded ethanol and xylene by the following steps: 1. 70% ethanol for 30 minutes 3 times; 2. 90% ethanol for 30 minutes 2 times; 3. 100% ethanol for 30 minutes 3 times; 4. Xylene for 20 minutes 3 times. Kidneys were then embedded in paraffin at 56 °C for 1 hour and sectioned into 10µm. After floating the kidney sections in distilled water at 56°C, sections were mounted onto gelatine-coated slides.

Antigen-retrieval: Sections were deparaffinised by xylene and rehydrated by graded ethanol and deionised water. Slides were then moved to boiling antigen-retrieval buffer (Santa Cruz) in a pressure cooker. Slides were cooled down with cold tap water after 3 minutes of full pressure boiling (**Figure 3.7**). Before the staining processes, circle the tissues with a hydrophobic pen.

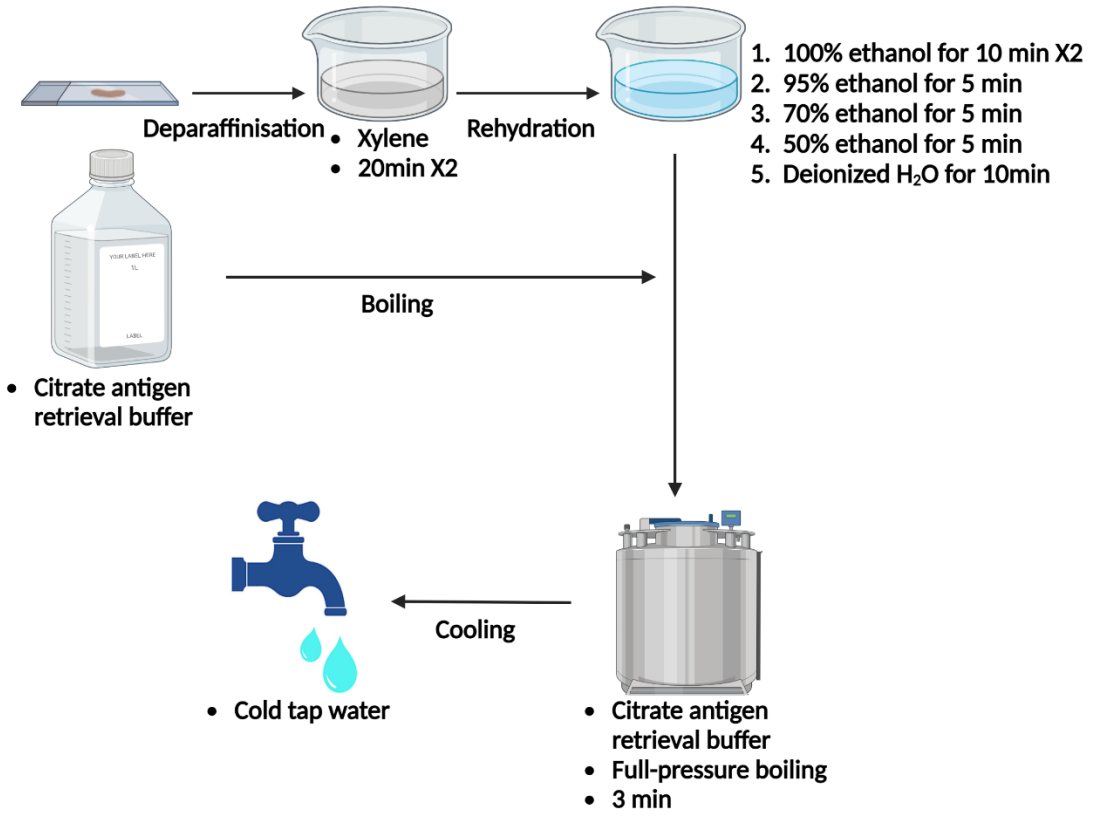

Figure 3. 7 Antigen-retrieval protocol

Slides were immersed in xylene for 20 minutes 2 times for deparaffinisation. Then slides were rehydrated in graded ethanol and water by the following steps: 1. 100% ethanol for 10 minutes 2 times; 95% ethanol for 5 minutes; 70% ethanol for 5 minutes; 50% ethanol for 5 minutes; deionised water for 10 minutes. Slides were then immersed in boiling citrate antigen-retrieval buffer at full pressure for 3 minutes. After that, slides were cooled down by cold tap water.

3.10.2 ICC preparation

Cells were seeded on coverslips (Thermo Fisher Scientific). After treatment, medium was removed, and coverslips were gently washed with ice-cold PBS. Then cells were fixed by 4% paraformaldehyde for 10 minutes. After being washed with PBS for three times, cells were ready for the following steps.

3.10.3 IHC and ICC Shared procedures

Tissues or cells were blocked and permeabilised in 5% normal donkey serum (NDS) in PBS with 0.05% Triton-X (PBST; Sigma-Aldrich) for 30 minutes. They were then incubated with primary antibodies at 4 °C overnight, followed by incubation with fluorescently conjugated secondary antibodies for 1 hour. They were then stained with 4',6-diamidino-2-phenylindole (DAPI) mounting solution (Vector Laboratories, Burlingame, USA) and prepared for examination (**Figure 3.8**). Antibodies used in IF were summarised in **Table 3.1**.

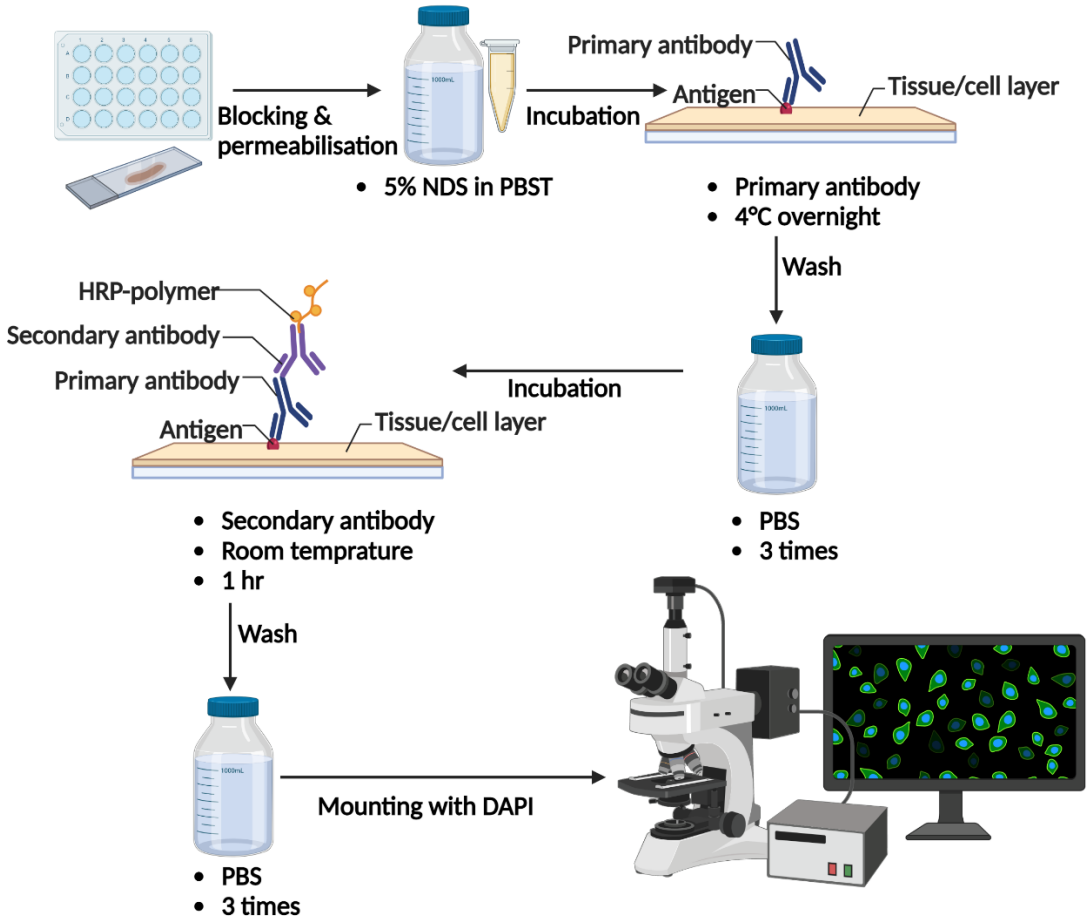

Figure 3. 8 An overview of IF

Tissues or cells were blocked and permeabilised in 5% NDS in PBST for 30 minutes. They were then incubated with primary antibodies at 4 °C overnight. After being washed with PBS for 3 times, slides were incubated with fluorescently conjugated secondary antibodies for 1 hour. Then slices were washed with PBS for 3 times and stained with DAPI mounting solution and prepared for examination.

NDS: normal donkey serum; PBS: phosphate buffered saline; PBST: PBS with 0.05% Triton-X; HRP: horseradish peroxidase; DAPI: 4’,6-diamidino-2-phenylindole.

Primary antibodies	Host species	Target species	Concentrations	Source
P-MLKL	Rabbit	Human; mouse	1:200	Abcam
E-cadherin	Rabbit	Human; mouse	1:1000	Abcam
A-SMA	Mouse	Human; mouse	1:200	eBioscience
TGF-β1	Mouse	Human	1:200	Abcam
NLRP3	Mouse	Human	1:200	Abcam
Collegen-1	Rabbit	Human	1:500	Abcam

Secondary antibodies	Host species	Target species	Concentrations	Source
Donkey anti-Rabbit Red	Donkey	Rabbit	1:1000	Cell signalling
Donkey anti-Rabbit Green	Donkey	Rabbit	1:1000	Cell signalling
Donkey anti-Mouse Red	Donkey	Mouse	1:1000	Cell signalling
Donkey anti-Mouse Green	Donkey	Mouse	1:1000	Cell signalling

Table 4. Immunofluorescence antibodies

P-MLKL: phosphorylated-mixed lineage domain-like protein; α-SMA: α-smooth muscle actin; TGF-β1: transforming growth factor-β1; NLRP3: NLR family pyrin domain containing 3

3.11 Western Blot

Western blot is a common analytical method for identifying particular proteins in a tissue homogenate or extract sample. In addition to identifying proteins, this method can be used to view, separate, and quantify the various proteins in a complex protein combination. The Western blot approach separates a particular protein from a complex by utilising three components: size separation, protein transfer from gel to a membrane, and visualisation of the target protein with primary and secondary antibodies.

3.11.1 Protein extraction

Tissues: Kidneys were dissected and immersed in ice-cold cell lysis solution which was made by cell lysis buffer (Cell Signalling Technology, Danvers, Massachusetts, USA), phosphatase inhibitor cocktail (Roche Holding AG, Basel, Switzerland), protease inhibitor cocktail (Roche Holding AG, Basel, Switzerland), and distilled water. Tissues were then homogenised by a manual homogeniser (Sigma-Aldrich) and a sonicator (Soniprep 150, Measuring and Scientific Equipment, Heathfield, UK) followed by constant agitation at 4 °C for two hours. The homogenates were then centrifuged at 16,000 x g for 20 min at 4 °C, and supernatant was collected for blotting.

Cells: After the removal of medium, cells were washed with ice-cold PBS for 3 times. Then cells were immersed in cell lysis solution and transferred into microcentrifuge tubes by scraping. Cell lysates were homogenised by a sonicator, followed by constant agitation at 4 °C for 20 minutes. The homogenates were then centrifuged at 16,000 x g for 20 min at 4 °C, and supernatant was collected for blotting (**Figure 3.9**).

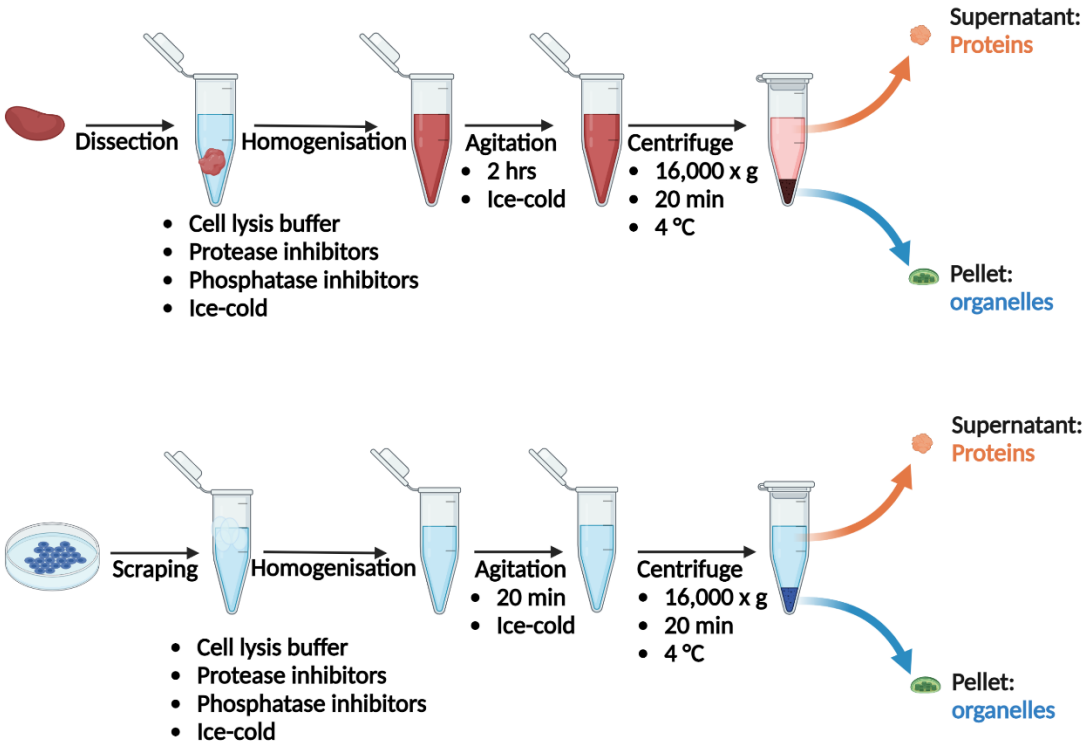

Figure 3. 9 Procedures of protein extraction

Dissected tissues or scrapped cells were immersed in ice-cold cell lysis solution which is composed of cell lysis buffer, protease inhibitors, and phosphatase inhibitors. They were homogenised, followed by constant agitation at 4 °C (2 hrs for tissues and 20 min for cells). The supernatant was then collected for blotting.

3.11.2 Protein blotting

Protein samples (80 g) were heated with NuPAGE lithium dodecyl sulphate (LDS) sample buffer (Invitrogen) at 95 °C for 5 minutes and then loaded onto a NuPAGE 10% Bis-Tris gel (1.5mm 10 well, Invitrogen) for electrophoresis. Proteins were then transferred onto a PVDF (polyvinylidene difluoride) membrane (Invitrogen) which was blocked in 5% non-fat milk in Tris-buffered saline with 0.1% Tween® 20 detergent (TBST, Sigma-Aldrich) for 1 hour, followed by incubation with primary antibodies in TBST at

4 °C overnight, followed by incubation with secondary antibodies for 1 hour. After incubation with antibodies, membranes were washed with TBST for 3 times. Membranes were developed in luminol agent (Santa Cruz) and visualised by GeneSnap Version 7.1 (Syngene, Cambridge, UK) (**Figure 3.10**). Protein band intensity was normalised with glyceraldehyde 3-phosphate dehydrogenase (GAPDH) and expressed as a ratio of control for data analysis. Antibodies used in western blot are summarised in **Table 3.2**.

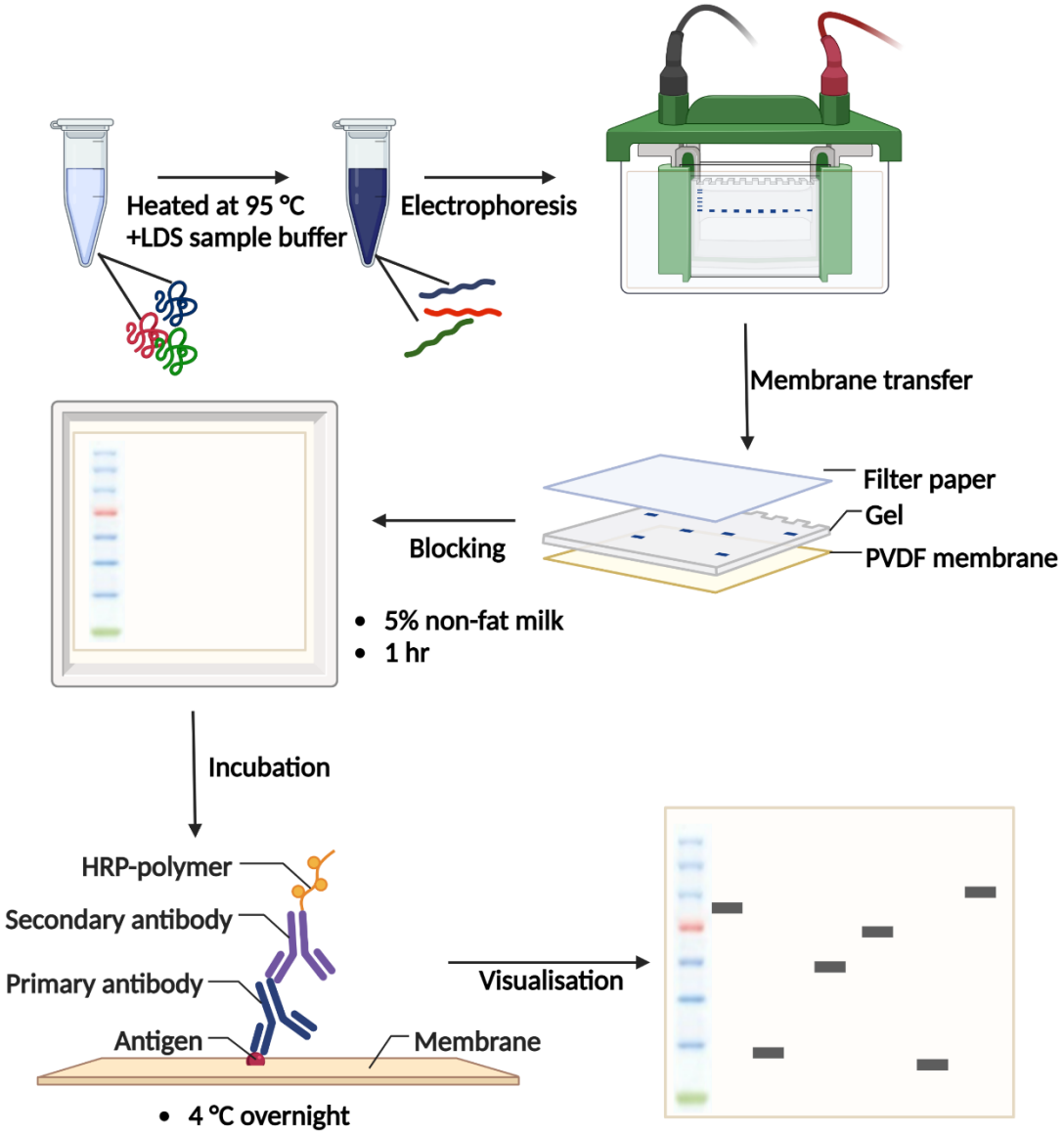

Figure 3. 10 Procedures of western blot

Protein samples were heated with LDS sample buffer at 95 °C for 5 minutes and then loaded onto a NuPAGE 10% Bis-Tris gel for electrophoresis. Proteins were then transferred onto a PVDF membrane which was blocked in 5% non-fat milk in TBST, followed by incubation with primary antibodies at 4 °C overnight. After incubating with secondary antibodies, membranes were developed in luminol agent and visualised. Membranes were washed with TBST after incubation with antibodies.
LDS: lithium dodecyl sulphate; PVDF: polyvinylidene difluoride; HRP: horseradish peroxidase. TBST: Tris-buffered saline with 0.1% Tween® 20

Primary antibodies	Host species	Target species	Concentrations	Source
P-RIP	Rabbit	Human	1:500	Cell signalling
RIP	Rabbit	Human	1:1000	Cell signalling
P-MLKL	Rabbit	Human; mouse	1:200	Abcam
MLKL	Rabbit	Human	1:1000	Abcam
E-cadherin	Rabbit	Human; mouse	1:1000	Abcam
Vimentin	Rabbit	Human	1:1000	Abcam
A-SMA	Mouse	Human; mouse	1:200	eBioscience
TGF-β1	Mouse	Human	1:200	Abcam
P-JNK	Rabbit	Human	1:500	Santa Cruz
JNK	Rabbit	Human	1:1000	Santa Cruz
GSDM-D	Rabbit	Human	1:500	Abcam
GAPDH	Mouse	Human;Mouse	1:20000	Millipore

Secondary antibodies	Host species	Target species	Concentrations	Source
Donkey anti-Rabbit	Donkey	Rabbit	1:1000	Cell signalling
Donkey anti-Mouse	Donkey	Mouse	1:1000	Cell signalling

Table 5. Western blot antibodies

RIP: receptor-interacting protein kinases; p-MLKL: phosphorylated-mixed lineage domain-like protein; α-SMA: α-smooth muscle actin; TGF-β1: transforming growth factor-β1; JNK: c-Jun N-terminal kinases; GSDM-D: gasdermin-D; GAPDH: glyceraldehyde 3-phosphate dehydrogenase

3.12 Data analysis

The intensity of protein bands and immunofluorescent images were measured using Image J. All data were expressed as mean ± standard deviation (SD) and presented as dot plot and then analysed using a one-way ANOVA followed by post hoc Tukey's test with GraphPad Prism 8. A p-value of less than 0.05 was considered to be of a statistical significance.

Chapter Four

Necroptosis and Toll-like receptor-4 Contribute to nephrotoxicity-Induced EMT Development in Renal Tubular Epithelial Cells

4.1 Introduction

Drug-induced nephrotoxicity is a common and significant clinical problem that can cause acute kidney injury (AKI) and progression of chronic kidney disease (CKD). Nephrotoxic agents, such as certain drugs or herbal ingredients, may contribute to kidney injuries towards CKD development. In fact, studies have indicated that at least one nephrotoxic agent was applied in about 25% of cases of AKI (200-202). Cell death has a vital role in the development of nephrotoxic AKI and even CKD. The death of affected cells not only directly causes a renal function decline, but also initiates immune reactions, inflammation, haemodynamic alterations, and cellular senescence, making it a central component in the development of nephrotoxicity (203). It is important to understanding the underlying mechanisms of cell death in nephrotoxicity to prevent and treat this serious issue. In this chapter, the nephrotoxic effects of four agents, cisplatin (CDDP), pemetrexed (PEM), gentamicin (GM), and aristolochic acid-I (AA-I), were investigated in human tubular epithelial cells (HK2 cells). The aim was to understand the relationship between cell death and the potential development of epithelial-mesenchymal transition in response to these nephrotoxic agents.

Cisplatin (CDDP) is a platinum-based alkylating agent that damages DNA. Despite its efficacy in treating various cancers, including ovarian, cervical, bladder, testicular, and lung cancer (204), its therapeutic use is limited due to its unpleasant side effects, including nephrotoxicity, which is the most common adverse effect (205). CDDP

nephrotoxicity can manifest as both AKI and CKD (206). Both apoptosis and regulated necrosis are involved in CDDP nephrotoxicity (207). However, detailed mechanisms remain to be elucidated.

PEM, a new generation antifolate agent, is widely recognized for its potent antineoplastic implications in mesothelioma and non-small cell lung cancer (NSCLC) (185). It interferes with the synthesis of DNA and RNA by blocking multiple folate-metabolizing enzymes (208). PEM has been approved as a first-line treatment for NSCLC (209) and is recommended for maintenance treatment for patients who have not experienced cancer progression (210). However, PEM has been reported to cause acute kidney injury (AKI) and even permanent kidney damage (211). A study showed that 49% of patients with advanced NSCLC who were given PEM maintenance developed acute kidney disease (AKD), of which 55% progressed to chronic kidney disease (CKD) (212). Despite its potential therapeutic benefits, the nephrotoxicity of PEM poses a challenge to its clinical use. There is currently limited knowledge on the underlying mechanisms.

Gentamicin is an antibiotic from the aminoglycoside family that is effective in the treatment of a diverse array of bacterial infections, such as Proteus and Staphylococcus (213, 214). Despite the availability of new generation antibiotics, gentamicin is still widely used due to its potent bactericidal activity, limited bacterial resistance, long-lasting effects, and cost-effectiveness. One major side effect of

gentamicin is nephrotoxicity (215), with estimates indicating that around 30% of patients taking gentamicin for a period exceeding seven days display signs of kidney injury (188, 216). The mechanisms behind gentamicin-induced nephrotoxicity include oxidative stress, production of reactive oxygen species, and induction of apoptosis and necrosis (217-220).

Aristolochic acids (AAs) are compounds found in plants from the Aristolochiaceae family (192) and have been used for therapeutic purposes, such as anti-inflammatory and diuretic treatments, for many years (221, 222). However, it has been shown that consuming herbal remedies containing AAs can lead to a progressive kidney disease known as aristolochic acid nephropathy (223). AA-I has been identified as a primary component of AAs with nephrotoxicity (192, 224). Research has linked the nephrotoxicity of Aristolochic acids to DNA damage, oxidative stress, mitochondrial dysfunction, and apoptosis (225-227), but more research is needed to fully understand the mechanisms and find effective treatments.

The mechanisms of cell death in nephrotoxicity are complex and involve various pathways, such as apoptosis, autophagy, and necrosis (228). Among these pathways, necroptosis, a newly recognised form of cell death, has attracted growing attention due to its unique characteristics and critical role in the progression of nephrotoxicity. Necroptosis is a type of regulated cell death characterised by cell membrane disruption and the release of intracellular contents, which trigger an immune response

and contribute to inflammation. Recent studies have revealed that necroptosis causes epithelial-mesenchymal transition (EMT) development in various cell types, such as nasopharyngeal carcinoma cells (229). EMT is a process in which epithelial cells lose their polarity and cellular adhesion and adopt a mesenchymal phenotype (141). EMT has been identified as a crucial factor in the development CKD, as it contributes to the loss of renal function and the formation of fibrosis (230). Therefore, this chapter aimed to investigate if nephrotoxic agents, including CDDP, PEM, GM, and AA-I, cause necroptosis and EMT, and study the correlations between necroptosis and EMT and the underlying molecular mechanisms.

4.2 Experimental design

4.2.1 Investigating the time course of EMT development in cultured human proximal tubular epithelial cells

Human proximal tubular epithelial cells (HK2) were treated with transforming growth factor (TGF)-β1, a classic inducer of EMT, for 12, 24, 48, and 72 hrs. Then the expressions of EMT markers, including E-cadherin, vimentin, and α-smooth muscle actin (α-SMA) were assessed by western blot.

4.2.2 Optimising the administration of CDDP, PEM, GM, and AA-I in HK2 cells

HK2 cells were treated with CDDP, PEM, GM, AA-I, or their respective vehicles, at different concentrations. Then, cell viability was assessed by CCK-8 assay.

4.2.3. Investigating CDDP, PEM, GM, and AA-I-induced cell death in HK2 cells

First, HK2 cells were either treated with CDDP, PEM, GM, or AA-I, or in combination with either a necroptosis inhibitor (Nec-1) or an apoptosis inhibitor (Z-VAD-FMK) at 50μM for 48 hrs, followed by CCK-8 assay to examine the cell viability. In the next experiment, cells were treated CDDP, PEM, GM, AA-I, or dimethyl sulfoxide (DMSO). Cells were stained with phosphorylated-mixed lineage kinase domain-like protein (p-MLKL), a specific necroptosis marker, and examined by immunocytochemistry (ICC). The ratio of phosphorylated-receptor-interacting protein kinase (RIP) to RIP and p-MLKL to MLKL, as indicators of necroptosis, were assessed by western blot.

4.2.4 Investigating if CDDP, PEM, GM, and AA-I causes EMT development in HK2 cells

HK2 cells were either treated with CDDP, PEM, GM, or AA-I for 48 hrs. Cell morphology was evaluated by light microscopy. EMT markers, such as E-cadherin and α-SMA, were assessed by ICC and western blot.

4.2.5 Investigating the correlation between necroptosis and EMT

HK2 cells were either treated with CDDP, PEM, GM, or AA-I, or in combination with Nec-1. EMT markers, such as E-cadherin and α-SMA, were assessed by ICC and western blot.

4.2.6 Investigating the associated signalling pathways

First, HK2 cells were either treated with CDDP, PEM, GM, or AA-I, or in combination with either a receptor for advanced glycation end products (RAGE) antagonist (RAGE antagonist peptide, RAP) or a Toll-like receptor (TLR)-4 antagonist (C34) for 48 hrs, followed by examination of necroptosis and EMT markers by western blot.

4.3 Results

4.3.1 Investigations on the time course of EMT development in HK2 cells

EMT is critical in the pathogenesis of renal fibrosis, whereby renal tubular epithelial cells lose their phenotype and gain features of mesenchymal cells. Transforming growth factor (TGF)-β1 is a classic inducer of EMT. In this study, human recombinant TGF-β1 was used to treat HK2 cells to determine the time window of EMT development (**Figure 4.1**). E-cadherin, a cadherin protein maintaining cellular adhesion, is a marker of cells with an epithelial phenotype (231). Vimentin is a structural protein that is predominantly expressed in mesenchymal cells (232). Alpha-smooth muscle action (α-SMA) is a marker of myofibroblasts. Theoretically, in the

process of EMT, E-cadherin expression is decreased, with increased expressions of vimentin and α-SMA.

HK2 cells were treated with TGF-β1 (5ng/ml) for 12, 24, 48, and 72 hrs. Our data show that overall, E-cadherin and vimentin expressions did not change significantly in response to TGF-β1, despite a slight decrease at 12 hrs (E-cadherin, 12 hrs, 0.78 ± 0.05, $p=0.07$; vimentin, 12 hrs, 0.88 ± 0.10, $p=0.35$). The expression of α-SMA increased significantly at 48 (α-SMA, 48 hrs, 1.60 ± 0.18, $p < 0.001$) and 72 hrs (α-SMA, 72 hrs, 1.63 ± 0.09, $p < 0.001$) of treatment, indicating that the signs of EMT development may require 48 hrs to manifest themselves *in vitro*. Therefore, cells were harvested 48 hrs after treatment in the following experiments.

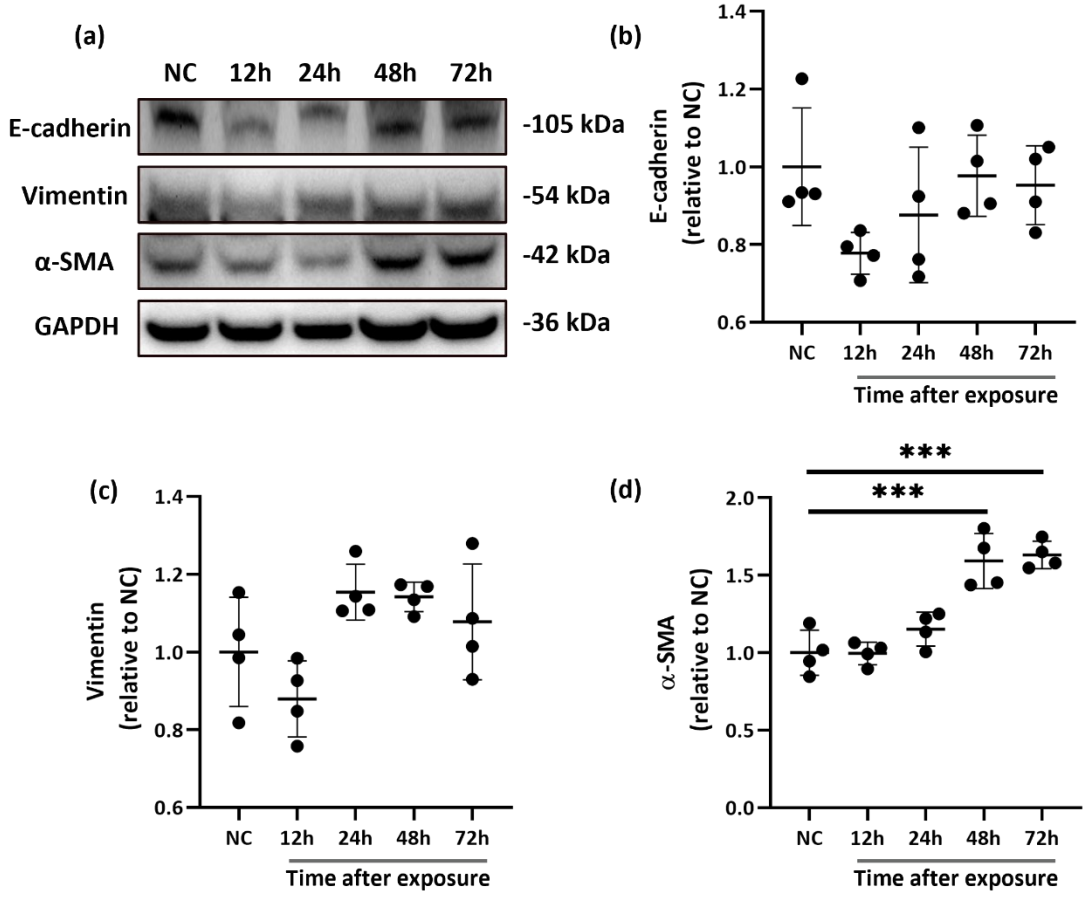

Figure 4. 1 Investigations on the time course of EMT development in HK2 cells

HK2 cells were treated with TGF-β1 (5ng/ml) for 12, 24, 48, and 72 hrs. (a) The representative blot of E-cadherin, vimentin, and α-SMA (n=4, each represent an independent experiment). (b-d) Quantitative analyses of α-SMA and E-cadherin. Data is presented as mean ± SD; * $p < 0.05$, ** $p < 0.01$ and *** $p < 0.001$.

NC: naïve control; α-SMA: α-smooth muscle actin; GAPDH: glyceraldehyde 3-phosphate dehydrogenase; HK2 cells: human kidney 2 cells; TGF-β1: transforming growth factor-1β.

4.3.2 Evaluation of the cytotoxicity of cisplatin, pemetrexed, gentamicin and aristolochic acid I on HK2 cells

CDDP, PEM, GM, and AA-I were dissolved in 0.9% NaCl, PBS (phosphate-buffered saline), distilled water, and DMSO (dimethyl sulfoxide), respectively. Their cytotoxicity was evaluated on HK2 cells by CCK-8 assay after 48 hrs of exposure (**Figure 4.2**). CDDP decreased cell viability significantly at 20 (CDDP, 20μM, 0.61 ± 0.11, $p < 0.01$) and 100μM (CDDP, 100μM, 0.46 ± 0.17, $p < 0.001$), while 3μM CDDP (CDDP, 3μM, 0.90 ± 0.20, $p = 0.75$) and 100μM 0.9% NaCl (NaCl, 1.14 ± 0.11, $p = 0.53$) did not affect cell viability with statistical significance. Similarly, PEM decreased cell viability at 20 (PEM, 20μM, 0.53 ± 0.10, $p < 0.01$) and 100μM (PEM, 100μM, 0.31 ± 0.11, $p < 0.001$), while 3μM PEM (PEM, 3μM, 1.00 ± 0.24, $p = 0.89$) and 100μM PBS (PBS, 1.06 ± 0.15, $p = 0.95$) did not affect cell viability significantly. GM decreased cell viability at 10 (GM, 10μM, 0.70 ± 0.08, $p < 0.05$), 20 (GM, 20μM, 0.52 ± 0.17, $p < 0.001$), and 100μM (GM, 100μM, 0.33 ± 0.10, $p < 0.001$). AA-I decreased cell viability at 1 (AA-I, 1μM, 0.66 ± 0.13, $p < 0.05$), 10 (AA-I, 10μM, 0.54 ± 0.17, $p < 0.001$), and 100μM (AA-I, 100μM, 0.38 ± 0.13, $p < 0.001$), while DMSO (DMSO, 0.94 ± 0.13, $p = 0.92$) did not have a significant effect. Cells therefore were treated with CDDP, PEM, GM, and AA-I at 20, 20, 10, 1μM in the following experiments, respectively.

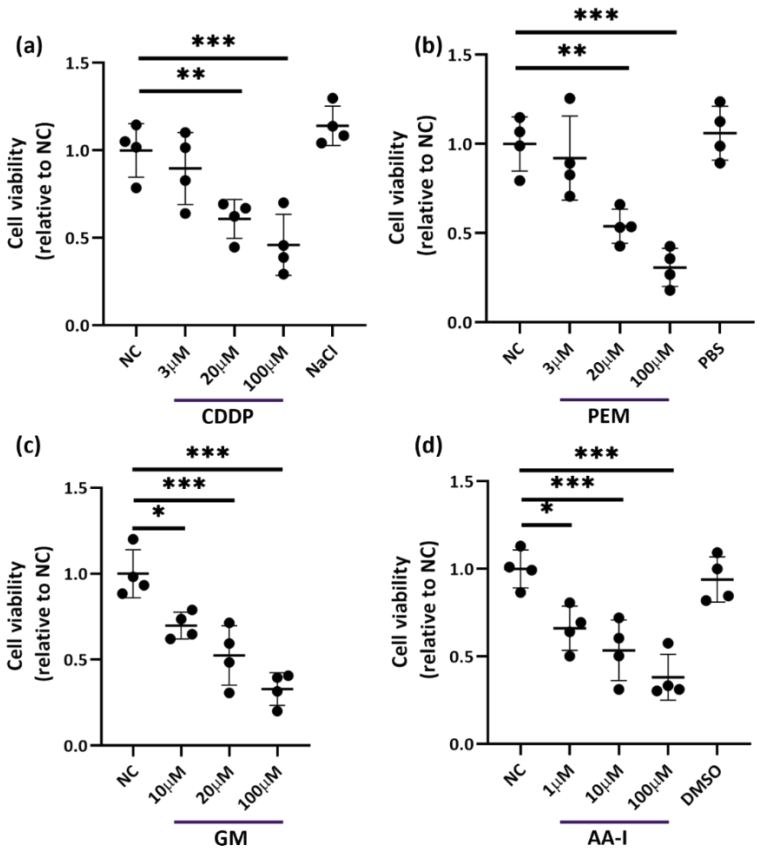

Figure 4. 2 Evaluation of the cytotoxicity of CDDP, PEM, GM, and AA-I on HK2 cells

HK2 cells were treated with CDDP, PEM, GM, and AA-I for 48 hrs at different concentrations. The cytotoxicity of CDDP (a), PEM (b), GM (c), and AA-I (d) were evaluated via CCK-8 assay. Data is presented as mean ± SD (n = 4, each represent an independent experiment); * $p < 0.05$, ** $p < 0.01$ and *** $p < 0.001$.

NC: naïve control; HK2 cells: human kidney 2 cells; CDDP: cisplatin; PEM: pemetrexed; GM: gentamicin; AA-I: aristolochic acid I; PBS: phosphate-buffered saline; DMSO (dimethyl sulfoxide); CCK-8 assay: cell counting-8 kit assay.

4.3.3 CDDP, PEM, and AA-I induced necroptosis in HK2 cells

Necroptosis inhibitor (Nec-1) and apoptosis inhibitor (Z-VAD-FMK) were applied in this study. Cells were either treated with CDDP, PEM, GM, AA-I or DMSO alone or in combination with either Nec-1 or Z-VAD-FMK for 48 hrs, followed by examinations by CCK-8 assay (**Figure 4.3a**). Results show that Nec-1 effectively alleviated CDDP, PEM and AA-I-induced cytotoxicity (CDDP *vs.* CDDP + Nec-1, 0.58 ± 0.09 *vs.* 0.79 ± 0.06, $p < 0.01$; PEM *vs.* PEM + Nec-1, 0.60 ± 0.14 *vs.* 0.84 ± 0.08, $p < 0.05$; AA-I *vs.* AA-1 + Nec-1, 0.50 ± 0.09 *vs.* 0.73 ± 0.08, $p < 0.05$), while Nec-1 did not significantly affect the cytotoxicity of GM and DMSO (GM *vs.* GM + Nec-1, 0.60 ± 0.11 *vs.* 0.64 ± 0.12, $p = 0.66$; DMSO *vs.* DMSO + Nec-1, 1.00 ± 0.15 *vs.* 1.02 ± 0.26, $p = 0.87$), indicating that CDDP, PEM, and AA-I exert their cytotoxicity via necroptosis. Z-VAD-FMK, on the other hand, significantly alleviated GM-induced cytotoxicity (GM *vs.* GM + Z-VAD-FMK, 0.60 ± 0.11 *vs.* 0.78 ± 0.06, $p < 0.05$), while it did not show significant cytotoxicity of CDDP, PEM, AA-I and DMSO, suggesting that GM decreased cell viability by inducing significant apoptosis. The presence of necroptosis was also demonstrated by ICC (**Figure 4.3b**). Phosphorylated-MLKL (p-MLKL) is the ultimate executioner of necroptosis. It was detected on the cell membrane and presented as a web-like feature (indicated by arrowheads). The percentage of p-MLKL increased significantly in CDDP, PEM, and AA-I group (NC *vs.* CDDP, 1.00 ± 0.18 *vs.* 2.60 ± 0.55, $p < 0.001$; NC *vs.* PEM, 1.00 ± 0.18 *vs.* 2.43 ± 0.10, $p < 0.001$; NC *vs.* AA-I, 1.00 ± 0.18 *vs.* 3.00 ± 0.07, $p < 0.001$). GM and DMSO failed to increase the percentage of p-MLKL in HK2 cells (NC *vs.* GM, 1.00 ± 0.18

vs. 1.30 ± 0.36, p = 0.77; NC *vs.* DMSO, 1.00 ± 0.18 *vs.* 1.34 ± 0.26, p = 0.67). This result was confirmed by western blot (**Figure 4.3d**). The ratios of phosphorylated-RIP (p-RIP) to RIP and p-MLKL to MLKL expressions were used as indicators of necroptosis. Compared to naïve controls, p-RIP/RIP and p-MLKL/MLKL significantly increased in response to CDDP (p-RIP/RIP, 2.14 ± 0.26, $p < 0.001$; p-MLKL/MLKL, 1.82 ± 0.25, $p < 0.01$), PEM (p-RIP/RIP, 2.00 ± 0.42, $p < 0.01$; p-MLKL/MLKL, 1.88 ± 0.23, $p < 0.01$), and AA-I (p-RIP/RIP, 1.99 ± 0.28, $p < 0.01$; p-MLKL/MLKL, 1.89 ± 0.28, $p < 0.01$), respectively. GM and DMSO did not have a significant effect on p-RIP/RIP (GM, 1.40 ± 0.38, p = 0.29; DMSO, 1.21 ± 0.23, p = 0.81) and p-MLKL/MLKL (GM, 1.18 ± 0.35, p = 0.81; DMSO, 1.14 ± 0.31, p = 0.93).

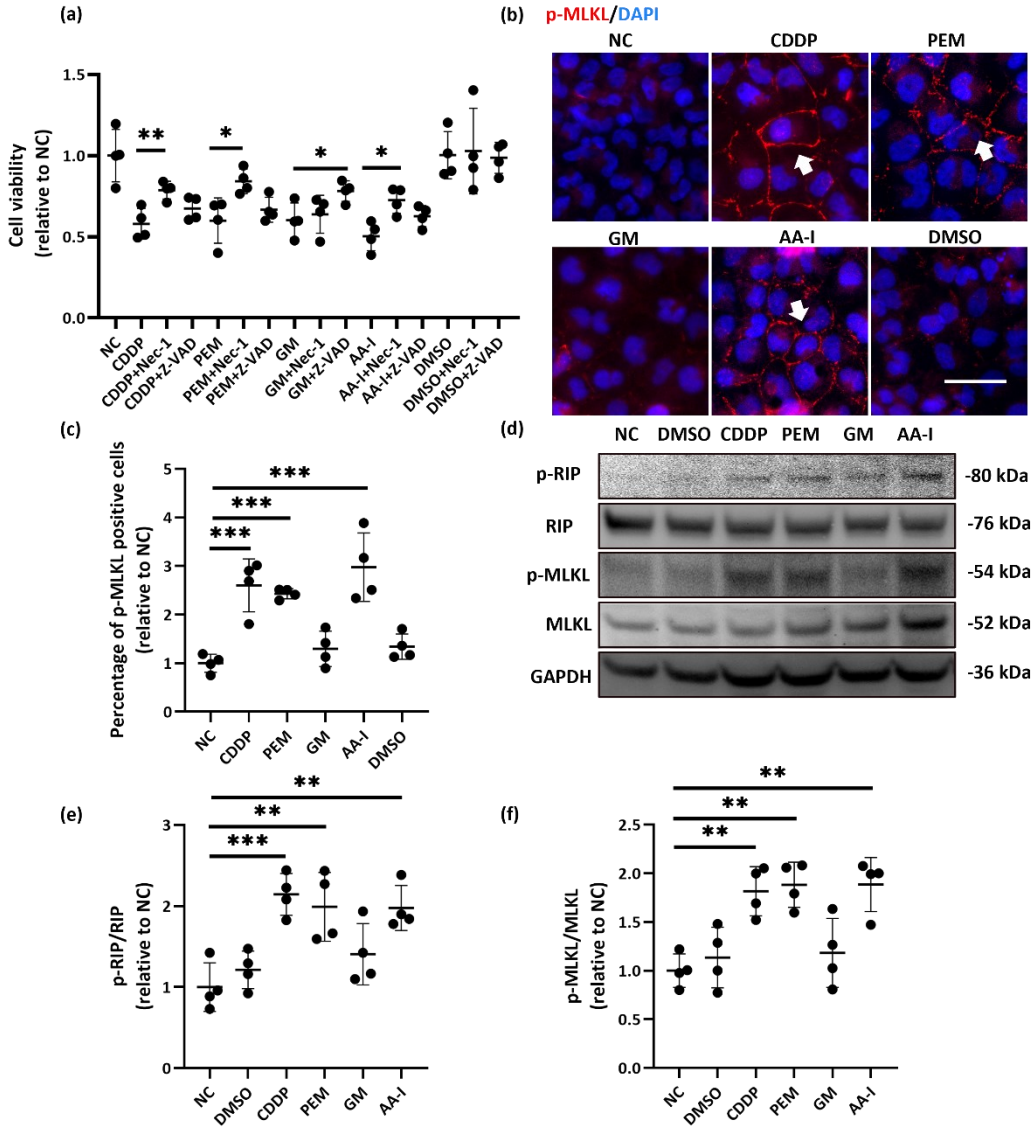

Figure 4. 3 CDDP, PEM, and AA-I induced necroptosis in HK2 cells

Cell death was demonstrated by CCK-8 assay, IF, and western blot. (a) Quantitative analysis of CCK8-assay results. (b) ICC of p-MLKL (red) in HK2 cells. Each dot represents an average value from four images of one sample. (c) Quantitative analysis of ICC results. (d) The representative western blot of p-RIP, RIP, p-MLKL, and MLKL (n=4, each represent an independent experiment). (e-f) Quantitative analysis of the expression of p-RIP/RIP and p-MLKL/MLKL, respectively. Data is presented as mean ± SD; * $p < 0.05$, ** $p < 0.01$ and *** $p < 0.001$. Scale bar = 50μm.

NC: naïve control; HK2 cells: human kidney 2 cells; CDDP: cisplatin; PEM: pemetrexed; GM: gentamicin; AA-I: aristolochic acid I; DMSO (dimethyl sulfoxide); CCK-8 assay: cell counting-8 kit assay; ICC: immunocytochemistry; RIP: receptor-interacting protein kinase; MLKL: mixed lineage kinase domain-like.

4.3.4 CDDP, PEM, and AA-I induced EMT in HK2 cells

Then we investigated if these nephrotoxic chemicals could induce EMT *in vitro.* HK2 cells were treated with CDDP, PEM, GM, and AA-I for 48 hrs. Cell morphology was assessed by light microscopy. In the naïve control group, cells were compact and adhesive with a rounded shape, while cells in the CDDP, PEM and AA-I groups transformed into an elongated, dispersed phenotype. In the GM group, no significant morphology change was observed, despite a noticeable decrease in cell density (**Figure 4.4a**). Then cells were double-stained with E-cadherin (green) and α-SMA (red) for ICC (**Figure 4.4b**) to examine EMT development. In theory, during EMT, the expression of E-cadherin decreased, with an increase in α-SMA expression. ICC results show that compared to naïve control, the level of E-cadherin did not markedly change (CDDP, 1.13 ± 0.16, $p = 0.88$; PEM, 1.10 ± 0.25, $p = 0.94$; GM, 1.10 ± 0.22, $p = 0.97$; AA-I, 1.11 ± 0.37, $p = 0.91$), while α-SMA expression significantly increased by the administration of CDDP (2.10 ± 0.35, $p < 0.01$), PEM (2.00 ± 0.29, $p < 0.01$), and AA-I (1.95 ± 0.48, $p < 0.01$) but not GM (1.29 ± 0.38, $p = 0.61$). EMT development was also evaluated by western blot (Figure 4.4e). Similarly, α-SMA expression significantly increased by CDDP (1.40 ± 0.16, $p < 0.05$), PEM (1.41 ± 0.19, $p < 0.05$), and AA-I (1.62 ± 0.27, $p < 0.001$) but not GM (1.12 ± 0.13, $p = 0.80$) and DMSO (0.89 ± 0.11, $p = 0.83$). The expressions of E-cadherin and vimentin had no significant differences.

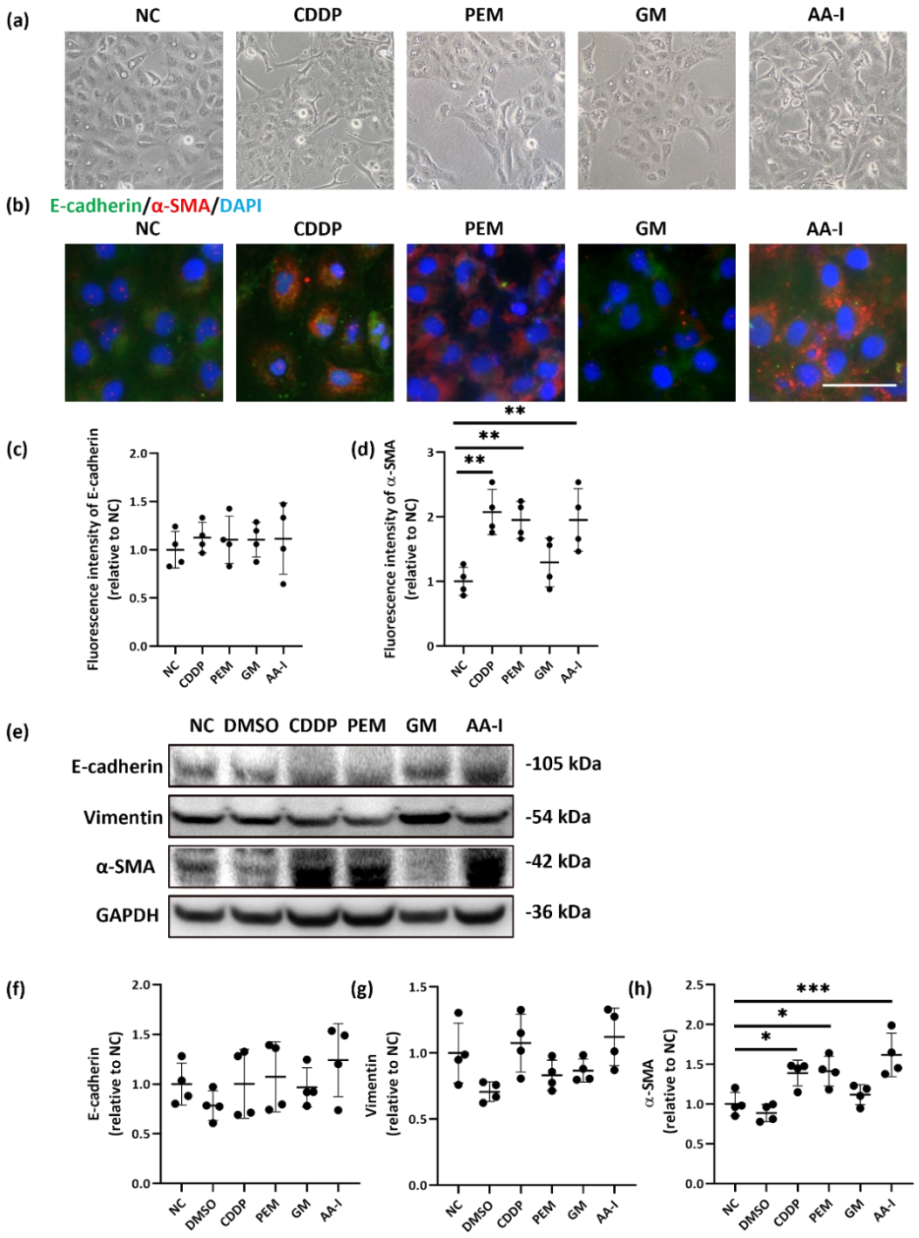

Figure 4. 4 CDDP, PEM, and AA-I induced EMT in HK2 cells

HK2 cells were treated with CDDP, PEM, GM, and AA-I for 48 hrs. (a) Cell morphology by light microscopy. (b) ICC of E-cadherin and α-SMA. (c-d) Quantitative analysis of ICC results (n=4, each represent an independent experiment). (e) The representative western blot of E-cadherin, vimentin and α-SMA (n=4, each represent an independent experiment). (f-h) Quantitative analysis of western blot. Data is presented as mean ± SD; * $p < 0.05$, ** $p < 0.01$ and *** $p < 0.001$. Scale bar = 50µm.

NC: naïve control; HK2 cells: human kidney 2 cells; CDDP: cisplatin; PEM: pemetrexed; GM: gentamicin; AA-I: aristolochic acid I; DMSO (dimethyl sulfoxide); ICC: immunocytochemistry; α-SMA: α-smooth muscle actin.

4.3.5 Inhibiting necroptosis by Nec-1 suppressed nephrotoxicity-induced EMT

Cells were either treated with CDDP, PEM or AAI alone, or in combination with Nec-1, respectively. ICC results suggest that Nec-1 effectively inhibited necroptosis, and inhibiting necroptosis by Nec-1 decreased α-SMA levels in response to CDDP, PEM, or AAI (**Figure 4.5a**). Western blot confirmed ICC results, as the expression of p-MLKL decreased significantly in Nec-1 treated group (CDDP *vs.* CDDP + Nec-1, 1.50 ± 0.12 *vs.* 1.12 ± 0.08, $p < 0.05$; PEM *vs.* PEM + Nec-1, 1.39 ± 0.19 *vs.* 1.03 ± 0.15, $p < 0.05$; AA-I *vs.* AA-I + Nec-1, 1.60 ± 0.18 *vs.* 1.09 ± 0.20, $p < 0.01$), along with a decrease in α-SMA expression (CDDP *vs.* CDDP + Nec-1, 1.28 ± 0.13 *vs.* 0.94 ± 0.11, $p < 0.05$; PEM *vs.* PEM + Nec-1, 1.29 ± 0.23 *vs.* 1.05 ± 0.07, $p < 0.05$; AA-I *vs.* AA-I + Nec-1, 1.53 ± 0.15 *vs.* 0.97 ± 0.16, $p < 0.01$) (**Figure 4.5b**).

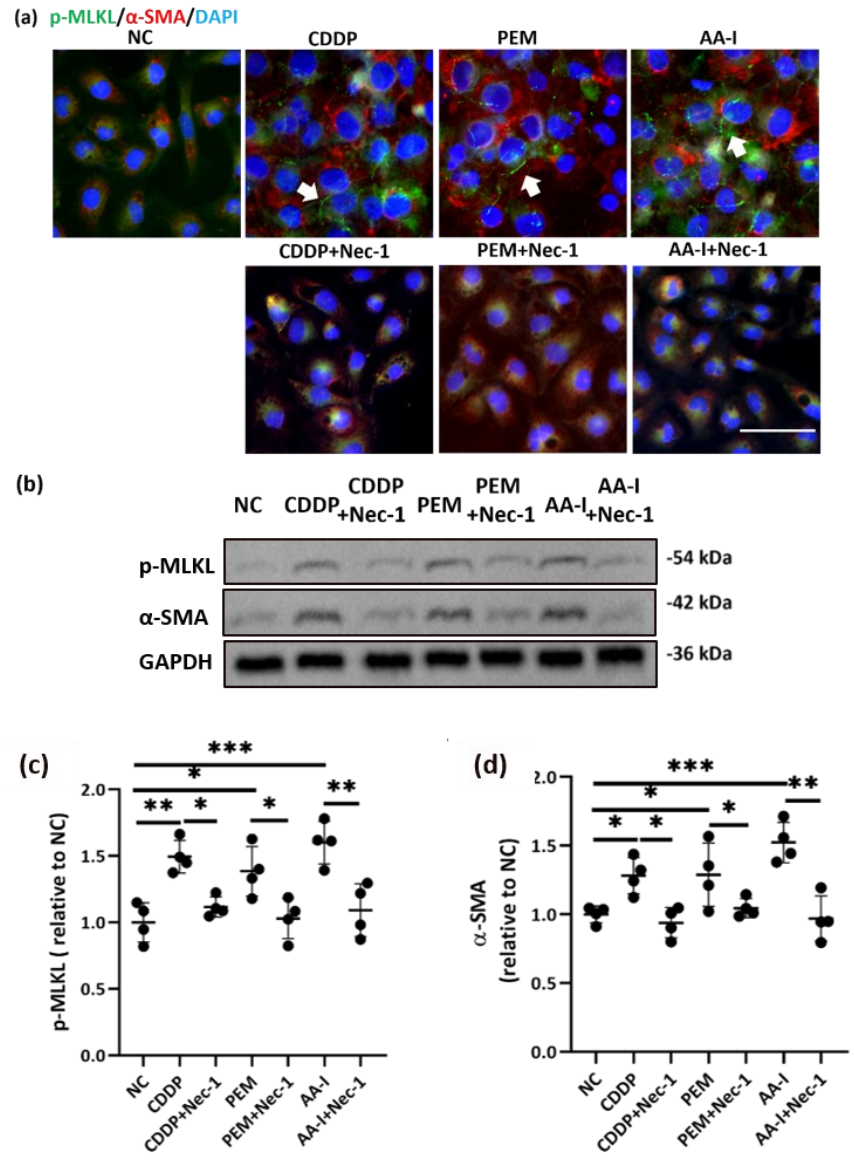

Figure 4. 5 CDDP, PEM, and AA-I induced EMT in HK2 cells

HK2 cells were treated with CDDP, PEM or AAI alone, or in combination with Nec-1, respectively. (a) ICC of p-MLKL and α-SMA (representative images, n=4, each represent an independent experiment). (b) The representative western blot of E-cadherin, p-MLKL, and α-SMA (n=4, each represent an independent experiment). (c-e) Quantitative analysis of western blot. Data is presented as mean ± SD; * $p < 0.05$, ** $p < 0.01$ and *** $p < 0.001$. Scale bar = 50μm.

NC: naïve control; HK2 cells: human kidney 2 cells; CDDP: cisplatin; PEM: pemetrexed; AA-I: aristolochic acid I; ICC: immunocytochemistry; MLKL: mixed lineage kinase domain-like; α-SMA: α-smooth muscle actin.

4.3.6 TLR-4, but not RAGE, was involved in CDDP, PEM, and AA-I-induced EMT

Receptor for Advanced Glycation End Products (RAGE) and Toll-like receptor-4 (TLR-4) are two receptors associated with necroptosis, DAMPs, and EMT (233-238). RAGE antagonist peptide (RAP) and a TLR4 inhibitor, C34, were applied to evaluate the involvement of RAGE and TLR-4 in CDDP, PEM, and AA-I-induced nephrotoxicity. HK2 cells were either treated with CDDP, PEM or AAI alone, or in combination either with RAGE or C34, respectively. Results show that RAP did not significantly change the ratio of p-MLKL to MLKL and α-SMA expression, while compared with administrating CDDP, PEM, and AA-I alone, co-administration with C34 significantly decreased p-MLKL/MLKL (CDDP *vs.* CDDP + Nec-1, 1.27 ± 0.11 *vs.* 1.04 ± 0.08, $p < 0.01$; PEM *vs.* PEM + Nec-1, 1.27 ± 0.09 *vs.* 1.05 ± 0.05, $p < 0.05$; AA-I *vs.* AA-I + Nec-1, 1.24 ± 0.11 *vs.* 1.02 ± 0.04, $p < 0.05$) and α-SMA expression (CDDP *vs.* CDDP + Nec-1, 1.19 ± 0.08 *vs.* 1.00 ± 0.10, $p < 0.05$; PEM *vs.* PEM + Nec-1, 1.23 ± 0.05 *vs.* 0.98 ± 0.08, $p < 0.05$; AA-I *vs.* AA-I + Nec-1, 1.31 ± 0.07 *vs.* 1.07 ± 0.14, $p < 0.05$), respectively.

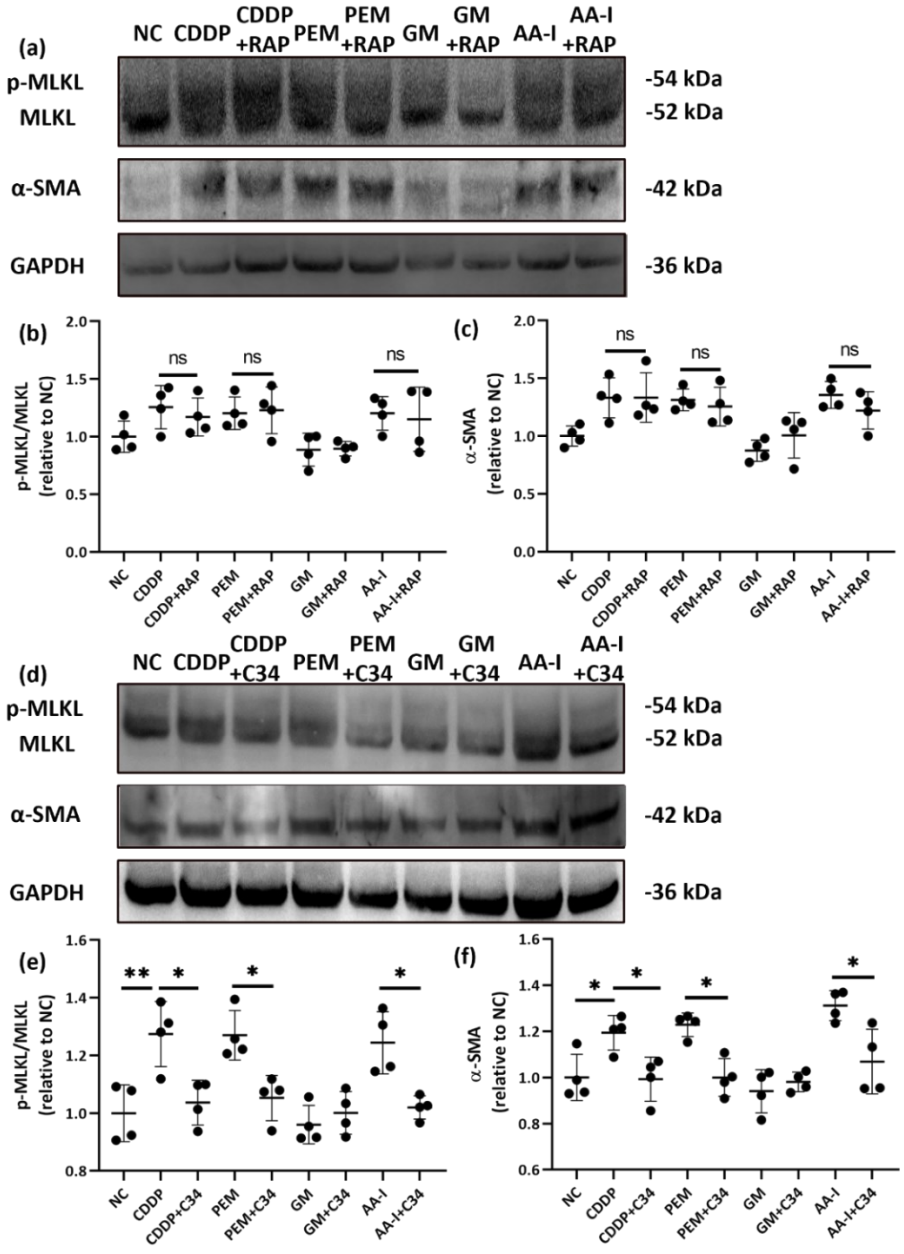

Figure 4. 6 TLR-4, but not RAGE, was involved in CDDP, PEM, and AA-I-induced EMT

HK2 cells were treated with CDDP, PEM or AAI alone, or in combination either with RAP or C34, respectively. (a and d) The representative western blot of p-MLKL, MLKL, and α-SMA (n=4, each represent an independent experiment). (b, c, e, and f) Quantitative analysis of western blot. Data is presented as mean ± SD; * $p < 0.05$ and ** $p < 0.01$.

NC: naïve control; HK2 cells: human kidney 2 cells; CDDP: cisplatin; PEM: pemetrexed; AA-I: aristolochic acid I; MLKL: mixed lineage kinase domain-like; α-SMA: α-smooth muscle actin.

4.4 Discussion

This chapter focuses on nephrotoxicity-induced tubular cell death and potential EMT development. Our data show EMT development, induced by TGF-β1, required 48 hrs in HK2 cells. CDDP, PEM, GM, and AA-I have cytotoxicity and decreased cell viability in a dose-dependent manner. In HK2 cells, CDDP, PEM, and AA-I caused significant necroptosis, while GM induced apoptosis-dominant cell death. CDDP, PEM, and AA-I increased α-SMA expression, which was attenuated by Nec-1. The RAGE antagonist, RAP, did not show any significant effects on p-MLKL/MLKL and α-SMA expressions, while C34, a TLR-4 antagonist, reversed the increase of p-MLKL/MLKL and α-SMA in response to CDDP, PEM, and AA-I. Our results suggest necroptosis, a highly pro-inflammatory form of cell death, contributes to EMT development, and TLR-4 is involved in CDDP, PEM, and AA-I-caused necroptosis and subsequent EMT.

Cell death has a critical role in nephrotoxic AKI and its associated CKD. It not only directly causes loss of the function of the affected cells but also leads to immune responses, inflammation, vascular dysfunction, and senescence, serving as a central hub in the pathogenesis of nephrotoxicity. Our findings demonstrate that in HK2 cells, CDDP, PEM, and AA-I induced significant necroptosis, whereas GM led to apoptosis as the dominant form of cell death. In fact, multiple types of cell death have been reported to be associated with these chemical's nephrotoxicity, as nephrotoxicity generally involves various complicated and overlapping mechanisms, including DNA

damage, mitochondrial pathology, oxidative stress, endoplasmic reticulum (ER) stress, and subsequent cell death and inflammation (67, 207, 218, 222, 239).

Apoptosis, a controlled form of cell death characterised by fragmentation, apoptotic bodies, and rapid phagocytosis by phagocytes, has an active role in CDDP, GM, and AA-I-induced nephrotoxicity, evidenced by the facts that pharmacological or genetically inhibiting apoptosis alleviated CDDP, GM and AA-I-induced nephrotoxicity in *vivo* and *in vitro* (217, 226, 240-244). Apoptosis can be induced by intrinsic, extrinsic and ER stress-related pathways. Intrinsically, CDDP, GM, and AA-I can trigger the tumour suppressor protein P53 (TP53), which leads to the transcriptional activation of Bcl-2-associated X protein (BAX) (245-249). Following activation, BAX is transported to the mitochondria and merges with BCL2 Antagonist/Killer 1 (BAK1) on the outer membrane. This interaction leads to the mitochondrial outer membrane permeabilisation (MOMP) and subsequent release of pro-apoptotic factors, such as cytochrome c, into the cytoplasm (247), resulting in the formation of apoptosomes which activates caspase 9, 3, and 7 and eventually apoptosis (250). Also, exposure to CDDP increased the expression of pro-apoptotic cytokines, such as tumour necrosis factor (TNF), leading to extrinsic apoptosis (251-253). ER stress can cause apoptosis in addition to intrinsic and extrinsic pathways. In response to severe ER stress, the C/EBP Homologous Protein (CHOP) is triggered, leading to BAX/BAK1 oligomerisation, MOMP, and apoptosis (254). It has been shown that pharmacologically inhibiting ER stress

decreased CDDP-induced apoptosis (243, 255-257). However, the involvement of apoptosis in PEM's nephrotoxicity is questionable due to limited research data that needs further studies.

Regulated necrosis, including necroptosis, ferroptosis, and pyroptosis, is a controlled cell death characterised by cell membrane disruption and release of danger-associated molecular patterns (DAMPs). Recently, it has been recognised that regulated necrosis also contributes to CDDP and GM-induced nephrotoxicity. Necroptosis, a RIP1-RIP3-MLKL-dependent regulated necrosis, is associated with various infectious and non-infectious kidney diseases (179). It was found that either genetic or pharmacological inhibition of necroptosis attenuated CDDP and GM-induced AKI (258-260), confirming the vital role of necroptosis in CDDP and GM-induced nephrotoxicity. In general, necroptosis can be caused intrinsically via ROS production (261) and DNA damage (262) or extrinsically via TNF superfamily receptors, TLRs, and interferon receptors (263). Applying TNF-α and deleting the TLR-4 gene showed protective effects against CDDP-induced AKI (264). However, the underlying signalling pathways, especially the intrinsic necroptosis in CDDP-induced AKI, remain unclear and require investigation in the future. To our knowledge, it is the first time to demonstrate that PEM and AA-I induce necroptosis in cultured proximal tubular epithelial cells, and Nec-1 effectively reverse PEM and AA-I's cytotoxicity. Our findings indicate that preventing necroptosis could be

a therapeutic strategy against PEM and AA-I-associated kidney injury, which is worth to be examined in animal studies.

Epithelial-mesenchymal transition (EMT) is a process in which epithelial cells lose their polarity and acquire mesenchymal characteristics such as increased migration, invasiveness, and resistance to apoptosis (141). EMT engages in various physiological and pathological processes, including tissue repair, cancer, and fibrosis (265). In the kidney, EMT allows epithelial cells to transform into fibroblasts, which are necessary for tissue repair. However, increased EMT during renal fibrosis is unfavourable because it can result in the overproduction of fibrotic scars, causing decreased renal function (143). We observed EMT development in response to CDDP, PEM, and AA-I, along with significant necroptosis. GM caused significant apoptosis and did not induce EMT in HK2 cells. In addition, inhibiting necroptosis by Nec-1 effectively suppressed EMT development. Collective findings suggest that necroptosis, rather than apoptosis, contributes to the progression of EMT and, potentially, AKI to CKD transition. Current literature demonstrated that inhibiting necroptosis can reduce EMT in various fibrosis models (266). For example, by comparing young and old mice livers, S. Mohammed et al. found an increased level of necroptosis marker in the livers of old mice, and short-term administration of Nec-1 decreased necroptosis, cell senescence, as well as fibrosis markers in the livers of aged mice (267). The mechanisms by which inhibiting necroptosis reduces EMT are not fully understood, but several theories have been

proposed. One theory is that necroptosis contributes to EMT by releasing DAMPs that trigger inflammation and oxidative stress, which in turn promote the EMT process (268). Inhibiting necroptosis can reduce the release of DAMPs and prevent the activation of pro-inflammatory signalling pathways, thereby reducing EMT. It has been well-documented that necroptotic cell death results in the massive release of DAMPs (269). However, the mechanisms of DAMPs-induced EMT remains partially understood and will be investigated in the next chapter.

TLR-4 is a member of the group of receptors known as pattern recognition receptors (PRRs). These receptors are widely conserved and are capable of identifying exogenous pathogens (pathogen-associated molecular patterns, PAMPs), making them the first line of defence against infection (270). Besides, these receptors are responsible for recognising endogenous molecules DAMPs, mediating a wide range of pro-inflammatory responses (271). Similar to TNFR, TLR-4 can initiate necroptosis signalling pathways (234, 272). By interacting with its corresponding ligands, TLR-4 recruits Toll-interleukin 1 receptor domain (TIR)-containing adaptor molecule (*TICAM*)-1 which activates TIR-domain-containing adapter-inducing interferon-β (TRIF) (273). Activated TRIF can stimulate RIP3 oligomerisation and phosphorylation, leading to phosphorylation of MLKL and subsequent membrane disruption (274, 275). TLR-4 is also associated with EMT and fibrosis in various *in vitro* models. For example, it was found that TLR4 signalling is required for lipopolysaccharide (LPS)-induced EMT in

human hepatocellular carcinoma cells (276). Our data demonstrate for the first time that the TLR-4 signalling is necessary for CDDP, PEM, and AA-I-induced necroptosis and EMT, indicating that TLR-4 signalling pathways can be therapeutic targets for their nephrotoxicity.

In conclusion, the results of this part of study provide valuable insights into the mechanisms of cell death in response to different drugs/chemicals and their potential impacts on epithelial- EMT development. The findings suggest that CDDP, PEM, and AA-I have cytotoxicity and decreased cell viability in a dose-dependent manner in HK2 cells, inducing significant necroptosis, while GM induced apoptosis-dominant cell death. The increased expression of α-SMA in response to CDDP, PEM, and AA-I was attenuated by the necroptosis inhibitor Nec-1, providing evidence for the role of necroptosis in EMT development. The results also suggest that TLR-4 is involved in CDDP, PEM, and AA-I-caused necroptosis and subsequent EMT, as the TLR-4 antagonist C34 reversed the increase of p-MLKL/MLKL and α-SMA expressions. These findings provide insights into the mechanisms of AKI to CKD progression. However, it is important to note that these results are based on in vitro experiments, and further research is needed to confirm these findings in vivo and to fully understand the underlying mechanisms and the translational value.

Chapter Five

Exploring the Interplay among Necroptosis, DAMPs, and EMT during Ischemia-Reperfusion Injury

5.1 Introduction

Ischemia-reperfusion injury (IRI) is a condition where blood flow to a particular area is temporarily cut off and then restored. The kidneys are particularly vulnerable to this injury, which can occur due to a range of medical conditions such as organ transplantation, trauma, heart attacks, and sepsis (277) . IRI is a frequent trigger AKI and has been linked to its progression into CKD (278-281). However, the mechanisms behind the progression from AKI to CKD are still not fully understood and an effective treatment for this progression is yet to be found.

Necroptosis is a controlled form of cell death that shares similar characteristics to necrosis but is regulated at the molecular level (282). Necroptosis can be triggered by various factors, such as death receptors, toll-like receptors (TLRs), interferons, and DNA-dependent activator of interferon regulatory factors in response to viruses and is executed by receptor-interacting protein kinase 3 (RIP3) and the mixed lineage kinase domain-like protein (MLKL) (162, 283). Recent studies have shown that necroptosis plays a significant role in IRI-induced AKI, as demonstrated by the protective effects of blocking necroptosis through pharmacological inhibitors or genetic deletion (171, 284, 285). Additionally, the role of necroptosis in chronic inflammation has been recognized (267, 286-288), making it reasonable to investigate the involvement of necroptosis and its associated necroinflammation in the progression from AKI to CKD.

DAMPs (danger-associated molecular patterns) are a group of endogenous molecules that function in preserving cell homeostasis (289). They are also recognised as danger signals when released into the extracellular space, mediating a series of cellular responses to eliminate pathogens and activate repair mechanisms (289, 290). In some cases, however, DAMPs can contribute to unfavourable outcomes, including CKD (156, 289, 291). Despite the recent advancements in understanding the role of DAMPs in various kidney disease models, few specific and effective therapies exist. Studying the effects of extracellular DAMPs has the potential to unveil new therapeutic targets for AKI and potential CKD.

This chapter examined effects of two representative DAMPs, histones and high-mobility group box-1 (HMGB-1), on cultured human tubular epithelial cells. Histones are nuclear proteins that are vital for chromosome structure. They form hetero-octamers that wrap around double-stranded DNA into chromatin (292). They have been reported to worsen AKI by their direct toxicity on renal cells and their pro-inflammatory actions (161). In addition, it has been demonstrated that the extracellular histone H4 contributes to chronic vascular inflammation (293). HMGB-1, on the other hand, is a protein that binds to DNA to stabilise chromosomes and involves transcription processes (294). It has been shown that extracellular HMGB-1 is a major pro-inflammatory mediator in several conditions, including IRI (295). In addition, the level of plasma HMGB-1 have been associated with renal function and

inflammatory biomarkers in CKD (296). These findings suggest that histones and HMGB-1 may play critical roles in the progression of renal fibrosis and subsequent CKD.

In this chapter, the role of necroptosis in the development of epithelial-mesenchymal transition (EMT) and fibrosis in the context of IRI was evaluated. The pro-fibrotic effects of histones and HMGB-1, as well as their underlying molecular mechanisms, were also examined in cultured tubular epithelial cells.

5.2 Experimental design

5.2.1 Investigating if IRI by renal pedicle clamping induce necroptosis and fibrosis, and if inhibiting necroptosis has anti-fibrotic effects

Mice were randomly assigned in untreated group (NC), sham surgery group (SH), IRI group (IRI), and necrostatin-1 treated IRI group (IRI + Nec-1) (n=3/group). The IRI and IRI + Nec-1 groups underwent bilateral renal pedicle clamping for 30 minutes. In the IRI + Nec-1 group, mice received Nec-1 intraperitoneally at 15 minutes before the onset of ischemia. The kidneys were collected 24 hours later for analysis of and α-SMA expression using immunohistochemistry (IHC) and western blot.

5.2.2 Investigating if oxygen-glucose deprivation (OGD) induces necroptosis in cultured tubular epithelial cells

OGD was used to mimic ischaemic injury *in vitro*. In brief, HK2 cells were incubated with pre-warmed OGD medium bubbled with 95% N_2 and 5% CO_2 and moved into a chamber flushed with the same gas combination. The chamber was then quickly

sealed and transferred into an incubator at 37 °C for 1 hour. After that, cells received 2 hrs reperfusion under normal growth conditions, followed by assessed of necroptosis markers via immunocytochemistry (ICC) and western blot.

5.2.3 Investigating if OGD induces EMT development in HK2 cells, and if inhibiting necroptosis reduces this EMT

After confirming OGD can induce necroptosis, we tested if OGD can cause EMT in HK2 cells. Cells received 48 hrs of recovery to allow EMT development (OGDR). For the OGDR+Nec-1 group, Nec-1 was added 30 min prior to the OGD treatment. After 48 hrs recovery, cells were collected for analysis of necroptosis markers and α-SMA expression using ICC and western blot.

5.2.4 Investigating of cellular content released from necroptotic cells induces EMT

Our hypothesis was that DAMPs released from necroptotic cells caused by OGD can lead to EMT. To eliminate the impact of IRI, we treated cells with OGD-conditioned medium. After OGD, the OGD-conditioned medium was collected, and the cells were treated with it, with (OGDM+Nec-1) or without Nec-1 (OGDM), for 48 hrs. ICC and western blot were used to examine necroptosis and EMT.

5.2.5 Investigating if histones and HMGB-1 induce EMT in HK2 cells

Cells were treated with total histones or HMGB-1 at different concentrations, followed by examination of EMT via ICC and western blot.

5.2.6 Investigating the molecular mechanisms of HMGB-1-induced EMT

To assess if receptor for advanced glycation end products (RAGE), Toll-like receptor-4 (TLR-4), and c-Jun N-terminal Kinase (JNK) signalling are involved in HMGB-1-indcued EMT development, HK2 cells were treated with HMGB-1 alone or in combination with either RAGE antagonist peptide (RAP), a TLR-4 inhibitor C34, or a JNK inhibitor SP-600125, respectively. Then EMT markers were examined by western blot.

5.3 Results

5.3.1 Nec-1 suppressed fibroblast activation during IRI in mice

IHC results show that IRI caused tubular oedema, vacuolisation, and immune infiltration, along with increased α-SMA fluorescence, which was attenuated by the administration of Nec-1 (**Figure 5.1a**). Western blots (**Figure 5.1b-d**) revealed that the IRI group had a significant increase in p-MLKL (1.52 ± 0.12, $p < 0.01$) and α-SMA (1.40 ± 0.14, $p < 0.05$) compared to the naïve controls (untreated, NC). Compared to the IRI group, IRI with Nec-1 had reduced p-MLKL (1.19 ± 0.13, $p < 0.05$) and α-SMA expressions (1.09 ± 0.12, $p < 0.05$). The results show that IRI triggered necroptosis and activation of fibroblasts, and that the inhibition of necroptosis diminished fibroblast activation *in vivo*.

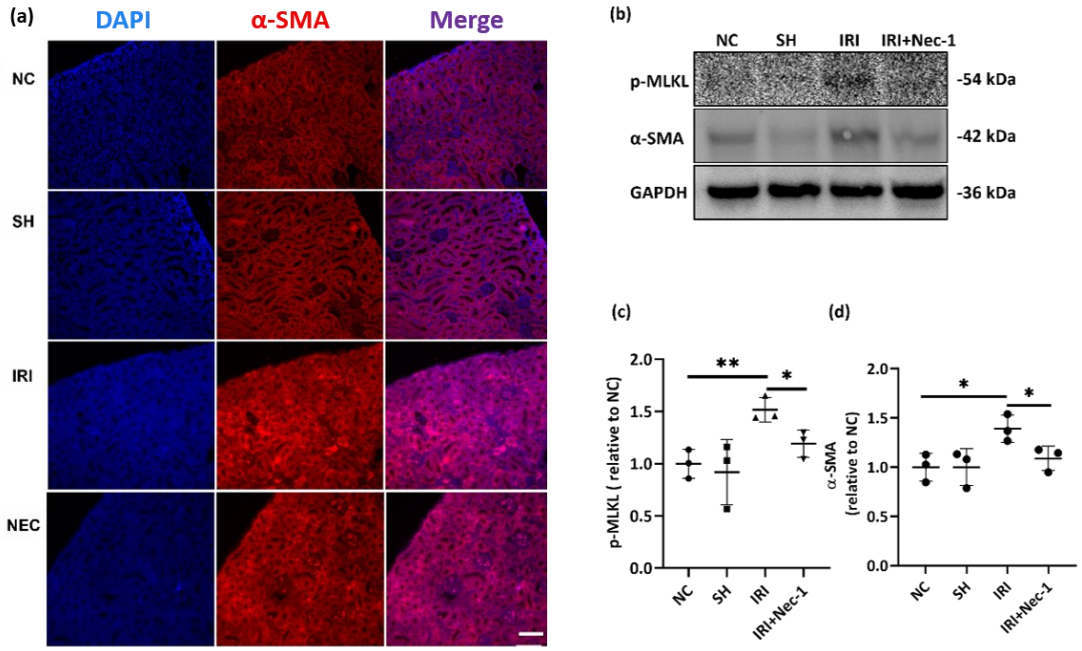

Figure 5. 1 Nec-1 suppressed fibroblast activation during IRI in mice

Mice were randomly assigned in the naïve control group (NC), sham surgery group (SH), IRI group (IRI), and necrostatin-1 treated IRI group (IRI + Nec-1). The IRI and IRI + Nec-1 groups underwent bilateral renal pedicle clamping for 30 minutes. In the IRI + Nec-1 group, mice received Nec-1 intraperitoneally at 15 minutes before the onset of ischemia. The kidneys were collected 24 hours later for analysis of P-MLKL and α-SMA expression using IHC and western blot. (a) The representative images of immunofluorescence of α-SMA (n=3, each represent an independent animal). (b) The representative western blot of p-MLKL and α-SMA (n=3, each represent an independent animal). (c-d) Quantitative analysis of western blot results. Data is presented as mean ± SD; * $p < 0.05$ and ** $p < 0.01$. Scale bar = 200μm.

NC: naïve control; SH: sham surgery control; IRI: ischaemic-reperfusion injury; Nec-1: necrostatin-1; IHC: immunohistochemistry; α-SMA: α-smooth muscle actin; p-MLKL: phosphorylated mixed lineage kinase domain-like.

5.3.2 OGD treatment induced necroptosis in HK2 cells

ICC results show that OGD induced necroptosis in HK2 cells, as seen by the appearance of web-like fluorescent dots on cell membranes (**Figure 5.2a**, indicated by arrowheads). The quantitative analysis showed that OGD significantly increased the proportion of cells positive for p-MLKL (2.29 ± 0.16, $p < 0.01$). The results from western blot were consistent with the ICC results, showing a significant increase in the expressions of p-RIP (1.69 ± 0.05, $p < 0.01$) and p-MLKL (2.18 ± 0.14, $p < 0.001$) (**Figure 5.2b**).

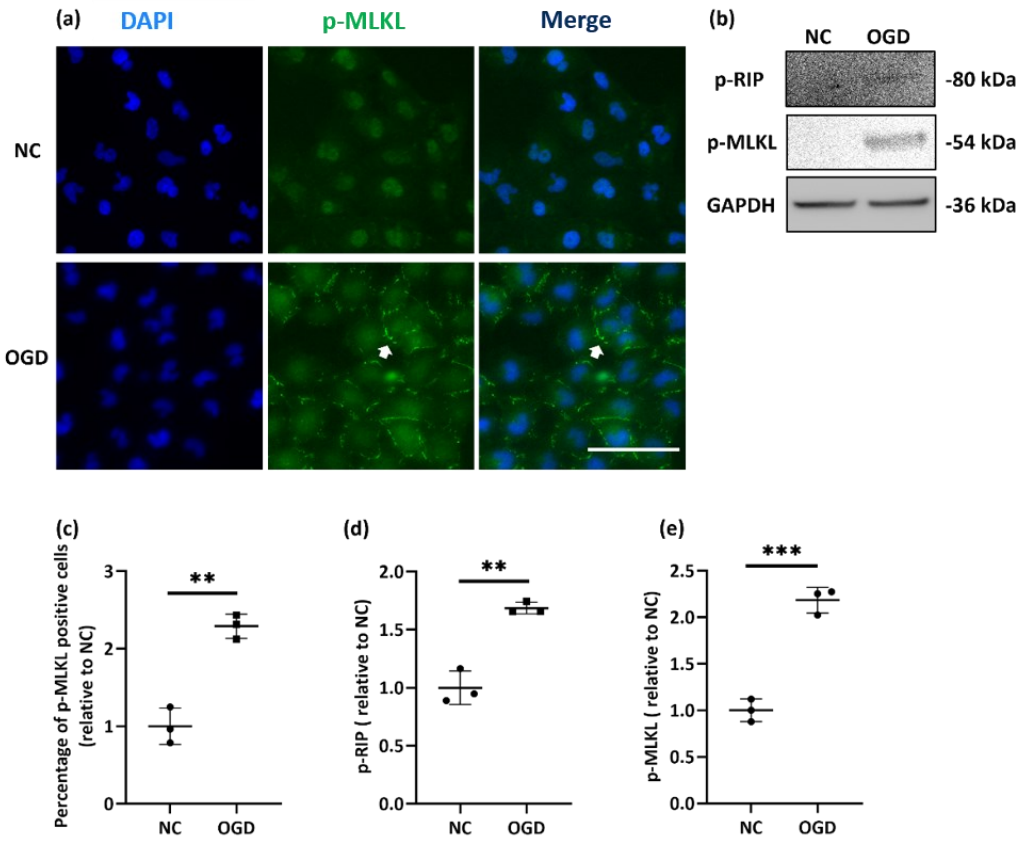

Figure 5. 2 OGD treatment induced necroptosis in HK2 cells

HK2 cells were treated with OGD or NC. (a) The representative ICC of p-MLKL (n=3, each represent an independent experiment). (b) The representative western blot of p-RIP and p-MLKL (n=3, each represent an independent experiment). (c) Quantitative analysis of ICC results (d-e) Quantitative analysis of western blot results. Data is presented as mean ± SD; ** $p < 0.01$ and *** $p < 0.001$. Scale bar = 50µm.

NC: naïve control; OGD: oxygen-glucose deprivation; ICC: immunocytochemistry; p-RIP: phosphorylated receptor-interacting protein kinase; p-MLKL: phosphorylated mixed lineage kinase domain-like.

5.3.3 OGD followed by 48 hrs of recovery induced EMT development in HK2 cells, which was attenuated by Nec-1

After confirming OGD can induce necroptosis, we tested if OGD can cause EMT in HK2 cells. Cells received 48 hrs of recovery after OGD (the OGDR group) to allow EMT development. For the OGDR+Nec-1 group, Nec-1 was added 30 min prior to the OGD treatment. The study found that OGDR caused EMT in HK2 cells, as evidenced by increased intensity of α-SMA in ICC results (1.48 ± 0.14, $p < 0.05$, **Figure 5.3a**) and increased expression of α-SMA in western blot results (1.43 ± 0.06, $p < 0.05$, **Figure 5.3d**). Nec-1 reduced this increase in α-SMA (1.17 ± 0.13 and 1.17 ± 0.08 in ICC and western blot, respectively). Different from the OGD treatment, OGDR had no significant effect on p-MLKL positive cells or p-RIP and p-MLKL expression, which may be because the necroptotic cells caused by OGD had died and were lost during the experiment.

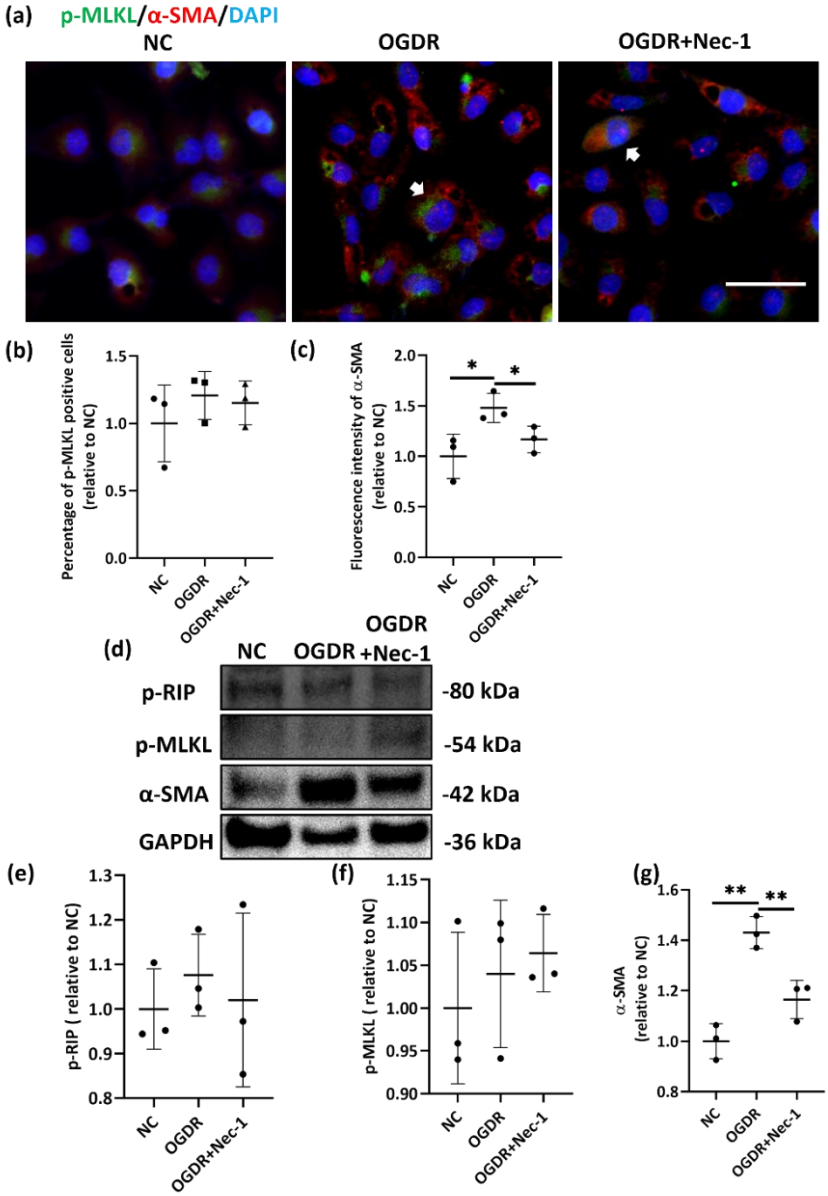

Figure 5. 3 OGDR induced EMT in HK2 cells

HK2 cells were either treated with OGD followed by 48 hrs of recovery (OGDR), OGDR with Nec-1 (OGDR+Nec-1), or naïve control (NC). (a) The representative ICC of p-MLKL and α-SMA (n=3, each represent an independent experiment). (b-c) Quantitative analysis of ICC results. (d) The representative western blot of p-RIP, p-MLKL, and α-SMA (n=3, each represent an independent experiment). (e-g) Quantitative analysis of western blot results. Data is presented as mean ± SD; * $p < 0.05$ and ** $p < 0.01$. Scale bar = 50µm.

NC: naïve control; OGD: oxygen-glucose deprivation; ICC: immunocytochemistry; p-RIP: phosphorylated receptor-interacting protein kinase; p-MLKL: phosphorylated mixed lineage kinase domain-like; α-SMA: α-smooth muscle actin.

5.3.4 OGD-conditioned medium induced EMT, and this was reduced by Nec-1

Our hypothesis was that DAMPs released from necroptotic cells caused by OGD can lead to EMT. To eliminate the impact of IRI, we treated cells with OGD-conditioned medium. After OGD, the OGD-conditioned medium was collected, and the cells were treated with it, with (OGDM+Nec-1) or without Nec-1 (OGDM), for 48 hrs. Results showed that OGDM caused EMT in HK2 cells, as seen by increased intensity of α-SMA in ICC (1.34 ± 0.07, $p < 0.01$, **Figure 5.4a**) and increased expression of α-SMA in western blot (4.07 ± 0.84, $p < 0.01$, **Figure 5.4b**). Nec-1 reduced this increase in α-SMA (1.12 ± 0.08 in ICC and 2.34 ± 0.35 in WB). Our results indicate that the cytoplasmic content released from necroptotic cells can cause EMT in HK2 cells.

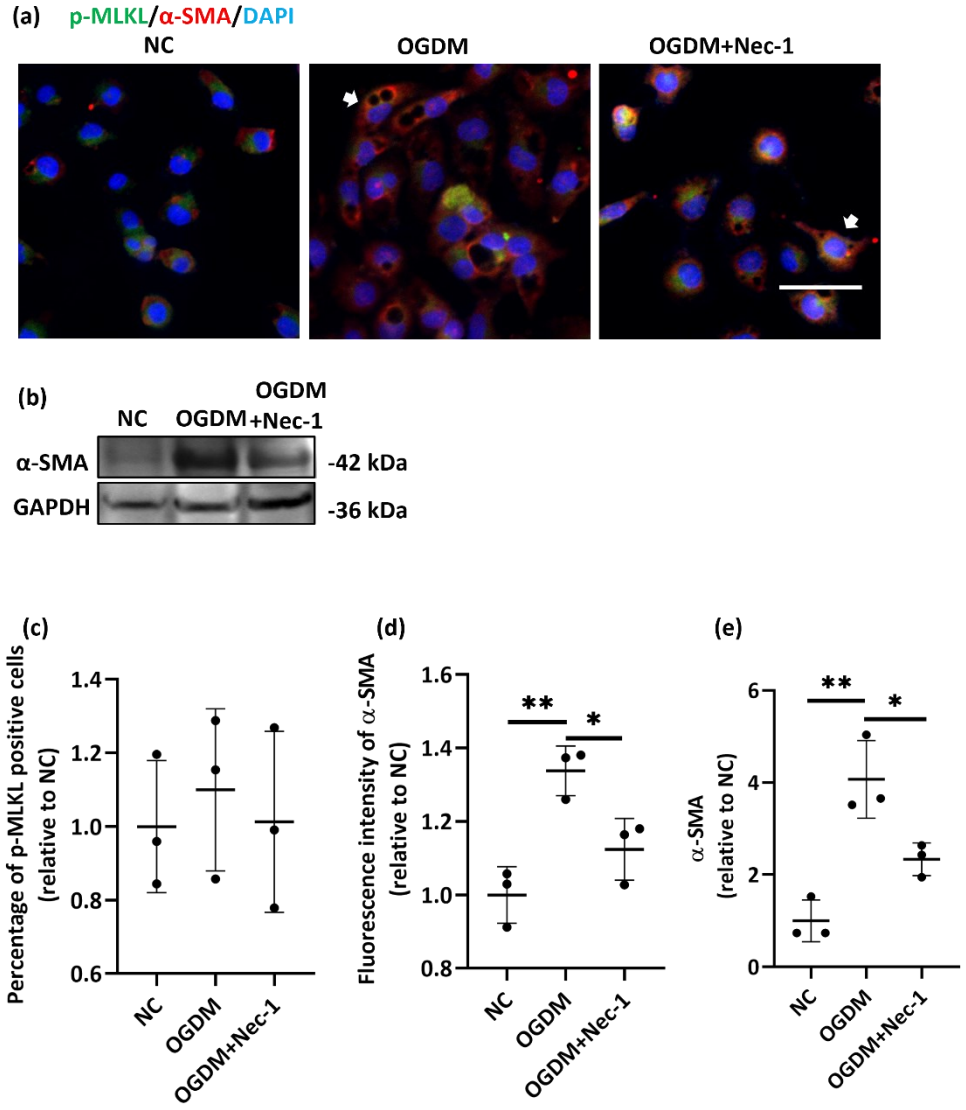

Figure 5. 4 OGDR induced EMT in HK2 cells, which was attenuated by Nec-1

HK2 cells were treated with OGD-conditioned medium, with (OGDM+Nec-1), without Nec-1 (OGDM), or naïve control (NC). (a) Representative ICC of p-MLKL and α-SMA (n=3). (b) The representative western blot of α-SMA (n=3. each represent an independent experiment). (c-d) Quantitative analysis of ICC results. (e) Quantitative analysis of western blot results. Data is presented as mean ± SD; * $p < 0.05$ and ** $p < 0.01$. Scale bar = 50μm.

NC: naïve control; OGD: oxygen-glucose deprivation; ICC: immunocytochemistry; p-MLKL: phosphorylated mixed lineage kinase domain-like; α-SMA: α-smooth muscle actin.

5.3.5 HMGB-1 induced EMT development in HK2 cells

HMGB-1 and histones are two well-known types of DAMPs that can initiate a series of danger signals and activate immune responses. We studied whether HMGB-1 and total histones could cause EMT development in HK2 cells. Cells were treated with total histones or HMGB-1. Western blot results showed that histones did not increase α-SMA expression, while HMGB-1 significantly increased α-SMA expression at 100μg/ml (1.45 ± 0.19, $p < 0.05$). The expressions of E-cadherin did not change significantly. ICC results showed similar results, with HMGB-1, but not histones, significantly increasing α-SMA intensity (1.51 ± 0.20, $p < 0.05$).

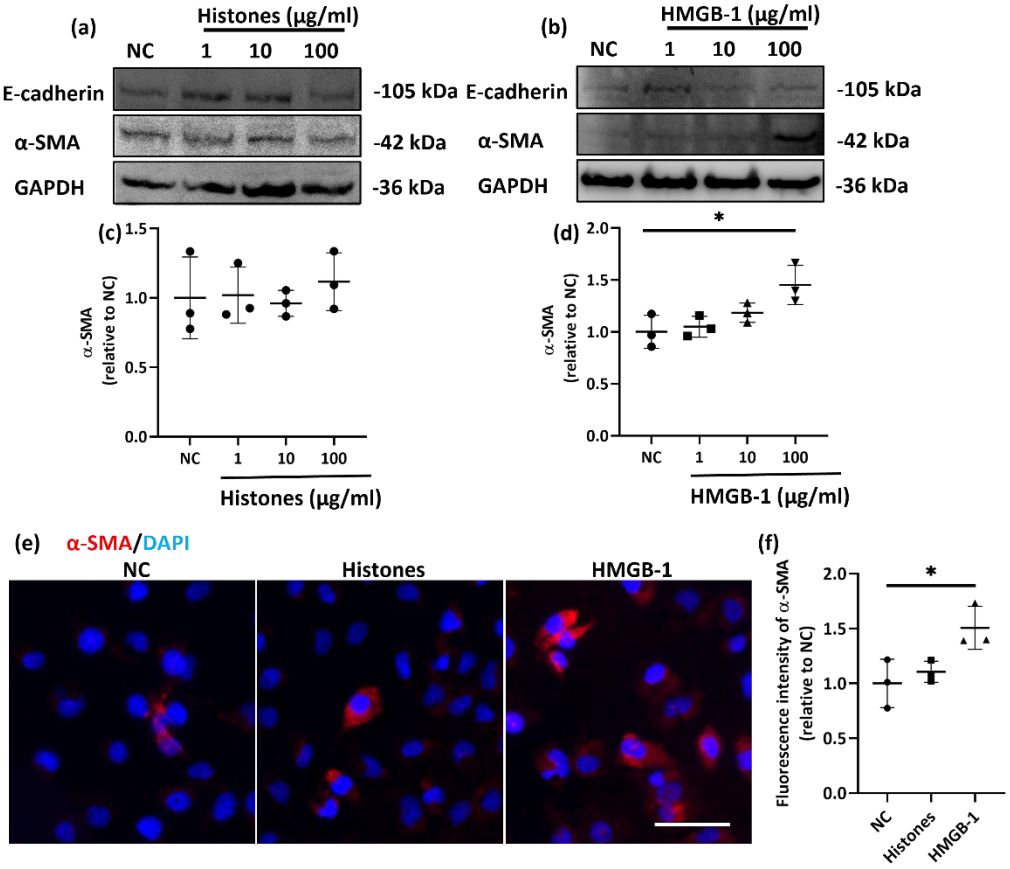

Figure 5. 5 HMGB-1 induced EMT development in HK2 cells

HK2 cells were treated histones or HMGB-1 at different concentrations. (a-b) The representative western blot of E-cadherin and α-SMA (n=3, each represent an independent experiment). (c-d) Quantitative analysis of western blot results (e) The representative ICC of α-SMA (n=3, each represent an independent experiment). (f) Quantitative analysis of ICC results. Data is presented as mean ± SD; * $p < 0.05$. Scale bar = 50μm.

NC: naïve control; ICC: immunocytochemistry; α-SMA: α-smooth muscle actin.

5.3.6 HMGB-1 induced EMT and production of TGF-β1 via TLR4/JNK signally pathways

RAGE antagonist peptide (RAP) and a TLR4 inhibitor, C34, were applied to evaluate the involvement of RAGE and TLR-4 in HMGB-1-induced EMT in HK2 cells. The inhibitors were applied 30 minutes prior to the HMGB-1 treatment. The cells were treated with HMGB-1 alone or in combination with either RAP at 2, 4, or 6 μg/ml (IC50 = 2 μg/ml) or with C34 at 5, 10, or 15 μg/ml (297). Compared to HMGB-1 alone, RAP slightly decreased the expressions of p-JNK (HMGB-1 vs. RAP [6 μg/ml], 1.50 ± 0.13 vs. 1.17 ± 0.11, $p = 0.14$), α-SMA (HMGB-1 vs. RAP [6 μg/ml], 1.35 ± 0.12 vs. 1.25 ± 0.08, $p = 0.83$), and TGF-β1 (HMGB-1 vs. RAP [6 μg/ml], 1.23 ± 0.03 vs. 1.14 ± 0.03, $p = 0.70$), but with no statistical significance. On the other hand, C34 significantly decreased the expressions of p-JNK (C34 [5 μg/ml], 0.84 ± 0.07, $p < 0.001$; C34 [10 μg/ml], 1.00 ± 0.34, $p < 0.01$; C34 [15 μg/ml], 0.88 ± 0.17, $p < 0.01$), α-SMA (C34 [5 μg/ml], 0.89 ± 0.09, $p < 0.001$; C34 [10 μg/ml], 0.90 ± 0.10, $p < 0.001$; C34 [15 μg/ml], 0.80 ± 0.07, $p < 0.001$), and TGF-β1 (C34 [5 μg/ml], 0.95 ± 0.04, $p < 0.001$; C34 [10 μg/ml], 1.08 ± 0.11, $p = 0.12$; C34 [15 μg/ml], 1.03 ± 0.10, $p < 0.01$). To demonstrate the role of JNK in HMGB-1-induced EMT, cells were treated with HMGB-1 alone or in combination with a selective JNK inhibitor SP-600125 at 40 or 90 nM (IC50 for JNK1/2 and JNK3, respectively). SP-600125 was applied 30 minutes prior to HMGB-1. Compared to HMGB-1 alone, treatment with SP-600125 effectively suppressed the phosphorylation of JNK (SP-600125 [40 nM], 0.73 ± 0.08, $p < 0.001$; SP-600125 [90 nM], 0.61 ± 0.06, p

< 0.001) and significantly decreased expressions of α-SMA (SP-600125 [40 nM], 0.95 ± 0.12, $p < 0.01$; SP-600125 [90 nM], 0.97 ± 0.12, $p < 0.05$) and TGF-β1 (SP-600125 [40nM], 0.89 ± 0.12, $p < 0.01$; SP-600125 [90nM], 0.99 ± 0.04, $p < 0.05$).

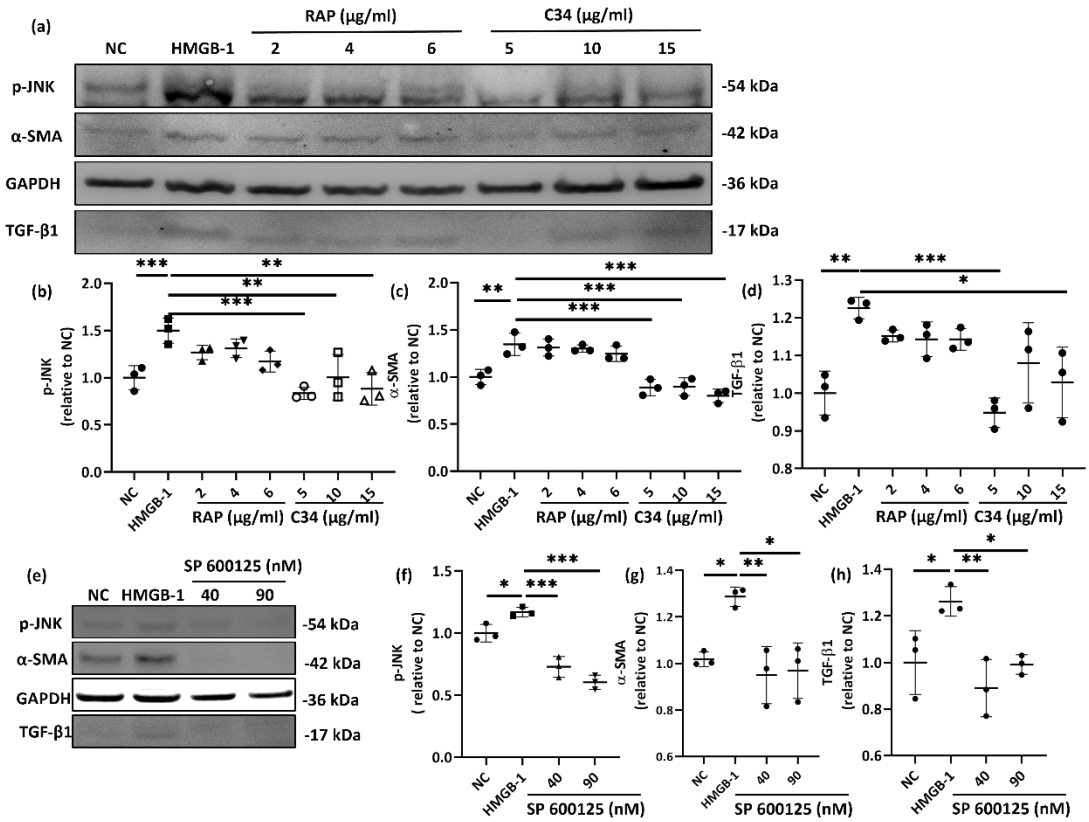

Figure 5. 6 HMGB-1 induced EMT and production of TGF-β1 via TLR4/JNK signally pathways

HK2 cells were treated with HMGB-1 alone or in combination with either RAP, C34, or SP-600125, respectively. (a and e) Representative western blot of p-JNK, α-SMA, and TGF-β1 (n=3, each represent an independent experiment). (b-d and f-h) Quantitative analysis of western blot results. Data is presented as mean ± SD; * $p < 0.05$, ** $p < 0.01$ and *** $p < 0.001$.

NC: naïve control; RAP: RAGE antagonist peptide; p-JNK: phosphorylated c-Jun N-terminal Kinase; α-SMA: α-smooth muscle actin; TGF-β1: transforming growth factor-β1.

5.4 Discussion

In this study, we demonstrated that IRI accomplished by bilateral pedicle clamping increased levels of α-SMA, which was attenuated by Nec-1. In vitro experiments showed that OGD treatment led to elevated expression of p-MLKL in HK2 cells and, after a 48-hour recovery period, the cells exhibited a significant increase in α-SMA expression. Nec-1 was effective in reducing both p-MLKL and α-SMA. Furthermore, OGD-conditioned medium induced EMT, which was decreased by Nec-1. In addition, we proved that HMGB-1, but not histones, led to the production of TGF-β1 and EMT in HK2 cells, and this was suppressed by blocking TLR-4 or JNK signalling. The lack of dose-dependence in the inhibition of C34 may be due to off-target effects and requires further investigation. Overall, these results suggest that necroptosis plays a role in promoting EMT development by releasing DAMPs, and HMGB-1 induces TGF-β1 production and EMT development through TLR-4/JNK signalling pathways.

Regulated cell death (RCD), accompanies the development of CKD, leading to persistent inflammation, progressive loss of tubular cells, cellular senescence, and fibrosis (155, 298-300). Therefore, investigating RCD in CKD is crucial for understanding the underlying mechanisms of disease progression and uncovering effective treatments. RCD can be divided into apoptosis and regulated necrosis based on their distinct morphological features and molecular mechanisms (301). Both types of RCD

have been found to be engaged in CKD progression (176, 302-312), which will be discussed in the following sections.

Apoptosis functions in normal kidneys as a way to clear out aged and damaged cells without causing inflammation (313). However, during chronic kidney disease (CKD), the increase in apoptosis of tubular cells leads to tubular atrophy and renal fibrosis, which contributes to the progression of CKD (302-306). Furthermore, promoting apoptosis by long non-coding RNA Neat1_2 was found to contribute to the progression of AKI to CKD (314). These findings indicate the important role of apoptosis in the development of CKD. However, since apoptosis has a critical role in haemostasis, interfering apoptosis normally have universal effects and may lead to unintended consequences such as cancer and degenerative diseases (315). As a result, targeting apoptosis for therapeutic purposes may not be a promising approach.

Recently, the contribution of regulated necrosis, including pyroptosis, ferroptosis, and necroptosis, to the development of CKD has been widely investigated. The upregulation of regulated necrosis-related genes has been found in various CKD models (287, 316, 317). The benefits of inhibiting regulated necrosis have also been investigated in vivo and in vitro. Deleting Gasdermin E (GSDME), an executor of pyroptosis, alleviated renal fibrosis and inflammation in CKD caused by unilateral ureteral ligation (UUO) and nephrectomy (318). Inhibition of ferroptosis by Ferrostatin-1 also exhibited anti-fibrotic effects against UUO and IRI-CKD models (311). Moreover,

inhibiting necroptosis showed protective effects in UUO (307, 308), nephrectomy (176), and IRI-induced CKD models (286). Consistent to these results, our study demonstrated that blocking necroptosis with Nec-1 mitigated IRI-induced fibrosis in mice and prevented IRI-induced EMT development in tubular epithelial cells. Collective findings suggest that regulated necrosis may be a key target in the prevention and treatment of CKD. Further studies are needed to confirm these findings and to develop safe and effective inhibitors of regulated necrosis for use in clinical settings.

It is believed that regulated necrosis contributes to chronic inflammation by releasing DAMPs into the extracellular space (156). In our study, OGD-conditioned medium caused EMT in tubular epithelial cells, and inhibiting necroptosis before the onset of OGD led to reduced EMT. It indicates that molecules that released from necroptotic cells, most likely DAMPs, can induce EMT development. Furthermore, our data demonstrated that extracellular HMGB-1 induces EMT and TGF-β1 production in tubular epithelial cells via TLR-4/JNK signalling pathways. These findings support the idea that regulated necrosis and the release of DAMPs play an important role in the development of CKD and suggest that targeting these processes may be a promising strategy for treating CKD.

In conclusion, this study demonstrates the role of necroptosis in promoting EMT development in the context of renal IRI. Also, our results indicate that extracellular

HMGB-1 induces TGF-β1 production and EMT development through TLR-4/JNK. Overall, these findings suggest that targeting necroptosis, HMGB-1, TLR4/JNK, and their downstream signalling pathways may be a promising strategy for preventing EMT and the development of CKD.

Chapter Six

Dexmedetomidine attenuates lipopolysaccharide-induced renal cell fibrotic phenotypic changes by inhibiting necroinflammation via activating α_2-adrenoceptor

6.1 Introduction

Sepsis is one of the major causes of AKI (10), and over 6% patients with sepsis-associated AKI (S-AKI) eventually develop CKD (319, 320). However, there is currently no effective treatment for this progression, and the precise mechanism underlying the transition from S-AKI to CKD remains to be elucidated.

Dexmedetomidine (Dex), a highly selective α_2-adrenoreceptor (α2-AR) agonist, is often used as an anaesthesia adjuvant or as a sedative for critically ill patients (321). Dex may be able to inhibit necroinflammation evidenced by its cytoprotective properties against several types of programmed necrosis (322-324). Dex treatment is also linked to lower DAMP levels (325, 326). Taken together, Dex may have anti-fibrotic properties in preventing renal fibrosis by suppressing necroinflammation which was investigated in the current study in LPS-induced sepsis models.

6.2 Experimental design

6.2.1 Investigating of Dex attenuates LPS-induced renal injury

An LPS-induced sepsis model was adapted to the role of Dex in S-AKI. The detailed procedures were explained in Methodology. In brief, mice were assigned in untreated group (naïve control, NC), LPS alone group (LPS), LPS with Dex group (LPS+Dex), and LPS, Dex, and Atipamezole (Atip) group (ATIP) (n=5/group). Atip is a potent antagonist of α2-AR. Haematoxylin and eosin (H&E) staining was used here to evaluate the protective effects of Dex against LPS-induced renal injury.

6.2.2 Investigating if Dex reduces fibrosis after LPS challenge

Kidney sections were stained with fibrotic markers collegen-1 and α-SMA, followed by assessment by immunohistochemistry (IHC).

6.2.3 Investigating if Dex reduces LPS-induced necroinflammation

Kidney sections were stained with necroptosis marker p-MLKL and pyroptosis-related marker NLR family pyrin domain containing 3 (NLRP3), followed by assessment by IHC.

6.2.4 Investigating if LPS induces EMT in HK2 cells

Cultured HK2 cells were treated either with LPS alone (LPS), LPS and Dex (LPS+DEX), LPS, Dex and Atip (ATIP), or naïve controls (NC) for 48 hours, followed by assessment of EMT markers by immunocytochemistry (ICC) and western blot.

6.2.5 Investigating if necroptosis suppresses LPS-induced regulated necrosis

Cultured HK2 cells were treated either with LPS alone (LPS), LPS and Dex (LPS+DEX), LPS, Dex and Atip (ATIP), or naïve controls (NC) for 48 hours. Cell necrosis were assessed by Annexin V/propidium iodide (PI) Flow cytometry. Then, necroptosis and pyroptosis markers were assessed by western blot.

6.2.6 Investigating if Dex attenuates transforming growth factor-β1 (TGF-β1) induced EMT in HK2 cells and the potential molecular mechanisms of Dex's protective effects

TGF-β1 is a classic inducer of EMT *in vitro*. Cultured HK2 cells were treated either with TGF-β1 alone (TGF-β1), TGF-β1 and Dex (TGF-β1 +DEX), TGF-β1, Dex and Atip (ATIP), or naïve controls (NC) for 48 hours, followed by assessment of EMT markers by ICC and western blot. The c-Jun N-terminal Kinase (JNK) signalling JNK is one of the downstream pathways of Toll like receptor-4 (TLR4), which mediates the inflammatory response induced by LPS. In addition, the JNK signalling pathway is involved in TGF-β1-induced EMT. The activation of the JNK signalling pathway was evaluated using western blot after stimulation with LPS, TGF-β1, or Dex.

6.3 Results

6.3.1 Dex attenuated LPS-induced kidney injury

LPS caused an increased interstitial oedema, brush border ablation, tubular and glomerular necrosis, and infiltration of leukocytes, attenuated by the administration of Dex (as indicated by arrow heads). The protective effects of Dex were abolished with Atip (**Figure 1a**). Histological injury score analysis revealed that the LPS group had a significant increase in both tubules (3.11 ± 0.49, $p < 0.001$, **Figure 1b**) and glomeruli (3.26 ± 0.32, $p < 0.01$, **Figure 1c**). Dex significantly reduced the injury scores in both the tubules (1.65 ± 0.29, $p < 0.01$) and the glomeruli (1.29 ± 0.48, $p < 0.01$), which were reversed by administering Atip to both the tubules (3.43 ± 0.38, $p < 0.01$) and glomeruli (3.34 ± 0.12, $p < 0.01$), indicating that Dex's organ protection was mediated through α_2-AR activation.

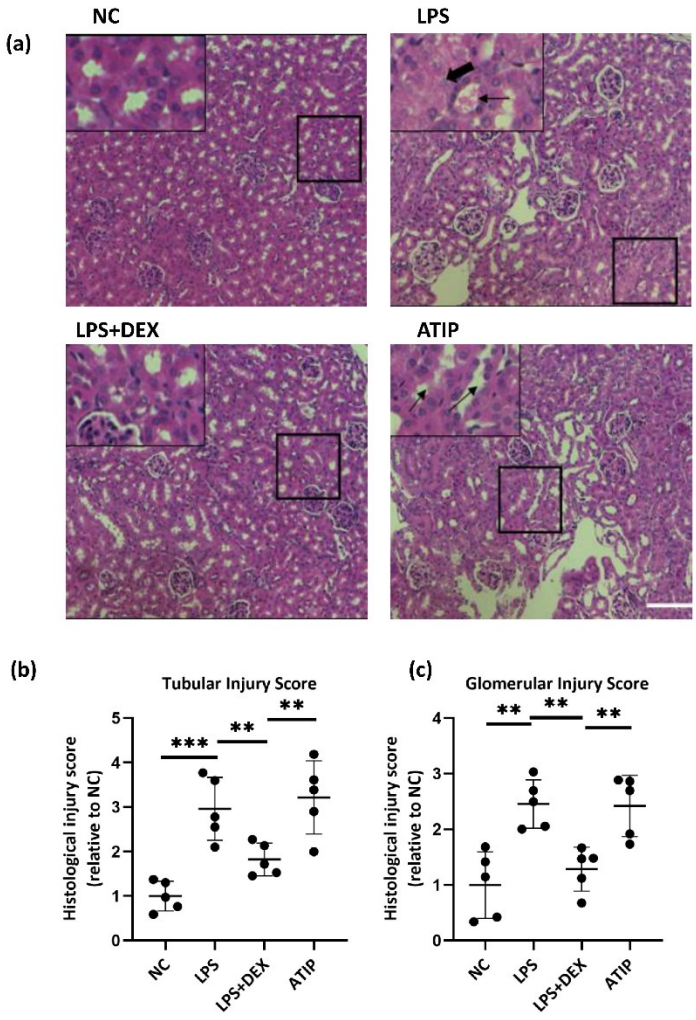

Figure 6. 1 DEX attenuated LPS-induced kidney injury in vivo via an α2-AR mechanism

C57BL/6 adult male mice were either injected with saline (NC), LPS alone (LPS), LPS with Dex (LPS+DEX) or LPS, DEX and Atip (ATIP). (a) The representative H&E staining of the mice kidney (renal cortex). (b-c) Quantitative analysis of injury scores (n=3, each represent an independent animal). Scale bar = 100μm. Data is presented as mean ± SD; ** $p < 0.01$ and *** $p < 0.001$.

LPS: lipopolysaccharide; Dex: dexmedetomidine; Atip: atipamezole; NC: naïve control.

6.3.2 Dex reduced fibroblast activation within kidney tubules

A-SMA and collagen-1 are classic markers that represent fibroblast activation and ECM formation, respectively, and are closely related to the degree of fibrosis (327, 328). The fluorescent intensity of α-SMA within the tubules (**Figure 2b**) was increased significantly in response to LPS injection (1.40 ± 0.09, $p < 0.001$). Furthermore, Dex ameliorated the increase in α-SMA (0.87 ± 0.14, $p < 0.001$), which was reversed by Atip administration (1.34 ± 0.09, $p < 0.001$). There were no significant differences observed in the expression of α-SMA in the glomeruli (**Figure 2c**) or in the expression of collagen-I in both the tubules and glomeruli across the four groups (**Figure 2d and e**).

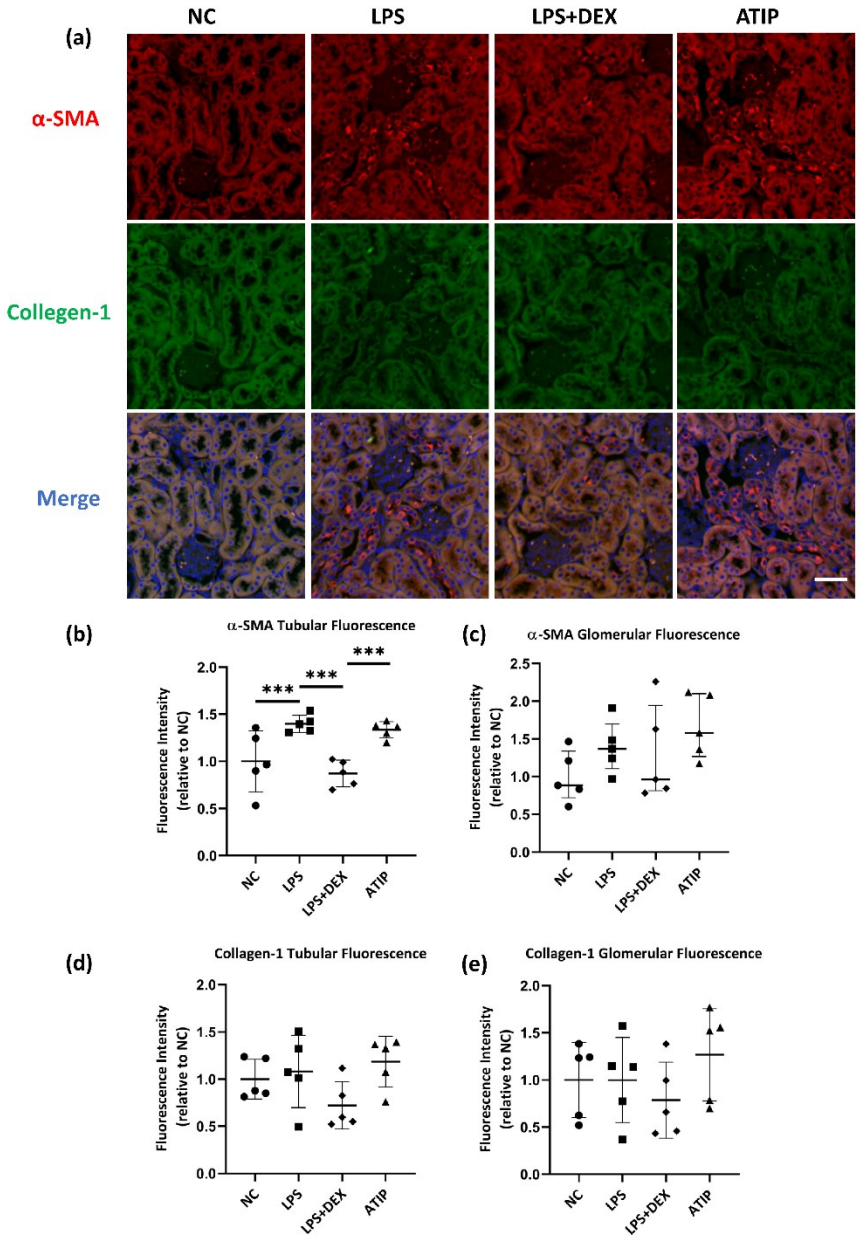

Figure 6. 2 Dex reduced myofibroblast activation within kidney tubules

C57BL/6 adult male mice were either injected with saline (NC), LPS alone (LPS), LPS with Dex (LPS+DEX) or LPS, DEX and Atip (ATIP). (a) The representative fluorescent staining of α-SMA and collegen-1 (renal cortex, n=5, each represent an independent animal). (b-e) The fluorescent intensity of α-SMA and collagen-1 within tubules and glomeruli. Scale bar = 50μm. Data is presented as mean ± SD; *** $p < 0.001$.
LPS: lipopolysaccharide; Dex: dexmedetomidine; Atip: atipamezole; NC: naïve control; α-SMA: α-smooth muscle actin.

6.3.3 Dex attenuated necroptosis and the formation of NLRP3 inflammasome

To investigate whether Dex may attenuate necroinflammation following an LPS challenge, two representative forms of programmed cell death, necroptosis and pyroptosis, were assessed with p-MLKL, an executioner of the necroptotic process, and NLRP3 which is associated with pyroptosis, respectively (**Figure 3a**). Compared to NC, the fluorescent intensities of p-MLKL (1.65 ± 0.43, $p < 0.01$) and NLRP3 (1.48 ± 0.47, $p < 0.05$) within tubules were significantly increased following LPS injection, respectively (Figure 3b). The p-MLKL (1.15 ± 0.21, $p < 0.05$) and NLRP3 (0.97 ± 0.16, $p < 0.05$) expressions within tubules were markedly decreased in the LPS+DEX group when compared to the LPS group. Atip reversed the effect of Dex by increasing the level of p-MLKL (1.50 ± 0.19, $p <0.05$) and NLRP3 (1.52 ± 0.33, $p < 0.05$).

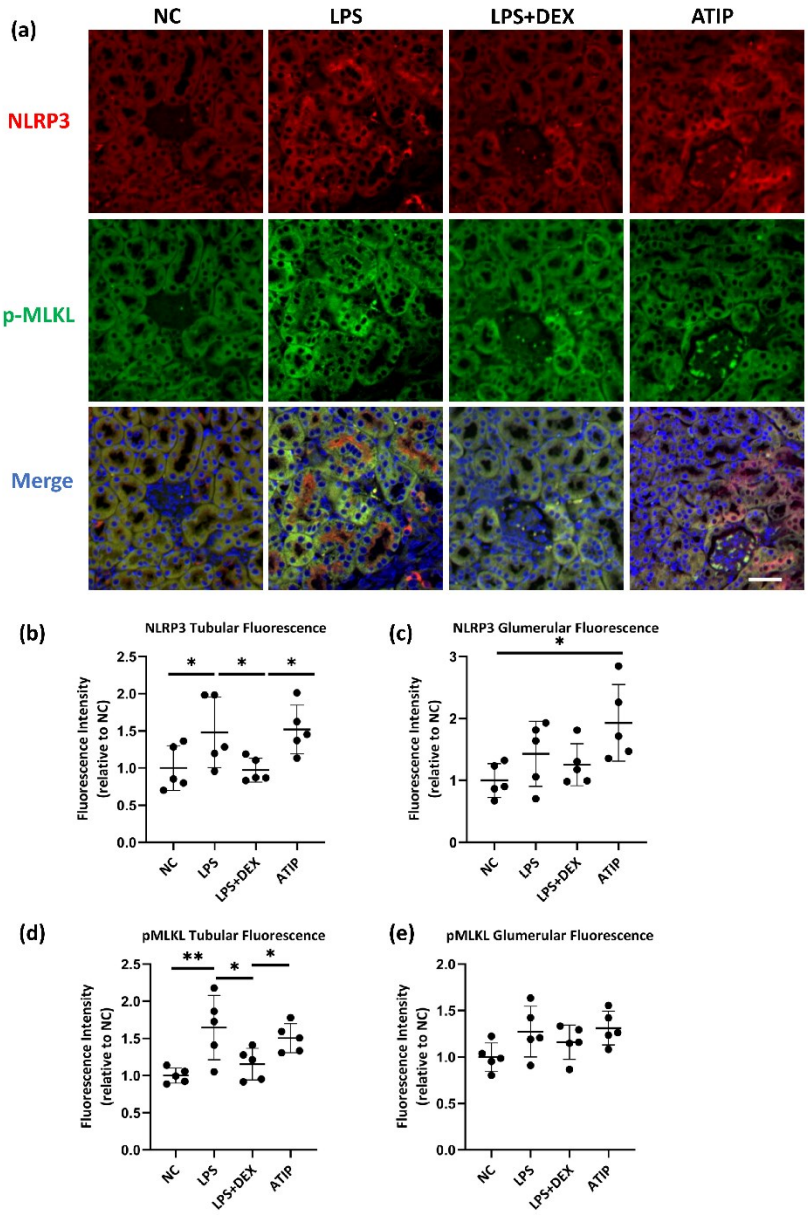

Figure 6. 3 Dex attenuated necroptosis and the formation of NLRP3 inflammasome

C57BL/6 adult male mice were either injected with saline (NC), LPS alone (LPS), LPS with Dex (LPS+DEX) or LPS, DEX and Atip (ATIP). Mice in control group were injected with comparable volumes of saline (NC). (a) The representative fluorescent staining of p-MLKL and NLRP3 (renal cortex, n=5, each represent an independent animal). (b-e) The fluorescent intensity of p-MLKL and NLRP3 within tubules and glomeruli. Scale bar = 50μm. Data is presented as mean ± SD; * $p < 0.05$ and ** $p < 0.01$. Arrows indicate positive staining.

LPS: lipopolysaccharide; Dex: dexmedetomidine; Atip: atipamezole; NC: naïve control; p-MLKL: phosphorylated mixed lineage kinase domain-like protein; NLRP3: NLR family pyrin domain containing 3.

6.3.4 Dex suppressed LPS-induced EMT *in vitro*

EMT is critical in the pathogenesis of renal fibrosis, whereby renal tubular epithelial cells increase α-SMA expression and lose epithelial cell markers, such as E-cadherin. To confirm our in vivo findings, we examined whether Dex is able to attenuate LPS-induced EMT in HK2 cells. Cultured HK2 cells were treated either with LPS alone (LPS), LPS and Dex (LPS+DEX), LPS, Dex and Atip (ATIP), or untreated naïve controls (NC) for 48 hours (**Figure 4a**). LPS significantly increased of α-SMA expression ($p < 0.01$), which was reversed following the administration of Dex ($p < 0.05$), whilst Atip administration did not have any significant effect (**Figure 4b**). There was no treatment induced any significant changes of E-cadherin expression (**Figure 4c**). The similar pattern changes were found within western blot analysis (**Figure 4d-f**).

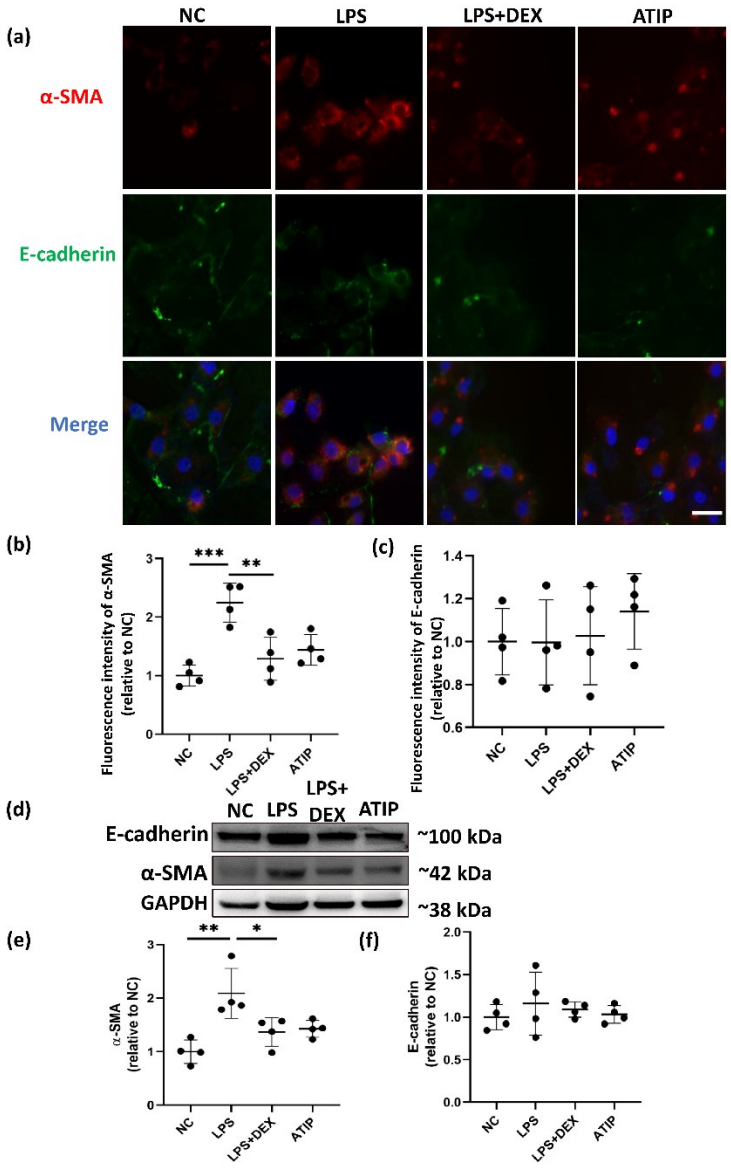

Figure 6. 4 Dex suppressed LPS-induced EMT in vitro

HK2 cells were either treated with LPS alone (LPS), LPS and Dex (LPS+DEX), LPS, Dex and Atip (ATIP) or untreated (NC) for 48 hours. (a) The representative IF of α-SMA and E-cadherin in HK2 cells (n=4, each represent an independent experiment). (b, c) Fluorescent intensity analysis of α-SMA and E-cadherin. (d) The representative western blot of α-SMA and E-cadherin in HK2 cells (n=4, each represent an independent experiment). (d, e) Quantitative analyses of α-SMA and E-cadherin. Scale bar = 100μm. Data is presented as mean ± SD; * $p < 0.05$ and ** $p < 0.01$. Arrows indicate positive staining.

HK2 cells: human kidney 2 cells, a proximal tubular epithelial cell line; LPS: lipopolysaccharide; Dex: dexmedetomidine; Atip: atipamezole; NC: naïve control; α-SMA: α-smooth muscle actin.

6.3.5 Dex inhibited LPS-induced necroptosis and pyroptosis *in vitro*

Flow cytometry was used to determine whether Dex has an anti-necrotic effect in response to LPS stimuli (Figure 6.5a). The treated cells and NC were stained with Annexin V and PI. The percentage of cells in Quadrant 3 (Q3, Annexin V-/PI+), which represents necrotic cells, was then compared between intervention groups. LPS challenge increased the percentage of cells in Q3 ($p < 0.05$), whereas Dex had an anti-necrotic effect, decreasing the rate of cells in Q3 in comparison to the LPS stimuli ($p < 0.05$) (Figure 6.5b). Western blotting was used to determine if Dex prevents necroptosis and pyroptosis (Figure 6.5c and e). P-MLKL and cleaved-GSDMD are executors of necroptosis and pyroptosis, respectively. LPS increased p-MLKL ($p < 0.01$), as well as cleaved-GSDMD expressions ($p < 0.01$), both of which were reduced following Dex treatment, respectively ($p < 0.05$) (Figure 6.5d and f).

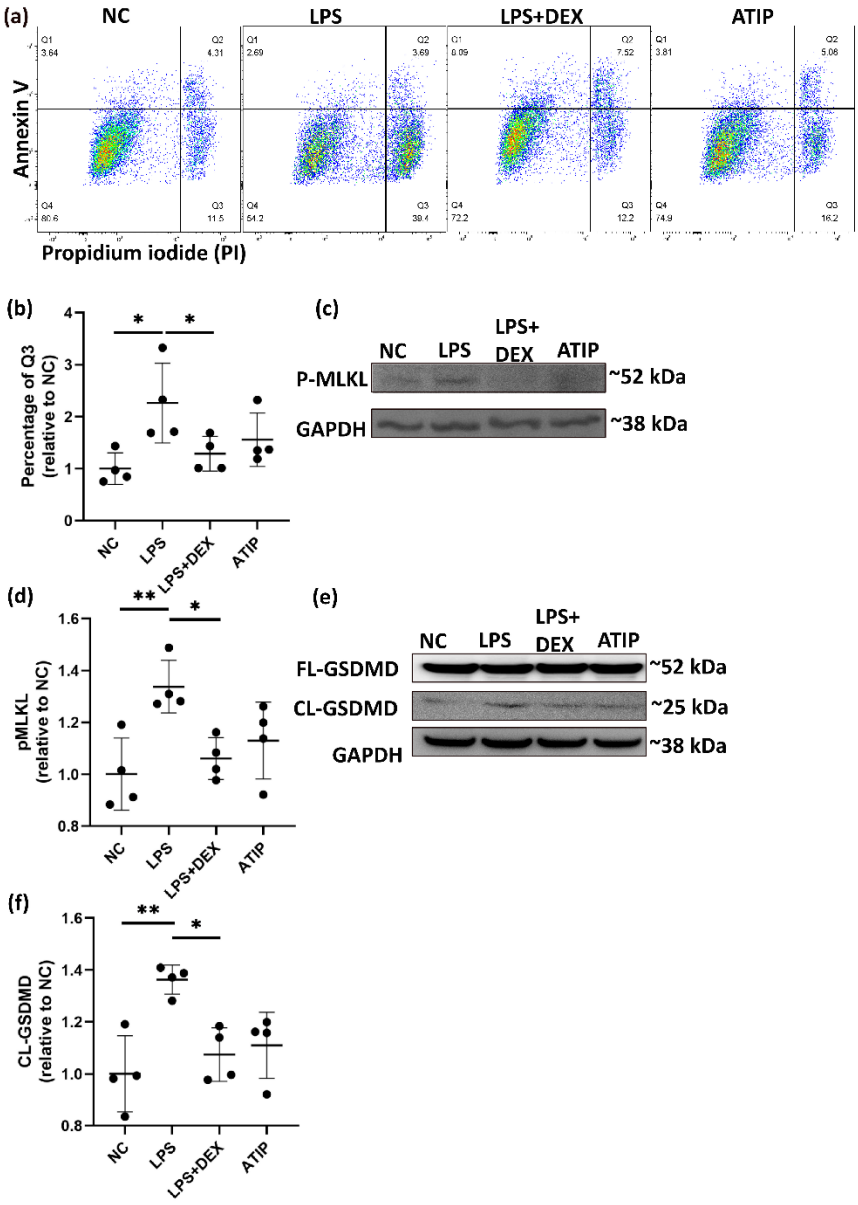

Figure 6. 5 Dex inhibited LPS-induced necrosis in vitro

HK2 cells were either treated with LPS alone (LPS), LPS and Dex (LPS+DEX), LPS, Dex and Atip (ATIP) or naïve control (NC) for 48 h. (a, b) The representative flowcytometry analysis of Annexin V and PI in HK2 cells (n=4, each represent an independent experiment). (c-f) The representative western blot of p-MLKL and GSDMD (full-length and cleaved) and their quantitative analyses (n=4, each represent an independent experiment). Data is presented as mean ± SD; * $p < 0.05$ and ** $p < 0.01$.

HK2 cells: human kidney 2 cells, a proximal tubular epithelial cell line; LPS: lipopolysaccharide; Dex: dexmedetomidine; Atip: atipamezole; NC: naïve control; PI: propidium iodide; MLKL: mixed lineage kinase domain-like protein; FL-: full-length-; CL-: cleaved-; GSDMD: Gasdermin D.

6.3.6 Dex suppressed TGF-β1-induced EMT

To demonstrate whether Dex directly inhibits EMT independent of its anti-necrotic properties, we administered TGF-β1 to induce EMT in HK2 cells. TGF-β1 is a classic EMT inducer, which helps to minimise the involvement of necrosis. Cells were either treated with TGF-β1 alone (TGF-β1), TGF-β1 and Dex (TGF-β1+DEX), TGF-β1, Dex and Atip (ATIP) or untreated naïve controls (NC) for 48 h. TGF-β1 significantly increases the fluorescent intensity of α-SMA, which was attenuated following Dex administration ($p < 0.01$ and $p < 0.05$, respectively; **Figure 6.6a and b**). Atip did not alter the fluorescent intensity of α-SMA relative to the Dex treatment. Western blot analysis revealed an increase of α-SMA expression induced by TGF-β1 ($p < 0.05$). TGF-β1-induced EMT was prevented by Dex, as evidenced by a decreased expression of α-SMA ($p < 0.05$; **Figure 6.6c and d**). Then we found that the anti-EMT effect of Dex is associated with phosphorylation of JNK (**Figure 6.6e**). The expressions of p-JNK were increased significantly after LPS ($p < 0.001$) and TGF-β1 ($p < 0.01$) administration, respectively. P-JNK expressions in the Dex groups were significantly lower than in the LPS or TGF-β1 groups ($p < 0.01$), consistent with lower α-SMA expression (**Figure 6.6f and g**), suggesting that the anti-EMT effects of Dex is associated with JNK phosphorylation.

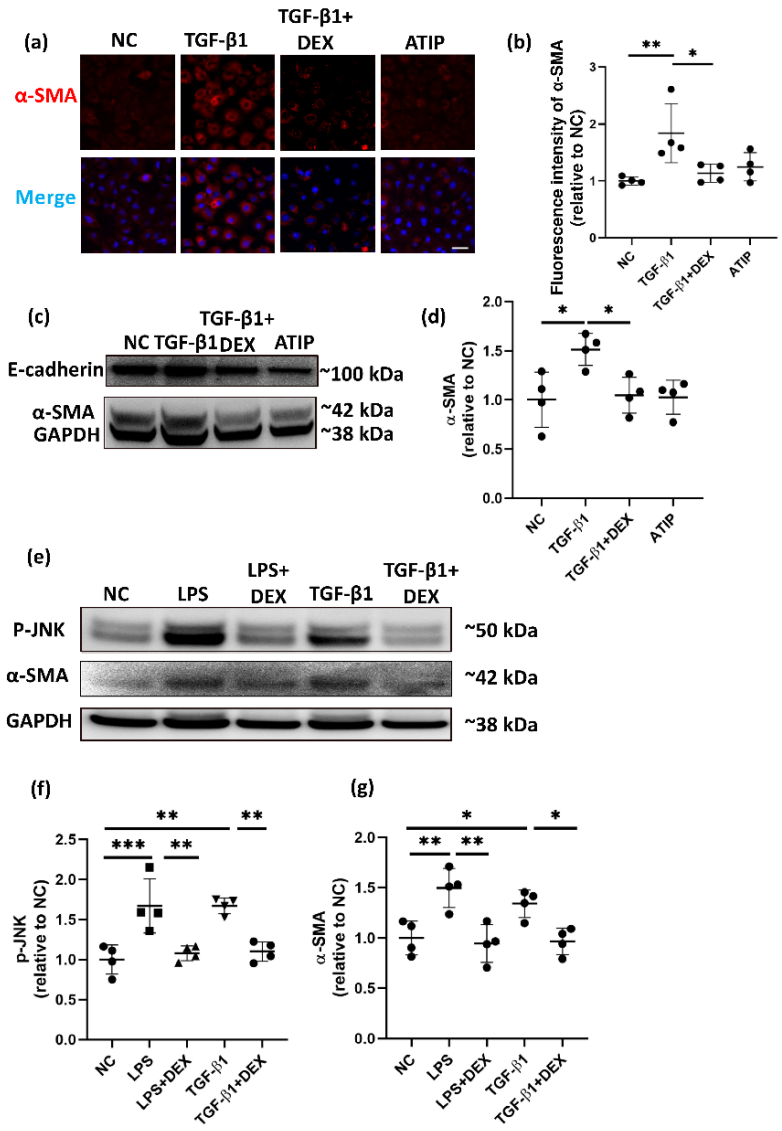

Figure 6. 6 Dex suppressed TGF-β1-induced necrosis in vitro

(a) IF of α-SMA in HK2 cells (n=4, each represent an independent experiment). (b) Fluorescent intensity analysis of α-SMA. (c) Western blot of α-SMA and E-cadherin in HK2 cells(n=4, each represent an independent experiment). (d) Quantitative analyses of α-SMA. (e) HK2 cells were either treated with LPS (LPS), LPS and Dex (LPS+DEX), TGF-β1 alone (TGF-β1), TGF-β1 and Dex (TGF-β1+DEX), or untreated (NC) for 48 h, respectively SMA (n=4, each represent an independent experiment). (f-g) Quantitative analyses of the p-JNK and α-SMA. Scale bar = 100μm. Data is presented as mean ± SD; * $p < 0.05$, ** $p < 0.01$ and *** $p < 0.001$.

HK2 cells: human kidney 2 cells, a proximal tubular epithelial cell line; TGF-β1: transforming growth factor beta 1; Dex: dexmedetomidine; Atip: atipamezole; NC: naïve control; IF: immunofluorescence; α-SMA: α-smooth muscle actin; JNK: c-Jun N-terminal Kinase.

6.4 Discussion

In this study, we found that Dex reduced renal injury in response to LPS-induced AKI. Dex inhibited myofibroblast proliferation while also decreased NLRP3 inflammasome formation and necroptosis. A_2-AR activation was at least partially responsible for the protective effects of Dex which was demonstrated in our *in vivo* experiments. *In vitro*, Dex also prevented EMT following LPS challenge. Dex significantly reduced two types of programmed cell death, necroptosis and pyroptosis suggesting that its anti-EMT effects were likely related to its cytoprotective properties. Dex also inhibited TGF-β1-induced EMT, indicating that Dex has an anti-EMT effect in addition to its cytoprotective properties. Furthermore, it was found that the JNK signalling pathway was involved in Dex's anti-EMT properties. Our findings suggest that Dex may be a promising treatment strategy to prevent renal fibrosis (**Figure 8**).

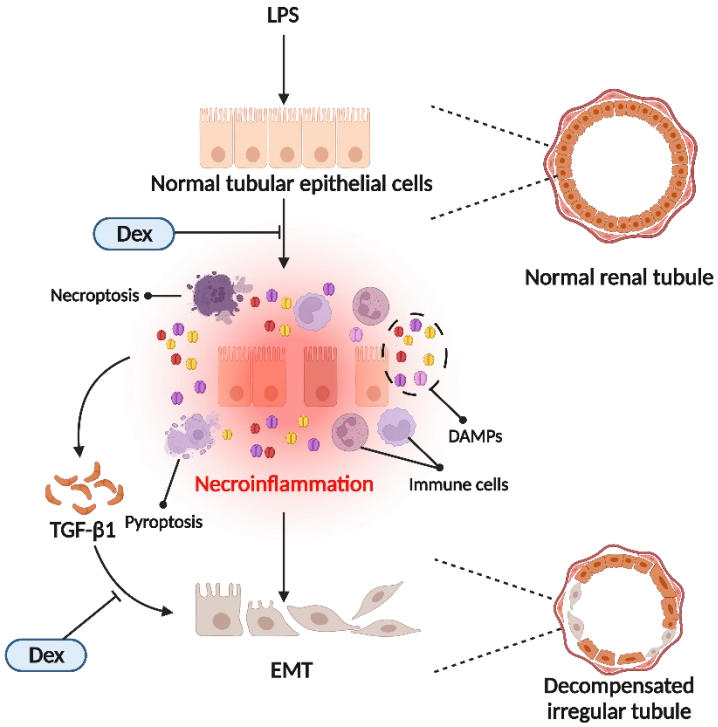

Figure 6. 7 The overall illustration of Dex-mediated protection against LPS-induced renal injury

In a normal renal tubule, renal tubule epithelial cells are tightly connected to each other by intracellular adhesion molecules, such as E-cadherin, and they attach to the TBM on their basal side. Upon the stimulation of LPS, tubular epithelial cells undergo programmed necrosis including necroptosis and pyroptosis, releasing DAMPs which recruit and activate immune cells. The intensive inflammation can directly cause EMT. In addition, the activated immune cells produce TGF-β1 which can also cause EMT. In the present study, this study demonstrates that Dex reduces EMT following LPS stimulation whilst simultaneously inhibiting pyroptosis and necroptosis. Dex can inhibit TGF-β1-induced EMT, indicating that Dex has a direct anti-EMT effect in addition to its cytoprotective properties.

TBM: tubular basement membrane; LPS: lipopolysaccharide; DAMPs: danger-associated molecular patterns; EMT: epithelial-mesenchymal transition; TGF-β1: transforming growth factor beta 1; Dex: dexmedetomidine.

Significant evidence suggests that acute kidney injury can trigger renal fibrosis development (1, 329, 330). Inflammation (331-333), DNA damage (334, 335), senescence (336, 337) and mitochondrial dysfunction (338, 339) are all possible contributors to the AKI-to-CKD transition. Inflammation is one of the most important factors that contribute to the progression of AKI to CKD, as many pro-inflammatory factors, such as tumour necrosis factor-α (TNF-α), C-reactive protein, and interleukins, are predictors and promoters of CKD (340). In addition, most of these factors interact positively with inflammation (341, 342). As a result, inflammation plays an important role in renal fibrosis. The necroinflammation theory may explain why inflammation persists after the acute phase of an injury in the transition from AKI to CKD. Initial damage to the kidney that induces programmed necrosis leads to a massive release of DAMPs that can sustain or amplify the inflammatory response and drive further necrosis, which ultimately results in renal fibrosis. Various DAMPs have been found to increase in CKD (289). A cross-sectional study of 225 patients showed that high mobility group box 1 (HMGB-1) was significantly elevated in patients with CKD and its concentration was inversely proportional to patients' renal function (343). In addition, heat shock proteins (HSPs) were reported to be higher in children and young adults with CKD (344). Hsp27, phospho-Hsp27, receptor for advanced glycation end-products (RAGE), and calreticulin expression were all increased in a unilateral ureteral obstruction (UUO) animal model (345-347). In addition to studies focusing on DAMPs, it has been reported that inhibiting programmed necrosis attenuates renal fibrosis

(348). Jiang *et al.* found that Coenzyme Q10 (CoQ10) prevented unilateral ureteral obstruction (UUO) induced necroptosis and renal fibrosis. Necrostatin-1 and GSK872, which are RIP inhibitors, had similar effects, indicating that the anti-fibrotic effect of CoQ10 may work through anti-RIP-mediated necroinflammation (348). Chen *et al.* demonstrated that the deletion of RIP3 or/and MLKL genes in mice reduced renal fibrosis in a model of ischemia-reperfusion injury (286). The evidence above clearly suggests an association between necroinflammation and CKD, indicating that necroinflammation may be a therapeutic target in tackling CKD.

Dex is a sedative with analgesic property and commonly used in perioperative medicine. The main target of this drug is the α_2-AR, which constitutes a family of guanine-nucleotide regulatory binding proteins (G proteins)–coupled receptors with at least three subtypes, α_{2A}, α_{2B}, and α_{2C} (349). The α_{2A} and α_{2B} subtypes are mainly expressed in the central nervous system, while the α_{2c} subtype is more commonly found peripherally. The α_2-AR's biological effects are mediated by G proteins, which modulate ion channel activity or initiate the second messenger system. Dex has recently been shown to have cytoprotective properties against several types of programmed necrosis. Dex, for example, has been shown to inhibit pyroptosis against myocardial ischemia-reperfusion injury (IRI) in rats (324). In cardiomyocytes, dexmedetomidine has also been shown to inhibit IRI-induced necroptosis (323). In our study, Dex significantly inhibited both pyroptosis and necroptosis while attenuating

EMT in vivo via a α_2-AR mechanism. Multiple studies have demonstrated that Dex exerts its organ-protective effects via α_2-AR activation in the brain, liver, and kidney (289, 350, 351). However, the precise signalling pathways remain unknown. It is necessary to better understand how α_2-AR interacts with necroptosis and pyroptosis signalling pathways.

EMT is a process in which epithelial cells lose their adhesion characteristics and phenotype but gain mesenchymal cell characteristics (141). EMT allows epithelial cells to transform into fibroblasts, which are necessary for tissue repair. However, increased EMT during renal fibrosis is unfavourable because it can result in overproduction of fibrotic scars, resulting in decreased renal function (143). The role of EMT in CKD has recently been called into question, as Le Bleu *et al.* demonstrated using genetic mouse models and fate-mapping techniques that, despite having a phenotype change, TECs did not cross the basement membrane into the interstitial space, indicating a partial-EMT status (352, 353). Surprisingly, S. Lovisa *et al.* discovered that this partial-EMT status also promoted renal fibrosis. Twist1 and Snai1, two transcriptional regulators of EMT, were conditionally deleted, which significantly reduced interstitial fibrosis (354). Our data demonstrate that Dex attenuates both LPS and TGF-β1-induced EMT via a mechanism related to JNK phosphorylation, indicating that Dex may have the potential to alleviate renal fibrosis in clinical practice. Multiple Dex studies further support this theory. For instance, Li *et al.* found that Dex attenuated renal fibrosis through the

inhibition of cellular senescence in an IRI model (355). An in vitro study found that Dex inhibited TGF-β1-induced ECM formation in airway smooth muscle cells by inhibiting MAPK signalling pathways (356). Collective findings suggest that Dex's anti-fibrotic effect might translate into clinical practice although it warrants further study.

JNK is a key member of the MAPK family (357), mediating a variety of cellular processes including cell proliferation, inflammation, and differentiation (358). JNK is primarily activated by multiple extracellular stimuli such as LPS, leading to increased pro-inflammatory transcriptional factors, chemokines, and cytokines, which potently activate host defensive mechanisms (359). Activation of the JNK signalling pathway is evident in various models of acute and chronic kidney injury (360). The JNK pathway also interacts with the TGF-1/Smad EMT pathway by phosphorylating mothers against decapentaplegic homolog 3 (Smad 3) directly (361). In this study, we found that Dex significantly inhibited JNK activation. The interaction between Dex and JNK can be found in various disease models. Dex, for example, has been shown to protect neonatal rats' hippocampus from isoflurane-induced neuro-apoptosis by inhibiting the JNK signalling pathway (362). Zhu et al. demonstrated that Dex protected against autophagy in focal cerebral IRI by suppressing JNK phosphorylation (363). Similar findings have also been demonstrated in acute stress-induced kidney Injury (364) and lung sepsis models (365). However, the mechanisms underlying the interaction between Dex and JNK remain to be studied.

This study has some limitations. Firstly, we mimicked S-AKI using an LPS model, which has some inherent drawbacks. LPS is only a single type of toxin that is released by gram-negative organisms during infection. Furthermore, the LPS-model neglects host-pathogen interactions as it essentially causes endotoxemia rather than a septic state. As a result, it may not result in actual inflammatory responses against infection. Secondly, the study course in both in vivo and in vitro is relatively short while renal fibrosis is chronic process, and the anti-fibrotic effect of Dex remains unknown. However, Dex inhibited pyroptosis and necroptosis induced by LPS stimulation reported here would no doubt protect kidney to be deteriorated pathologically and functionally.

In summary, this study demonstrates that Dex attenuated EMT following LPS challenge whilst simultaneously inhibited pyroptosis and necroptosis via α_2-AR activation in the kidney. Our findings suggest that Dex may have potential to reduce renal fibrosis through suppressing necroinflammation. Dex's anti-fibrotic properties may provide further justification of using Dex on patients have a risk of developing AKI towards CKD during perioperative period.

Chapter Seven

Final discussion

7.1 Rationale of the study

Chronic Kidney Disease (CKD) has become a major global health issue, with an estimated worldwide prevalence of over 9% (366). The disease is characterised by a gradual loss of kidney function over time, which can result in reduced quality of life, increased mortality, and various complications, such as hypertension, acute kidney injury (AKI), and cardiovascular disease (10, 17, 18). A wide range of conditions can lead to the development of CKD and can be categorised as systematic diseases (e.g., diabetes), genetic disorders (e.g., polycystic kidney disease), and AKI (e.g., sepsis-induced AKI) (24). Currently, treatment options are mainly focused on conservative management and addressing the underlying causes (24). However, there is no effective treatment to prevent or slow down CKD developed from AKI. This study aims to investigate the mechanisms behind the transition from AKI to CKD, with a particular focus on the role of necroptosis, as well as the potential therapeutic interventions. The findings from this study have the potential to provide new therapeutic targets for the AKI-CKD transition, which could be further developed and eventually translated into clinical practice.

7.2 Summary of the findings

In chapter 4, we explored the mechanisms of cell death triggered by various nephrotoxic agents, including cisplatin (CDDP), pemetrexed (PEM), gentamicin (GM), and aristolochic acid-I (AA-I), and their effect on the development of epithelial-

mesenchymal transition (EMT) in human tubular epithelial cells (HK2). Our findings indicate that CDDP, PEM, and AA-I induce cytotoxicity and decreased cell viability in a dose-dependent manner in HK2 cells, leading to significant necroptosis. On the other hand, GM causes apoptosis-dominated cell death. The upregulation of α-smooth muscle actin (α-SMA) in response to CDDP, PEM, and AA-I was suppressed by the necroptosis inhibitor Necrostatin-1 (Nec-1), suggesting the involvement of necroptosis in the development of EMT. Furthermore, the results suggest that the Toll-like receptor-4 (TLR-4) is implicated in CDDP, PEM, and AA-I-induced necroptosis and subsequent EMT, as the TLR-4 antagonist C34 reversed the increase in p-MLKL/MLKL (MLKL, mixed lineage domine-like protein) and α-SMA expressions.

In chapter 5, we studied the correlation between necroptosis and EMT in ischaemia-reperfusion injury (IRI) settings. Our findings demonstrate that ischemia-reperfusion injury (IRI) caused by bilateral pedicle clamping led to an increase in the levels of p-MLKL and α-SMA, which was mitigated by Nec-1. Our *in vitro* experiments reveal that oxygen-glucose deprivation (OGD) treatment resulted in increased expression of p-MLKL in HK2 cells. After a 48-hour recovery period, the cells displayed a noticeable increase in α-SMA expression, which was reduced by Nec-1. Additionally, we found that OGD-conditioned medium induced EMT, and this effect was diminished by Nec-1. Furthermore, our results prove that high mobility group box 1 (HMGB-1) triggered transforming growth factor-β1 (TGF-β1) production and EMT in HK2 cells, but histones

did not. These effects were suppressed by blocking TLR-4 or c-Jun N-terminal kinase (JNK) signalling. Overall, these findings suggest that necroptosis contributes to the promotion of EMT development by releasing damage-associated molecular patterns (DAMPs), and HMGB-1-mediated EMT development occurs through TLR-4/JNK signalling pathways.

In chapter 6, our study investigated the impact of Dexmedetomidine (Dex), an anaesthetic with cytoprotective properties, on fibrotic changes triggered by lipopolysaccharide (LPS). Results showed that Dex effectively reduced renal injury caused by LPS-induced AKI. The drug inhibited myofibroblast proliferation while also reducing the expression of the NLR family pyrin domain containing 3 (NLRP3) inflammasome and necroptosis. Our in vivo experiments revealed that the protective effects of Dex were at least partially due to activation of the α2-adrenoceptor (α2-AR). In vitro, Dex prevented EMT following LPS challenge. Dex significantly reduced two forms of programmed cell death, necroptosis and pyroptosis, suggesting that its anti-EMT effects may be linked to its cytoprotective properties. Furthermore, Dex inhibited TGF-β1-induced EMT, indicating that it has both cytoprotective and anti-EMT properties. Our results showed that the JNK signalling pathway was involved in Dex's anti-EMT effects. Overall, our findings suggest that Dex may have potential to decrease renal fibrosis by suppressing necroinflammation and may provide further justification

for its use in patients at risk of developing AKI and progressing to CKD during the perioperative period.

To summarise, necroptosis-associated necroinflammation plays a role in AKI and the subsequent development of EMT, which may be through activation of the TLR4/JNK cellular signalling pathways. These pathways can be therapeutic targets for future treatment of AKI and its progression to CKD. The results of our studies show that the use of Dex has a protective effect against necroptosis, pyroptosis, and EMT, making it a valuable option for clinical applications.

7.3 Scientific and clinical implications

7.3.1 Necroptosis and DNA damage

Necroptosis is a type of cell death that is regulated by a complex pathway involving the RIP1, RIP3, and MLKL proteins (367). It can be triggered by various extrinsic pathways including tumour necrosis factor receptor (TNFR)-dependent pathways, TLR-dependent pathways, and interferon receptor-dependent pathways (263). Recent studies have shown that DNA damage may lead to necroptosis as an intrinsic mechanism, as evidenced by the induction of necroptosis by DNA-damaging agents, such as cisplatin and etoposide (368). Our findings further support this conclusion, as PEM and AA-I, two compounds with DNA-damaging properties, induced significant necroptosis in HK2 cells. However, little is known about the molecular mechanisms underlying DNA damage-induced necroptosis.

Cells have developed intricate processes to handle DNA damage, which is commonly occurring due to sources such as ultraviolet (UV) light and reactive oxygen species (ROS) (262). While cells can repair mild DNA damage, severe and irreparable damage can lead to cell death via damage checkpoints Ataxia-Telangiectasia mutated (ATM) and ATM- and Rad3-related (ATR), which initiate signalling pathways leading to apoptosis (369). In certain situations, signals from ATM and ATR may also activate RIP1 and RIP3, resulting in the induction of necroptosis (370, 371). Further research is needed to fully understand the interactions between DNA damage and necroptosis, and how these processes can be manipulated or improved to prevent necroptosis, which may have important implications for a wide range of fields, including cancer research, aging, regenerative medicine, and CKD.

7.3.2 Necroinflammation and chronic inflammation

The development of CKD is accompanied by necroinflammation, a self-perpetuating cycle resulting from the mutually enhanced effects of necrosis and inflammation (155, 298-300). Upon the stimulation of insults, normal cells develop necrosis which causes massive release of danger-associated molecular patterns (DAMPs) including ATP, HMGB-1, HSP, DNA, etc (156). By interacting with pattern recognition receptors (PRRs), DAMPs not only induce cell death on neighbouring cells but also recruit and activate immune cells that amplify the inflammation and drive further, persistent cell death

(157). This leads to sustained inflammation, the decline in tubular cells, aging of cells, and fibrosis (155, 298-300).

The inhibition of necroptosis, pyroptosis, or ferroptosis has shown protective effects against CKD in various models, indicating the involvement of these forms of regulated necrosis in the development of CKD (176, 302-312). However, none of these findings have been translated into clinical practice. This may be due to the fundamental differences between experimental and clinical settings. In experimental settings, the inhibition of a specific type of cell death, either through pharmacological agents or genetic deletion, occurs prior to the injury, which does not occur in clinical settings. Additionally, in the case of the AKI-CKD transition, there may be a predominant type of cell death present in the early stages of injury. As the disease progresses, multiple types of cell death may coexist. Thus, inhibiting only one type of cell death may not be a promising approach for CKD. The effects of co-inhibiting regulated necrosis warrant further investigation.

7.3.3 HMGB-1, TLR-4, and RAGE

HMGB-1 is a nonhistone nuclear protein that has various functions based on its location within a cell (372). Within the nucleus, it acts as a DNA chaperone, preserving chromosome structure and function. In the cytoplasm, it can promote autophagy by binding to the Beclin-1 protein. Upon release, extracellular HMGB-1 acts as a DAMP molecule and regulates inflammation and immune responses through various

receptors (372). This molecule plays a role in several inflammatory conditions, such as sepsis, chronic inflammatory bowel diseases, and burns (373).

HMGB-1 may also be a pro-inflammatory mediator in CKD, as its levels in the serum have been linked to pro-inflammatory markers and declining kidney function in CKD patients (296). Additionally, in vitro studies have shown that HMGB-1 promotes fibrotic phenotypes (374-376). Our research further confirms that HMGB-1 induces epithelial-mesenchymal transition (EMT) in tubular epithelial cells, making it a potential therapeutic target for preventing EMT and CKD.

The classic HMGB1 receptors include RAGE, TLRs (TLR2, TLR4, and TLR9), CXCR4, and T cell immunoglobulin mucin-3 (TIM-3) (377). Currently, only RAGE and TLR4 have been confirmed as established HMGB1 receptors (372). Our study showed that HMGB-1 induces EMT in HK2 cells via TLR-4, suggesting that the HMGB-1/TLR-4 system may be a therapeutic target for CKD treatment. Our data also showed that the RAGE antagonist peptide slightly reduced HMGB-1-induced EMT and TGF-β1 production, though this was statistically insignificant, possibly due to HMGB-1's relatively lower affinity for RAGE compared to TLR-4. Further investigation is necessary to fully understand the role of RAGE in HMGB-1-induced EMT.

7.3.4 JNK signalling

JNK, which is a member of the MAPK family (357), is responsible for regulating several cellular processes like cell growth, inflammation, and differentiation (358). It is

activated by various extrinsic stimuli, leading to an increase in pro-inflammatory factors, chemokines, and cytokines that activate the body's defence mechanisms (359). The activation of the JNK signalling pathway can be observed in multiple cell types, including glomerular cells, tubular epithelial cells and infiltrating leukocytes, in various models of acute and chronic kidney injury (360). Inhibiting JNK has been shown to protect against kidney injury and prevent the UUO-induced renal fibrosis (378). JNK activation in tubular epithelial cells may be a pivotal mechanism in determining the outcome of both acute kidney injury and progression of chronic. Multiple studies, as well as our results, demonstrate that JNK mediates EMT in tubular epithelial cells (379, 380). Tubular epithelial cells are also a major source of pro-fibrotic factors in tubulointerstitial fibrosis (381). In our study, JNK inhibitor SP-600125 significantly reduced HMGB-1-induced TGF-β1 production in tubular epithelial cells, suggesting an important role of JNK in the formation of fibrosis. In summary, the JNK signalling pathway is an important contributor to fibrosis in the kidneys, and inhibiting JNK enzymes has the potential to become an effective treatment approach for CKD.

7.3.5 Dexmedetomidine and renal fibrosis

Dex is a medication with sedative and pain-relieving effects commonly used in perioperative procedures. It primarily works by targeting α2-AR, which is activated by G proteins and can influence ion channel function or trigger the secondary messenger system (349). Dex has recently been shown to have cytoprotective properties against several types of programmed necrosis (323, 324). Consistently, our results show that Dex significantly inhibited both pyroptosis and necroptosis against LPS-induced renal injury in vivo via an α_2-AR mechanism, with significant anti-fibrotic effects. It is likely that Dex reduced fibrotic changes though its cytoprotective properties, indicating the potential anti-fibrotic effects of cytoprotective agents. Dex also directly suppressed TGF-β1-induced EMT, indicating that Dex has an anti-EMT effect in addition to its cytoprotective properties. The mechanisms of this, however, require further investigations. In addition, it was found in our study that the JNK signalling pathway was involved in Dex's anti-EMT properties. Recently, it has been demonstrated that Dex can attenuate inflammation through downregulated TLR-4 expression via an α7 nicotinic acetylcholine receptor-dependent pathway (67), which may explain how Dex interacts with JNK. Overall, our findings suggest that the use of Dex may have benefits for patients at risk of developing AKI and progressing to CKD during the perioperative period. Dex-associated anti-fibrotic mechanisms may provide novel therapeutic targets and warrant further study.

7.4 Limitations of the study

The current study, while contributing some valuable insights into the mechanisms of AKI and its progression to renal fibrosis, has several limitations that have to be acknowledged.

Primarily, the sample size in the study, particularly some experiments in Chapter 5, was relatively small due to the impact of the COVID-19 pandemic, which affected the validity of the findings. Future studies with larger sample sizes are necessary to confirm the reproducibility and applicability of these results.

The methodological approach also has limitations. The study presents a limitation in its design due to the absence of negative controls in the *in vivo* experiments. This can lead to ambiguity when distinguishing between baseline expression levels and true positive signals. Without these controls, differentiating between inherent background activity and genuine experimental outcomes became challenging, potentially compromising the reliability of the study's findings.

Furthermore, the absence of an *in vivo* model to corroborate the nephrotoxicity-induced AKI findings leaves a gap in translational validity. The use of the LPS model, while informative and classic, does not simulate host-pathogen interactions, as it essentially causes endotoxemia rather than a septic state. As a result, it may not result in actual inflammatory responses against infection. Furthermore, the duration of the study was relatively short in comparison to the chronic nature of renal fibrosis, possibly

weakening the strength of the evidence. Besides, employing genetically modified animal models, such as RIP3-knockout mice, may also enhance the validity of the data. Future studies should validate these findings in a solid model of CKD.

Moreover, the study did not include comprehensive measurements of renal function such as glomerular filtration rate (GFR) or serum creatinine levels, and other inflammation markers, which are critical for assessing kidney health and function. The absence of these assessment leaves the evaluation of AKI severity and the overall kidney function assessment incomplete. Comprehensive physiological assessments should be integrated into future studies.

7.5 Overall summary

The present study focused on the role of necroptosis and its potential as a therapeutic target in the AKI to CKD transition. Through both *in vitro* and *in vivo* models, we have demonstrated that necroptosis contributes to EMT, a key process in kidney fibrosis and functional impairment, via the TLR4/JNK signalling pathway.

Using nephrotoxic agents such as CDDP, PEM, GM, and AA-I, we induced nephrotoxicity-associated AKI in HK2 cells and observed a dose-dependent decrease in cell viability. CDDP, PEM, and AA-I significantly induced necroptosis and subsequent EMT through TLR-4 activation. The necroptosis pathway inhibitor Nec-1 effectively mitigated these effects, implicating necroptosis in the pathogenesis of EMT and suggesting its potential as an intervention point.

Further investigations into IRI-induced AKI, both in murine models and HK2 cells subjected to renal pedicle clamping and OGD, respectively, confirmed the induction of necroptosis and EMT, with Nec-1 again providing protective effects. The involvement of high mobility group box-1 protein (HMGB-1) in inducing EMT via the TLR/JNK signalling pathway was also elucidated.

Additionally, we explored the protective properties of Dex, an α2-adrenoceptor agonist, in a sepsis-AKI model. Dex demonstrated the capacity to attenuate LPS-induced renal injury and EMT, inhibit necroinflammation, and protect against TGF-β1-induced EMT, with these effects being associated with JNK pathway inhibition.

In summary, the research identified necroptosis-associated necroinflammation as a driving force in the AKI to CKD transition, mediated through TLR4/JNK cellular signalling pathways. The inhibition of necroptosis by Nec-1 provided a protective effect against EMT and renal cell impairment. Moreover, Dex was demonstrated potent anti-EMT and renal protective effects, suggesting its therapeutic potential. These findings highlight novel therapeutic targets for AKI management and CKD prevention, warranting further investigation and development for clinical application.

References

1. Hsu RK, Hsu CY. The Role of Acute Kidney Injury in Chronic Kidney Disease. Semin Nephrol. 2016;36(4):283-92.
2. Zeisberg M, Maeshima Y, Mosterman B, Kalluri R. Renal fibrosis. Extracellular matrix microenvironment regulates migratory behavior of activated tubular epithelial cells. The American journal of pathology. 2002;160(6):2001-8.
3. Yuan Q, Tan RJ, Liu Y. Myofibroblast in Kidney Fibrosis: Origin, Activation, and Regulation. In: Liu B-C, Lan H-Y, Lv L-L, editors. Renal Fibrosis: Mechanisms and Therapies. Singapore: Springer Singapore; 2019. p. 253-83.
4. Mulay SR, Linkermann A, Anders H-J. Necroinflammation in Kidney Disease. Journal of the American Society of Nephrology. 2016;27(1):27-39.
5. Levey AS, Eckardt KU, Tsukamoto Y, Levin A, Coresh J, Rossert J, et al. Definition and classification of chronic kidney disease: a position statement from Kidney Disease: Improving Global Outcomes (KDIGO). Kidney Int. 2005;67(6):2089-100.
6. James SL, Abate D, Abate KH, Abay SM, Abbafati C, Abbasi N, et al. Global, regional, and national incidence, prevalence, and years lived with disability for 354 diseases and injuries for 195 countries and territories, 1990–2017: a systematic analysis for the Global Burden of Disease Study 2017. The Lancet. 2018;392(10159):1789-858.
7. Hoerger TJ, Simpson SA, Yarnoff BO, Pavkov ME, Ríos Burrows N, Saydah SH, et al. The Future Burden of CKD in the United States: A Simulation Model for the CDC CKD Initiative. American Journal of Kidney Diseases. 2015;65(3):403-11.
8. Carney EF. The impact of chronic kidney disease on global health. Nature Reviews Nephrology. 2020;16(5):251-.
9. Senanayake S, Gunawardena N, Palihawadana P, Bandara P, Haniffa R, Karunarathna R, et al. Symptom burden in chronic kidney disease; a population based cross sectional study. BMC Nephrology. 2017;18(1):228.
10. Romagnani P, Remuzzi G, Glassock R, Levin A, Jager KJ, Tonelli M, et al. Chronic kidney disease. Nature Reviews Disease Primers. 2017;3(1):17088.
11. Pham PC, Khaing K, Sievers TM, Pham PM, Miller JM, Pham SV, et al. 2017 update on pain management in patients with chronic kidney disease. Clinical kidney journal. 2017;10(5):688-97.
12. Davison SN, Rathwell S, Ghosh S, George C, Pfister T, Dennett L. The Prevalence and Severity of Chronic Pain in Patients With Chronic Kidney Disease: A Systematic Review and Meta-Analysis. Canadian journal of kidney health and disease. 2021;8:2054358121993995.
13. Iwagami M, Mansfield KE, Hayes JF, Walters K, Osborn DP, Smeeth L, et al. Severe mental illness and chronic kidney disease: a cross-sectional study in the United Kingdom. Clinical epidemiology. 2018;10:421-9.
14. Cogley C, Carswell C, Bramham K, Chilcot J. Chronic Kidney Disease and Severe Mental Illness: Addressing Disparities in Access to Health Care and Health Outcomes. Clinical Journal of the American Society of Nephrology. 2022;17(9).
15. Peng T, Hu Z, Guo L, Xia Q, Li D, Yang X. Relationship Between Psychiatric Disorders and Quality of Life in Nondialysis Patients With Chronic Kidney Disease. The American Journal of the Medical Sciences. 2013;345(3):218-21.

16. Pereira BDS, Fernandes NDS, de Melo NP, Abrita R, Grincenkov F, Fernandes N. Beyond quality of life: a cross sectional study on the mental health of patients with chronic kidney disease undergoing dialysis and their caregivers. Health and quality of life outcomes. 2017;15(1):74.
17. Yang M, Fox CH, Vassalotti J, Choi M. Complications of Progression of CKD. Advances in Chronic Kidney Disease. 2011;18(6):400-5.
18. Bello AK, Alrukhaimi M, Ashuntantang GE, Basnet S, Rotter RC, Douthat WG, et al. Complications of chronic kidney disease: current state, knowledge gaps, and strategy for action. Kidney International Supplements. 2017;7(2):122-9.
19. Valderrábano F, Jofre R, López-Gómez JM. Quality of life in end-stage renal disease patients. American Journal of Kidney Diseases. 2001;38(3):443-64.
20. Finkelstein FO, Arsenault KL, Taveras A, Awuah K, Finkelstein SH. Assessing and improving the health-related quality of life of patients with ESRD. Nature Reviews Nephrology. 2012;8(12):718-24.
21. Levin A, Stevens PE. Summary of KDIGO 2012 CKD Guideline: behind the scenes, need for guidance, and a framework for moving forward. Kidney International. 2014;85(1):49-61.
22. Kerr M, Bray B, Medcalf J, O'Donoghue DJ, Matthews B. Estimating the financial cost of chronic kidney disease to the NHS in England. Nephrology Dialysis Transplantation. 2012;27(suppl_3):iii73-iii80.
23. Saran R, Robinson B, Abbott KC, Agodoa LYC, Bhave N, Bragg-Gresham J, et al. US Renal Data System 2017 Annual Data Report: Epidemiology of Kidney Disease in the United States. American journal of kidney diseases : the official journal of the National Kidney Foundation. 2018;71(3 Suppl 1):A7.
24. Levin A SP, Bilous RW, Coresh J, De Francisco ALM, De Jong PE et al. Kidney disease: Improving global outcomes (KDIGO) CKD work group. KDIGO 2012 clinical practice guideline for the evaluation and management of chronic kidney disease. Kidney International Supplements. 2013;3(1):1-150.
25. Kalantar-Zadeh K, Jafar TH, Nitsch D, Neuen BL, Perkovic V. Chronic kidney disease. The Lancet. 2021;398(10302):786-802.
26. Snyder S, Pendergraph B. Detection and evaluation of chronic kidney disease. American family physician. 2005;72(9):1723-32.
27. Levey AS, de Jong PE, Coresh J, El Nahas M, Astor BC, Matsushita K, et al. The definition, classification, and prognosis of chronic kidney disease: a KDIGO Controversies Conference report. Kidney International. 2011;80(1):17-28.
28. Effect of a long-term behavioural weight loss intervention on nephropathy in overweight or obese adults with type 2 diabetes: a secondary analysis of the Look AHEAD randomised clinical trial. The lancet Diabetes & endocrinology. 2014;2(10):801-9.
29. Chang AR, Grams ME, Ballew SH, Bilo H, Correa A, Evans M, et al. Adiposity and risk of decline in glomerular filtration rate: meta-analysis of individual participant data in a global consortium. BMJ. 2019;364:k5301.

30. Lee S, Kang S, Joo YS, Lee C, Nam KH, Yun H-R, et al. Smoking, Smoking Cessation, and Progression of Chronic Kidney Disease: Results From KNOW-CKD Study. Nicotine & Tobacco Research. 2021;23(1):92-8.
31. Kasiske BL, Lakatua JD, Ma JZ, Louis TA. A meta-analysis of the effects of dietary protein restriction on the rate of decline in renal function. American journal of kidney diseases : the official journal of the National Kidney Foundation. 1998;31(6):954-61.
32. Robertson L, Waugh N, Robertson A. Protein restriction for diabetic renal disease. Cochrane Database Syst Rev. 2007;2007(4):Cd002181.
33. Jones-Burton C, Mishra SI, Fink JC, Brown J, Gossa W, Bakris GL, et al. An in-depth review of the evidence linking dietary salt intake and progression of chronic kidney disease. American journal of nephrology. 2006;26(3):268-75.
34. KDIGO 2022 Clinical Practice Guideline for Diabetes Management in Chronic Kidney Disease. Kidney Int. 2022;102(5s):S1-s127.
35. KDIGO 2021 Clinical Practice Guideline for the Management of Blood Pressure in Chronic Kidney Disease. Kidney Int. 2021;99(3s):S1-s87.
36. Liu Y. Renal fibrosis: new insights into the pathogenesis and therapeutics. Kidney international. 2006;69(2):213-7.
37. Bülow RD, Boor P. Extracellular Matrix in Kidney Fibrosis: More Than Just a Scaffold. The journal of histochemistry and cytochemistry : official journal of the Histochemistry Society. 2019;67(9):643-61.
38. Liu Y. Cellular and molecular mechanisms of renal fibrosis. Nature reviews Nephrology. 2011;7(12):684-96.
39. Karin M, Clevers H. Reparative inflammation takes charge of tissue regeneration. Nature. 2016;529(7586):307-15.
40. Chung AC, Lan HY. Chemokines in renal injury. Journal of the American Society of Nephrology. 2011;22(5):802-9.
41. Vielhauer V, Kulkarni O, Reichel CA, Anders H-J, editors. Targeting the recruitment of monocytes and macrophages in renal disease. Semin Nephrol; 2010: Elsevier.
42. Duffield JS, editor Macrophages and immunologic inflammation of the kidney. Semin Nephrol; 2010: Elsevier.
43. Liu Y. Cellular and molecular mechanisms of renal fibrosis. Nature Reviews Nephrology. 2011;7(12):684-96.
44. Eyden B. Fibronexus junctions associated with in vivo human endothelium. Ultrastructural Pathology. 2009;33(1):28-32.
45. Margadant C, Sonnenberg A. Integrin-TGF-beta crosstalk in fibrosis, cancer and wound healing. EMBO reports. 2010;11(2):97-105.
46. Kellum JA, Lameire N, Aspelin P, Barsoum RS, Burdmann EA, Goldstein SL, et al. Kidney disease: improving global outcomes (KDIGO) acute kidney injury work group. KDIGO clinical practice guideline for acute kidney injury. Kidney international supplements. 2012;2(1):1-138.
47. Khwaja A. KDIGO clinical practice guidelines for acute kidney injury. Nephron Clinical Practice. 2012;120(4):c179-c84.

48. Gameiro J, Fonseca JA, Outerelo C, Lopes JA. Acute Kidney Injury: From Diagnosis to Prevention and Treatment Strategies. Journal of clinical medicine. 2020;9(6).
49. Lameire N, Van Biesen W, Vanholder R. The changing epidemiology of acute renal failure. Nature clinical practice Nephrology. 2006;2(7):364-77.
50. Bagshaw SM, George C, Bellomo R. Changes in the incidence and outcome for early acute kidney injury in a cohort of Australian intensive care units. Critical care. 2007;11(3):1-9.
51. Chertow GM, Burdick E, Honour M, Bonventre JV, Bates DW. Acute kidney injury, mortality, length of stay, and costs in hospitalized patients. Journal of the American Society of Nephrology. 2005;16(11):3365-70.
52. Ehrmann S, Helms J, Joret A, Martin-Lefevre L, Quenot JP, Herbrecht JE, et al. Nephrotoxic drug burden among 1001 critically ill patients: impact on acute kidney injury. Ann Intensive Care. 2019;9(1):106.
53. Makris K, Spanou L. Acute Kidney Injury: Definition, Pathophysiology and Clinical Phenotypes. The Clinical biochemist Reviews. 2016;37(2):85-98.
54. Liu B-C, Tang T-T, Lv L-L, Lan H-Y. Renal tubule injury: a driving force toward chronic kidney disease. Kidney International. 2018;93(3):568-79.
55. Kellum JA, Romagnani P, Ashuntantang G, Ronco C, Zarbock A, Anders H-J. Acute kidney injury. Nature Reviews Disease Primers. 2021;7(1):52.
56. e Silva VTC, Marçal LJ, Burdmann EA. Risk factors for vancomycin nephrotoxicity: still a matter of debate. Critical care medicine. 2014;42(12):2635-6.
57. Joyce EL, Kane-Gill SL, Priyanka P, Fuhrman DY, Kellum JA. Piperacillin/tazobactam and antibiotic-associated acute kidney injury in critically ill children. Journal of the American Society of Nephrology: JASN. 2019;30(11):2243.
58. Fu EL, Trevisan M, Clase CM, Evans M, Lindholm B, Rotmans JI, et al. Association of acute increases in plasma creatinine after renin-angiotensin blockade with subsequent outcomes. Clinical journal of the American Society of Nephrology: CJASN. 2019;14(9):1336.
59. Mulay SR, Shi C, Ma X, Anders HJ. Novel Insights into Crystal-Induced Kidney Injury. Kidney diseases (Basel, Switzerland). 2018;4(2):49-57.
60. Gunness P, Aleksa K, Koren G. The effect of acyclovir on the tubular secretion of creatinine in vitro. J Transl Med. 2010;8:139.
61. Małyszko J, Kozłowska K, Kozłowski L, Małyszko J. Nephrotoxicity of anticancer treatment. Nephrology Dialysis Transplantation. 2017;32(6):924-36.
62. Santos MLC, de Brito BB, da Silva FAF, Botelho A, de Melo FF. Nephrotoxicity in cancer treatment: An overview. World journal of clinical oncology. 2020;11(4):190-204.
63. Morales-Alvarez MC. Nephrotoxicity of Antimicrobials and Antibiotics. Advances in Chronic Kidney Disease. 2020;27(1):31-7.
64. Ghane Shahrbaf F, Assadi F. Drug-induced renal disorders. Journal of renal injury prevention. 2015;4(3):57-60.
65. Tune BM. Nephrotoxicity of beta-lactam antibiotics: mechanisms and strategies for prevention. Pediatric Nephrology. 1997;11(6):768-72.

66. Roger C, Louart B. Beta-Lactams Toxicity in the Intensive Care Unit: An Underestimated Collateral Damage? Microorganisms. 2021;9(7):1505.
67. Mingeot-Leclercq MP, Tulkens PM. Aminoglycosides: nephrotoxicity. Antimicrobial agents and chemotherapy. 1999;43(5):1003-12.
68. Bodeker G, Ong C-K. WHO global atlas of traditional, complementary and alternative medicine: World Health Organization; 2005.
69. Rashrash M, Schommer JC, Brown LM. Prevalence and Predictors of Herbal Medicine Use Among Adults in the United States. Journal of patient experience. 2017;4(3):108-13.
70. Jain A, Olivero JJ. Herbal Nephropathy. Methodist DeBakey cardiovascular journal. 2019;15(3):228-30.
71. Dudek I, Rybak N, Skubel T, Czarnota J, Dobrzyński M, Drozd M. Herbal nephropathy – a serious condition based on the innocence of nature. Journal of Education, Health and Sport. 2022;12(9):92-8.
72. Prakash J, Murthy AS, Vohra R, Rajak M, Mathur SK. Acute renal failure in the intensive care unit. The Journal of the Association of Physicians of India. 2006;54:784-8.
73. Wu L, Xiong X, Wu X, Ye Y, Jian Z, Zhi Z, et al. Targeting Oxidative Stress and Inflammation to Prevent Ischemia-Reperfusion Injury. Frontiers in Molecular Neuroscience. 2020;13.
74. Basile DP, Friedrich JL, Spahic J, Knipe N, Mang H, Leonard EC, et al. Impaired endothelial proliferation and mesenchymal transition contribute to vascular rarefaction following acute kidney injury. American journal of physiology Renal physiology. 2011;300(3):F721-33.
75. Kinsey GR, Li L, Okusa MD. Inflammation in acute kidney injury. Nephron Experimental nephrology. 2008;109(4):e102-7.
76. Verma S, Fedak PWM, Weisel RD, Butany J, Rao V, Maitland A, et al. Fundamentals of Reperfusion Injury for the Clinical Cardiologist. Circulation. 2002;105(20):2332-6.
77. Murphy E, Steenbergen C. Mechanisms underlying acute protection from cardiac ischemia-reperfusion injury. Physiological reviews. 2008;88(2):581-609.
78. Epstein T, Xu L, Gillies RJ, Gatenby RA. Separation of metabolic supply and demand: aerobic glycolysis as a normal physiological response to fluctuating energetic demands in the membrane. Cancer & Metabolism. 2014;2(1):7.
79. Tian J, Xie ZJ. The Na-K-ATPase and calcium-signaling microdomains. Physiology (Bethesda, Md). 2008;23:205-11.
80. Brini M, Carafoli E. Calcium Pumps in Health and Disease. Physiological reviews. 2009;89(4):1341-78.
81. Okamoto F, Allen BS, Buckberg GD, Young H, Bugyi H, Leaf J. Reperfusate composition: interaction of marked hyperglycemia and marked hyperosmolarity in allowing immediate contractile recovery after four hours of regional ischemia. The Journal of thoracic and cardiovascular surgery. 1986;92(3 Pt 2):583-93.
82. HONDA HM, KORGE P, WEISS JN. Mitochondria and Ischemia/Reperfusion Injury. Annals of the New York Academy of Sciences. 2005;1047(1):248-58.
83. Granger DN, Kvietys PR. Reperfusion injury and reactive oxygen species: The evolution of a concept. Redox biology. 2015;6:524-51.

84. Hayyan M, Hashim MA, AlNashef IM. Superoxide Ion: Generation and Chemical Implications. Chemical Reviews. 2016;116(5):3029-85.
85. Xing P, Ma K, Wu J, Long W, Wang D. Protective effect of polysaccharide peptide on cerebral ischemia-reperfusion injury in rats. Molecular Medicine Reports. 2018;18(6):5371-8.
86. Xu X, Zhang L, Ye X, Hao Q, Zhang T, Cui G, et al. Nrf2/ARE pathway inhibits ROS-induced NLRP3 inflammasome activation in BV2 cells after cerebral ischemia reperfusion. Inflammation Research. 2018;67(1):57-65.
87. Somolinos M, García D, Pagán R, Mackey B. Relationship between sublethal injury and microbial inactivation by the combination of high hydrostatic pressure and citral or tert-butyl hydroquinone. Applied and environmental microbiology. 2008;74(24):7570-7.
88. Walmsley SJ, Broeckling C, Hess A, Prenni J, Curthoys NP. Proteomic analysis of brush-border membrane vesicles isolated from purified proximal convoluted tubules. American journal of physiology Renal physiology. 2010;298(6):F1323-31.
89. Mooseker MS, Bonder EM, Conzelman KA, Fishkind DJ, Howe CL, Keller TC, 3rd. Brush border cytoskeleton and integration of cellular functions. The Journal of cell biology. 1984;99(1 Pt 2):104s-12s.
90. Goligorsky MS, Lieberthal W, Racusen L, Simon EE. Integrin receptors in renal tubular epithelium: new insights into pathophysiology of acute renal failure. The American journal of physiology. 1993;264(1 Pt 2):F1-8.
91. Li S, Jiang S, Zhang Q, Jin B, Lv D, Li W, et al. Integrin β3 Induction Promotes Tubular Cell Senescence and Kidney Fibrosis. Frontiers in Cell and Developmental Biology. 2021;9.
92. Maderna P, Godson C. Phagocytosis of apoptotic cells and the resolution of inflammation. Biochimica et Biophysica Acta (BBA) - Molecular Basis of Disease. 2003;1639(3):141-51.
93. Lockshin RA, Zakeri Z. Apoptosis, autophagy, and more. The international journal of biochemistry & cell biology. 2004;36(12):2405-19.
94. Oppenheim RW, Flavell RA, Vinsant S, Prevette D, Kuan CY, Rakic P. Programmed cell death of developing mammalian neurons after genetic deletion of caspases. J Neurosci. 2001;21(13):4752-60.
95. Elmore S. Apoptosis: a review of programmed cell death. Toxicologic pathology. 2007;35(4):495-516.
96. Poon IKH, Lucas CD, Rossi AG, Ravichandran KS. Apoptotic cell clearance: basic biology and therapeutic potential. Nature Reviews Immunology. 2014;14(3):166-80.
97. D'Arcy MS. Cell death: a review of the major forms of apoptosis, necrosis and autophagy. Cell Biology International. 2019;43(6):582-92.
98. Kanduc D, Mittelman A, Serpico R, Sinigaglia E, Sinha AA, Natale C, et al. Cell death: apoptosis versus necrosis (review). International journal of oncology. 2002;21(1):165-70.
99. Fiers W, Beyaert R, Declercq W, Vandenabeele P. More than one way to die: apoptosis, necrosis and reactive oxygen damage. Oncogene. 1999;18(54):7719-30.
100. Sun L, Wang H, Wang Z, He S, Chen S, Liao D, et al. Mixed lineage kinase domain-like protein mediates necrosis signaling downstream of RIP3 kinase. Cell. 2012;148(1-2):213-27.

101. Zhang DW, Shao J, Lin J, Zhang N, Lu BJ, Lin SC, et al. RIP3, an energy metabolism regulator that switches TNF-induced cell death from apoptosis to necrosis. Science. 2009;325(5938):332-6.
102. He S, Wang L, Miao L, Wang T, Du F, Zhao L, et al. Receptor interacting protein kinase-3 determines cellular necrotic response to TNF-alpha. Cell. 2009;137(6):1100-11.
103. Teng X, Degterev A, Jagtap P, Xing X, Choi S, Denu R, et al. Structure-activity relationship study of novel necroptosis inhibitors. Bioorganic & medicinal chemistry letters. 2005;15(22):5039-44.
104. Degterev A, Huang Z, Boyce M, Li Y, Jagtap P, Mizushima N, et al. Chemical inhibitor of nonapoptotic cell death with therapeutic potential for ischemic brain injury. Nature Chemical Biology. 2005;1(2):112-9.
105. Berghe TV, Linkermann A, Jouan-Lanhouet S, Walczak H, Vandenabeele P. Regulated necrosis: the expanding network of non-apoptotic cell death pathways. Nature Reviews Molecular Cell Biology. 2014;15(2):135-47.
106. Zhang G, Wang J, Zhao Z, Xin T, Fan X, Shen Q, et al. Regulated necrosis, a proinflammatory cell death, potentially counteracts pathogenic infections. Cell Death & Disease. 2022;13(7):637.
107. Coca SG, Singanamala S, Parikh CR. Chronic kidney disease after acute kidney injury: a systematic review and meta-analysis. Kidney international. 2012;81(5):442-8.
108. Ishani A, Nelson D, Clothier B, Schult T, Nugent S, Greer N, et al. The magnitude of acute serum creatinine increase after cardiac surgery and the risk of chronic kidney disease, progression of kidney disease, and death. Archives of internal medicine. 2011;171(3):226-33.
109. Mehta S, Chauhan K, Patel A, Patel S, Pinotti R, Nadkarni GN, et al. The prognostic importance of duration of AKI: a systematic review and meta-analysis. BMC nephrology. 2018;19(1):1-10.
110. Thakar CV, Christianson A, Himmelfarb J, Leonard AC. Acute kidney injury episodes and chronic kidney disease risk in diabetes mellitus. Clinical journal of the American Society of Nephrology: CJASN. 2011;6(11):2567.
111. Ferenbach DA, Bonventre JV. Mechanisms of maladaptive repair after AKI leading to accelerated kidney ageing and CKD. Nature reviews Nephrology. 2015;11(5):264-76.
112. Schmitt R, Cantley LG. The impact of aging on kidney repair. American Journal of Physiology-Renal Physiology. 2008;294(6):F1265-F72.
113. Venkatachalam MA, Weinberg JM, Kriz W, Bidani AK. Failed tubule recovery, AKI-CKD transition, and kidney disease progression. Journal of the American Society of Nephrology: JASN. 2015;26(8):1765.
114. Basile DP, Donohoe D, Roethe K, Osborn JL. Renal ischemic injury results in permanent damage to peritubular capillaries and influences long-term function. American Journal of Physiology-Renal Physiology. 2001.
115. Ferenbach DA, Bonventre JV. Mechanisms of maladaptive repair after AKI leading to accelerated kidney ageing and CKD. Nature Reviews Nephrology. 2015;11(5):264-76.
116. Yang L, Besschetnova TY, Brooks CR, Shah JV, Bonventre JV. Epithelial cell cycle arrest in G2/M mediates kidney fibrosis after injury. Nature medicine. 2010;16(5):535-43.
117. Hsu RK, Hsu C-Y. The Role of Acute Kidney Injury in Chronic Kidney Disease. Semin Nephrol. 2016;36(4):283-92.

118. Bertram JF, Douglas-Denton RN, Diouf B, Hughson MD, Hoy WE. Human nephron number: implications for health and disease. Pediatric nephrology. 2011;26(9):1529-33.
119. Schnaper HW. Remnant nephron physiology and the progression of chronic kidney disease. Pediatric nephrology (Berlin, Germany). 2014;29(2):193-202.
120. Denic A, Glassock RJ, Rule AD. Structural and Functional Changes With the Aging Kidney. Adv Chronic Kidney Dis. 2016;23(1):19-28.
121. Mari C, Winyard P. Concise Review: Understanding the Renal Progenitor Cell Niche In Vivo to Recapitulate Nephrogenesis In Vitro. Stem Cells Translational Medicine. 2015;4(12):1463-71.
122. Andrianova NV, Buyan MI, Zorova LD, Pevzner IB, Popkov VA, Babenko VA, et al. Kidney Cells Regeneration: Dedifferentiation of Tubular Epithelium, Resident Stem Cells and Possible Niches for Renal Progenitors. Int J Mol Sci. 2019;20(24):6326.
123. Hoy WE, Bertram JF, Hughson MD. Nephron hypertrophy and glomerulosclerosis in normal donor kidneys. Clinical journal of the American Society of Nephrology : CJASN. 2014;9(11):1832-4.
124. McArdle Z, Schreuder MF, Moritz KM, Denton KM, Singh RR. Physiology and Pathophysiology of Compensatory Adaptations of a Solitary Functioning Kidney. Frontiers in physiology. 2020;11.
125. Laouari D, Burtin M, Phelep A, Martino C, Pillebout E, Montagutelli X, et al. TGF-alpha mediates genetic susceptibility to chronic kidney disease. Journal of the American Society of Nephrology : JASN. 2011;22(2):327-35.
126. Canaud G, Bonventre JV. Cell cycle arrest and the evolution of chronic kidney disease from acute kidney injury. Nephrology, dialysis, transplantation : official publication of the European Dialysis and Transplant Association - European Renal Association. 2015;30(4):575-83.
127. Vogetseder A, Picard N, Gaspert A, Walch M, Kaissling B, Le Hir M. Proliferation capacity of the renal proximal tubule involves the bulk of differentiated epithelial cells. American Journal of Physiology-Cell Physiology. 2008;294(1):C22-C8.
128. Witzgall R. Are renal proximal tubular epithelial cells constantly prepared for an emergency? Focus on “the proliferation capacity of the renal proximal tubule involves the bulk of differentiated epithelial cells”. American Journal of Physiology-Cell Physiology. 2008;294(1):C1-C3.
129. He S, Sharpless NE. Senescence in health and disease. Cell. 2017;169(6):1000-11.
130. Herranz N, Gil J. Mitochondria and senescence: new actors for an old play. The EMBO journal. 2016;35(7):701-2.
131. Lin X, Jin H, Chai Y, Shou S. Cellular senescence and acute kidney injury. Pediatric nephrology (Berlin, Germany). 2022;37(12):3009-18.
132. Jin H, Zhang Y, Ding Q, Wang SS, Rastogi P, Dai D-F, et al. Epithelial innate immunity mediates tubular cell senescence after kidney injury. JCI insight. 2019;4(2).
133. Yang L, Besschetnova TY, Brooks CR, Shah JV, Bonventre JV. Epithelial cell cycle arrest in G2/M mediates kidney fibrosis after injury. Nat Med. 2010;16(5):535-43, 1p following 143.
134. Cohen EP. Fibrosis causes progressive kidney failure. Medical hypotheses. 1995;45(5):459-62.
135. Strutz F, Zeisberg M. Renal Fibroblasts and Myofibroblasts in Chronic Kidney Disease. Journal of the American Society of Nephrology. 2006;17(11):2992.

136. Sheng L, Zhuang S. New Insights Into the Role and Mechanism of Partial Epithelial-Mesenchymal Transition in Kidney Fibrosis. Frontiers in physiology. 2020;11.
137. Piera-Velazquez S, Li Z, Jimenez SA. Role of endothelial-mesenchymal transition (EndoMT) in the pathogenesis of fibrotic disorders. The American journal of pathology. 2011;179(3):1074-80.
138. Basile DP. The endothelial cell in ischemic acute kidney injury: implications for acute and chronic function. Kidney Int. 2007;72(2):151-6.
139. Castellano G, Stasi A, Intini A, Gigante M, Di Palma AM, Divella C, et al. Endothelial dysfunction and renal fibrosis in endotoxemia-induced oliguric kidney injury: possible role of LPS-binding protein. Critical care (London, England). 2014;18(5):520.
140. Curci C, Castellano G, Stasi A, Divella C, Loverre A, Gigante M, et al. Endothelial-to-mesenchymal transition and renal fibrosis in ischaemia/reperfusion injury are mediated by complement anaphylatoxins and Akt pathway. Nephrology, dialysis, transplantation : official publication of the European Dialysis and Transplant Association - European Renal Association. 2014;29(4):799-808.
141. Fan J-M, Ng Y-Y, Hill PA, Nikolic-Paterson DJ, Mu W, Atkins RC, et al. Transforming growth factor-β regulates tubular epithelial-myofibroblast transdifferentiation in vitro. Kidney International. 1999;56(4):1455-67.
142. Peifer M, McEwen DG. The Ballet of Morphogenesis: Unveiling the Hidden Choreographers. Cell. 2002;109(3):271-4.
143. Zeisberg M, Kalluri R. The role of epithelial-to-mesenchymal transition in renal fibrosis. Journal of Molecular Medicine. 2004;82(3):175-81.
144. Yang J, Liu Y. Dissection of Key Events in Tubular Epithelial to Myofibroblast Transition and Its Implications in Renal Interstitial Fibrosis. The American journal of pathology. 2001;159(4):1465-75.
145. Xu J, Lamouille S, Derynck R. TGF-beta-induced epithelial to mesenchymal transition. Cell Res. 2009;19(2):156-72.
146. Poniatowski Ł A, Wojdasiewicz P, Gasik R, Szukiewicz D. Transforming growth factor Beta family: insight into the role of growth factors in regulation of fracture healing biology and potential clinical applications. Mediators of inflammation. 2015;2015:137823.
147. Zhang YE. Non-Smad pathways in TGF-beta signaling. Cell research. 2009;19(1):128-39.
148. Schnaper HW, Hayashida T, Poncelet AC. It's a Smad world: regulation of TGF-beta signaling in the kidney. Journal of the American Society of Nephrology : JASN. 2002;13(4):1126-8.
149. Heldin CH, Miyazono K, ten Dijke P. TGF-beta signalling from cell membrane to nucleus through SMAD proteins. Nature. 1997;390(6659):465-71.
150. Massague J. How cells read TGF-beta signals. Nature reviews Molecular cell biology. 2000;1(3):169-78.
151. Kavsak P, Rasmussen RK, Causing CG, Bonni S, Zhu H, Thomsen GH, et al. Smad7 binds to Smurf2 to form an E3 ubiquitin ligase that targets the TGF beta receptor for degradation. Molecular cell. 2000;6(6):1365-75.

152. Chung ACK, Zhang H, Kong Y-Z, Tan J-J, Huang XR, Kopp JB, et al. Advanced Glycation End-Products Induce Tubular CTGF via TGF-β–Independent Smad3 Signaling. Journal of the American Society of Nephrology. 2010;21(2):249.
153. Ko GJ, Grigoryev DN, Linfert D, Jang HR, Watkins T, Cheadle C, et al. Transcriptional analysis of kidneys during repair from AKI reveals possible roles for NGAL and KIM-1 as biomarkers of AKI-to-CKD transition. American journal of physiology Renal physiology. 2010;298(6):F1472-83.
154. Lee SB, Kalluri R. Mechanistic connection between inflammation and fibrosis. Kidney Int Suppl. 2010(119):S22-S6.
155. Linkermann A, Stockwell BR, Krautwald S, Anders H-J. Regulated cell death and inflammation: an auto-amplification loop causes organ failure. Nature Reviews Immunology. 2014;14(11):759-67.
156. Roh JS, Sohn DH. Damage-Associated Molecular Patterns in Inflammatory Diseases. Immune network. 2018;18(4):e27.
157. Mulay SR, Linkermann A, Anders HJ. Necroinflammation in Kidney Disease. Journal of the American Society of Nephrology : JASN. 2016;27(1):27-39.
158. Rubartelli A, Lotze MT. Inside, outside, upside down: damage-associated molecular-pattern molecules (DAMPs) and redox. Trends in immunology. 2007;28(10):429-36.
159. Chen Q, Guan X, Zuo X, Wang J, Yin W. The role of high mobility group box 1 (HMGB1) in the pathogenesis of kidney diseases. Acta pharmaceutica Sinica B. 2016;6(3):183-8.
160. Shen F, Zhuang S. Histone Acetylation and Modifiers in Renal Fibrosis. Front Pharmacol. 2022;13:760308.
161. Allam R, Scherbaum CR, Darisipudi MN, Mulay SR, Hägele H, Lichtnekert J, et al. Histones from dying renal cells aggravate kidney injury via TLR2 and TLR4. Journal of the American Society of Nephrology : JASN. 2012;23(8):1375-88.
162. Linkermann A, Green DR. Necroptosis. New England Journal of Medicine. 2014;370(5):455-65.
163. Pasparakis M, Vandenabeele P. Necroptosis and its role in inflammation. Nature. 2015;517(7534):311-20.
164. Vanlangenakker N, Vanden Berghe T, Bogaert P, Laukens B, Zobel K, Deshayes K, et al. cIAP1 and TAK1 protect cells from TNF-induced necrosis by preventing RIP1/RIP3-dependent reactive oxygen species production. Cell Death Differ. 2011;18(4):656-65.
165. Lamothe B, Lai Y, Xie M, Schneider MD, Darnay BG. TAK1 is essential for osteoclast differentiation and is an important modulator of cell death by apoptosis and necroptosis. Mol Cell Biol. 2013;33(3):582-95.
166. Zhao H, Jaffer T, Eguchi S, Wang Z, Linkermann A, Ma D. Role of necroptosis in the pathogenesis of solid organ injury. Cell Death Dis. 2015;6:e1975.
167. Vanlangenakker N, Bertrand MJ, Bogaert P, Vandenabeele P, Vanden Berghe T. TNF-induced necroptosis in L929 cells is tightly regulated by multiple TNFR1 complex I and II members. Cell Death Dis. 2011;2:e230.

168. Zhao J, Jitkaew S, Cai Z, Choksi S, Li Q, Luo J, et al. Mixed lineage kinase domain-like is a key receptor interacting protein 3 downstream component of TNF-induced necrosis. Proceedings of the National Academy of Sciences of the United States of America. 2012;109(14):5322-7.
169. Galluzzi L, Kroemer G. Necroptosis: A Specialized Pathway of Programmed Necrosis. Cell. 2008;135(7):1161-3.
170. Xu Y, Ma H, Shao J, Wu J, Zhou L, Zhang Z, et al. A Role for Tubular Necroptosis in Cisplatin-Induced AKI. Journal of the American Society of Nephrology. 2015;26(11):2647.
171. Pefanis A, Ierino FL, Murphy JM, Cowan PJ. Regulated necrosis in kidney ischemia-reperfusion injury. Kidney Int. 2019;96(2):291-301.
172. Jun W, Benjanuwattra J, Chattipakorn SC, Chattipakorn N. Necroptosis in renal ischemia/reperfusion injury: A major mode of cell death? Archives of Biochemistry and Biophysics. 2020;689:108433.
173. Sureshbabu A, Patino E, Ma KC, Laursen K, Finkelsztein EJ, Akchurin O, et al. RIPK3 promotes sepsis-induced acute kidney injury via mitochondrial dysfunction. JCI insight. 2018;3(11).
174. Takahashi E, Nagano O, Ishimoto T, Yae T, Suzuki Y, Shinoda T, et al. Tumor Necrosis Factor-α Regulates Transforming Growth Factor-β-dependent Epithelial-Mesenchymal Transition by Promoting Hyaluronan-CD44-Moesin Interaction2. Journal of Biological Chemistry. 2010;285(6):4060-73.
175. Bolognese AC, Yang W-L, Hansen LW, Denning N-L, Nicastro JM, Coppa GF, et al. Inhibition of necroptosis attenuates lung injury and improves survival in neonatal sepsis. Surgery. 2018;164(1):110-6.
176. Zhu Y, Cui H, Xia Y, Gan H. RIPK3-mediated necroptosis and apoptosis contributes to renal tubular cell progressive loss and chronic kidney disease progression in rats. PloS one. 2016;11(6):e0156729.
177. Liu W, Chen B, Wang Y, Meng C, Huang H, Huang X-R, et al. RGMb protects against acute kidney injury by inhibiting tubular cell necroptosis via an MLKL-dependent mechanism. Proceedings of the National Academy of Sciences. 2018;115(7):E1475-E84.
178. Anders HJ. Necroptosis in Acute Kidney Injury. Nephron. 2018:342-8.
179. Kolbrink B, von Samson-Himmelstjerna FA, Murphy JM, Krautwald S. Role of necroptosis in kidney health and disease. Nature Reviews Nephrology. 2023.
180. Ryan MJ, Johnson G, Kirk J, Fuerstenberg SM, Zager RA, Torok-Storb B. HK-2: an immortalized proximal tubule epithelial cell line from normal adult human kidney. Kidney Int. 1994;45(1):48-57.
181. Yang Y, Hong S, Wang Q, Wang S, Xun Y. Exosome-mediated crosstalk between epithelial cells amplifies the cell injury cascade in CaOx stone formation. Journal of Biological Engineering. 2023;17(1):16.
182. Zhang XQ, Dong JJ, Cai T, Shen X, Zhou XJ, Liao L. High glucose induces apoptosis via upregulation of Bim expression in proximal tubule epithelial cells. Oncotarget. 2017;8(15):24119-29.
183. Rajkumar P, Mathew BS, Das S, Isaiah R, John S, Prabha R, et al. Cisplatin Concentrations in Long and Short Duration Infusion: Implications for the Optimal Time of Radiation Delivery. J Clin Diagn Res. 2016;10(7):Xc01-xc4.

184. Jazaeri AA, Shibata E, Park J, Bryant JL, Conaway MR, Modesitt SC, et al. Overcoming platinum resistance in preclinical models of ovarian cancer using the neddylation inhibitor MLN4924. Molecular cancer therapeutics. 2013;12(10):1958-67.
185. Genova C, Rijavec E, Truini A, Coco S, Sini C, Barletta G, et al. Pemetrexed for the treatment of non-small cell lung cancer. Expert opinion on pharmacotherapy. 2013;14(11):1545-58.
186. Li KM, Rivory LP, Clarke SJ. Pemetrexed pharmacokinetics and pharmacodynamics in a phase I/II study of doublet chemotherapy with vinorelbine: implications for further optimisation of pemetrexed schedules. British journal of cancer. 2007;97(8):1071-6.
187. Chen X, Yang Y, Berger I, Khalid U, Patel A, Cai J, et al. Early detection of pemetrexed-induced inhibition of thymidylate synthase in non-small cell lung cancer with FLT-PET imaging. Oncotarget. 2017;8(15):24213-23.
188. Ali B. Agents ameliorating or augmenting experimental gentamicin nephrotoxicity: some recent research. Food and Chemical Toxicology. 2003;41(11):1447-52.
189. Dahlgren JG, Anderson ET, Hewitt WL. Gentamicin blood levels: a guide to nephrotoxicity. Antimicrobial agents and chemotherapy. 1975;8(1):58-62.
190. Hamilton KS, Gopal KV, Moore EJ, Gross GW. Pharmacological response sensitization in nerve cell networks exposed to the antibiotic gentamicin. Eur J Pharmacol. 2017;794:92-9.
191. Nightingale J, Patel S, Suzuki N, Buxton R, Takagi K-i, Suzuki J, et al. Oncostatin M, a Cytokine Released by Activated Mononuclear Cells, Induces Epithelial Cell-Myofibroblast Transdifferentiation via Jak/Stat Pathway Activation. Journal of the American Society of Nephrology. 2004;15(1).
192. Kumar V, Prasad AK, Parmar VS. Naturally occurring aristolactams, aristolochic acids and dioxoaporphines and their biological activities. Natural product reports. 2003;20(6):565-83.
193. Bloch KM, Evans A, Lock EA. Aristolochic acids — Induced transcriptomic responses in rat renal proximal tubule cells in vitro. Genomics Data. 2015;5:254-6.
194. Li W, Zhang J, Yu X, Meng F, Huang J, Zhang L, et al. Aristolochic acid I exposure decreases oocyte quality. Frontiers in Cell and Developmental Biology. 2022;10.
195. Yang CC, Wu CT, Chen LP, Hung KY, Liu SH, Chiang CK. Autophagy induction promotes aristolochic acid-I-induced renal injury in vivo and in vitro. Toxicology. 2013;312:63-73.
196. Chen YY, Chung JG, Wu HC, Bau DT, Wu KY, Kao ST, et al. Aristolochic acid suppresses DNA repair and triggers oxidative DNA damage in human kidney proximal tubular cells. Oncology reports. 2010;24(1):141-53.
197. Sommer CJ. Ischemic stroke: experimental models and reality. Acta neuropathologica. 2017;133(2):245-61.
198. Goss G. Theory and Practice of Histological Techniques. The American Journal of Surgical Pathology. 2009;33(2).
199. Schick MA, Isbary TJ, Schlegel N, Brugger J, Waschke J, Muellenbach R, et al. The impact of crystalloid and colloid infusion on the kidney in rodent sepsis. Intensive care medicine. 2010;36(3):541-8.
200. Loghman-Adham M, Kiu Weber CI, Ciorciaro C, Mann J, Meier M. Detection and management of nephrotoxicity during drug development. Expert opinion on drug safety. 2012;11(4):581-96.

201. Bonventre JV, Vaidya VS, Schmouder R, Feig P, Dieterle F. Next-generation biomarkers for detecting kidney toxicity. Nature biotechnology. 2010;28(5):436-40.
202. McCullough PA, Murray P, Mehta RL, Kellum J. ADQI consensus on AKI biomarkers and cardiorenal syndromes. ADQI Consensus on AKI Biomarkers and Cardiorenal Syndromes. 2013:1-204.
203. Linkermann A, Chen G, Dong G, Kunzendorf U, Krautwald S, Dong Z. Regulated cell death in AKI. Journal of the American Society of Nephrology : JASN. 2014;25(12):2689-701.
204. Miller RP, Tadagavadi RK, Ramesh G, Reeves WB. Mechanisms of Cisplatin nephrotoxicity. Toxins. 2010;2(11):2490-518.
205. Arany I, Safirstein RL, editors. Cisplatin nephrotoxicity. Semin Nephrol; 2003: Elsevier.
206. Latcha S, Jaimes EA, Patil S, Glezerman IG, Mehta S, Flombaum CD. Long–term renal outcomes after cisplatin treatment. Clinical Journal of the American Society of Nephrology. 2016;11(7):1173-9.
207. Tang C, Livingston MJ, Safirstein R, Dong Z. Cisplatin nephrotoxicity: new insights and therapeutic implications. Nature Reviews Nephrology. 2023;19(1):53-72.
208. Britten CD, Izbicka E, Hilsenbeck S, Lawrence R, Davidson K, Cerna C, et al. Activity of the multitargeted antifolate LY231514 in the human tumor cloning assay. Cancer chemotherapy and pharmacology. 1999;44:105-10.
209. Ricciardi S, Tomao S, de Marinis F. Pemetrexed as first-line therapy for non-squamous non-small cell lung cancer. Therapeutics and clinical risk management. 2009;5:781-7.
210. Paz-Ares L, de Marinis F, Dediu M, Thomas M, Pujol J-L, Bidoli P, et al. Maintenance therapy with pemetrexed plus best supportive care versus placebo plus best supportive care after induction therapy with pemetrexed plus cisplatin for advanced non-squamous non-small-cell lung cancer (PARAMOUNT): a double-blind, phase 3, randomised controlled trial. The lancet oncology. 2012;13(3):247-55.
211. Zattera T, Londrino F, Trezzi M, Palumbo R, Granata A, Tatangelo P, et al. Pemetrexed-induced acute kidney failure following irreversible renal damage: two case reports and literature review. J Nephropathol. 2017;6(2):43-8.
212. Visser S, Huisbrink J, van 't Veer NE, van Toor Jermo J, van Boxem AJM, van Walree NC, et al. Renal impairment during pemetrexed maintenance in patients with advanced nonsmall cell lung cancer: a cohort study. European Respiratory Journal. 2018;52(4):1800884.
213. Zembower TR, Noskin GA, Postelnick MJ, Nguyen C, Peterson LR. The utility of aminoglycosides in an era of emerging drug resistance. International journal of antimicrobial agents. 1998;10(2):95-105.
214. Buabeng KO, Mackenzie AR, Laing RBS, Cook I, Jappy B, Gould IM. Assessment of the efficacy, safety and quality of gentamicin use in Aberdeen Royal Infirmary. Journal of Antimicrobial Chemotherapy. 1999;44(6):843-5.
215. Selby NM, Shaw S, Woodier N, Fluck RJ, Kolhe NV. Gentamicin-associated acute kidney injury. QJM: An International Journal of Medicine. 2009;102(12):873-80.

216. Ali BH, Al Za'abi M, Blunden G, Nemmar A. Experimental Gentamicin Nephrotoxicity and Agents that Modify it: A Mini-Review of Recent Research. Basic & Clinical Pharmacology & Toxicology. 2011;109(4):225-32.
217. Bledsoe G, Crickman S, Mao J, Xia C-F, Murakami H, Chao L, et al. Kallikrein/kinin protects against gentamicin-induced nephrotoxicity by inhibition of inflammation and apoptosis. Nephrology Dialysis Transplantation. 2006;21(3):624-33.
218. Balakumar P, Rohilla A, Thangathirupathi A. Gentamicin-induced nephrotoxicity: Do we have a promising therapeutic approach to blunt it? Pharmacological Research. 2010;62(3):179-86.
219. Martinez-Salgado C, López-Hernández FJ, López-Novoa JM. Glomerular nephrotoxicity of aminoglycosides. Toxicology and applied pharmacology. 2007;223(1):86-98.
220. Abdel-Raheem IT, Abdel-Ghany AA, Mohamed GA. Protective effect of quercetin against gentamicin-induced nephrotoxicity in rats. Biological and Pharmaceutical Bulletin. 2009;32(1):61-7.
221. Arlt VM, Stiborova M, Schmeiser HH. Aristolochic acid as a probable human cancer hazard in herbal remedies: a review. Mutagenesis. 2002;17(4):265-77.
222. Anger EE, Yu F, Li J. Aristolochic Acid-Induced Nephrotoxicity: Molecular Mechanisms and Potential Protective Approaches. Int J Mol Sci. 2020;21(3).
223. Hranjec T, Kovač A, Kos J, Mao W, Chen JJ, Grollman AP, et al. Endemic nephropathy: the case for chronic poisoning by aristolochia. Croatian medical journal. 2005;46(1).
224. Shibutani S, Dong H, Suzuki N, Ueda S, Miller F, Grollman AP. Selective toxicity of aristolochic acids I and II. Drug metabolism and disposition. 2007;35(7):1217-22.
225. Yu F-Y, Wu T-S, Chen T-W, Liu B-H. Aristolochic acid I induced oxidative DNA damage associated with glutathione depletion and ERK1/2 activation in human cells. Toxicology In Vitro. 2011;25(4):810-6.
226. Shi H, Feng J-m. Aristolochic acid induces apoptosis of human umbilical vein endothelial cells in vitro by suppressing PI3K/Akt signaling pathway. Acta pharmacologica Sinica. 2011;32(8):1025-30.
227. Pozdzik A, Salmon IJ, Debelle F, Decaestecker C, Van Den Branden C, Verbeelen D, et al. Aristolochic acid induces proximal tubule apoptosis and epithelial to mesenchymal transformation. Kidney international. 2008;73(5):595-607.
228. Barnett LMA, Cummings BS. Nephrotoxicity and Renal Pathophysiology: A Contemporary Perspective. Toxicological Sciences. 2018;164(2):379-90.
229. Dong Y, Sun Y, Huang Y, Fang X, Sun P, Dwarakanath B, et al. Depletion of MLKL inhibits invasion of radioresistant nasopharyngeal carcinoma cells by suppressing epithelial-mesenchymal transition. Annals of translational medicine. 2019;7(23):741.
230. Grande MT, Sánchez-Laorden B, López-Blau C, De Frutos CA, Boutet A, Arévalo M, et al. Snail1-induced partial epithelial-to-mesenchymal transition drives renal fibrosis in mice and can be targeted to reverse established disease. Nat Med. 2015;21(9):989-97.
231. Loh CY, Chai JY, Tang TF, Wong WF, Sethi G, Shanmugam MK, et al. The E-Cadherin and N-Cadherin Switch in Epithelial-to-Mesenchymal Transition: Signaling, Therapeutic Implications, and Challenges. Cells. 2019;8(10).

232. Larsson Å, Wilhelmsson U, Pekna M, Pekny M. Increased cell proliferation and neurogenesis in the hippocampal dentate gyrus of old GFAP−/− Vim−/− mice. Neurochemical research. 2004;29:2069-73.
233. Faust H, Lam LM, Hotz MJ, Qing D, Mangalmurti NS. RAGE interacts with the necroptotic protein RIPK3 and mediates transfusion-induced danger signal release. Vox Sanguinis. 2020;115(8):729-34.
234. Liu T, Zong H, Chen X, Li S, Liu Z, Cui X, et al. Toll-like receptor 4-mediated necroptosis in the development of necrotizing enterocolitis. Pediatric Research. 2022;91(1):73-82.
235. Jing YY, Han ZP, Sun K, Zhang SS, Hou J, Liu Y, et al. Toll-like receptor 4 signaling promotes epithelial-mesenchymal transition in human hepatocellular carcinoma induced by lipopolysaccharide. BMC medicine. 2012;10:98.
236. Jing Y-Y, Han Z-P, Sun K, Zhang S-S, Hou J, Liu Y, et al. Toll-like receptor 4 signaling promotes epithelial-mesenchymal transition in human hepatocellular carcinoma induced by lipopolysaccharide. BMC medicine. 2012;10(1):98.
237. Zhang J, Shao S, Han D, Xu Y, Jiao D, Wu J, et al. High mobility group box 1 promotes the epithelial-to-mesenchymal transition in prostate cancer PC3 cells via the RAGE/NF-κB signaling pathway. International journal of oncology. 2018;53(2):659-71.
238. Raghavan CT, Nagaraj RH. AGE-RAGE interaction in the TGFβ2-mediated epithelial to mesenchymal transition of human lens epithelial cells. Glycoconjugate journal. 2016;33(4):631-43.
239. Walker PD, Barri Y, Shah SV. Oxidant Mechanisms in Gentamicin Nephrotoxicity. Renal Failure. 1999;21(3-4):433-42.
240. Jiang M, Wang CY, Huang S, Yang T, Dong Z. Cisplatin-induced apoptosis in p53-deficient renal cells via the intrinsic mitochondrial pathway. American journal of physiology Renal physiology. 2009;296(5):F983-93.
241. Wei Q, Dong G, Yang T, Megyesi J, Price PM, Dong Z. Activation and involvement of p53 in cisplatin-induced nephrotoxicity. American journal of physiology Renal physiology. 2007;293(4):F1282-91.
242. Zhang D, Liu Y, Wei Q, Huo Y, Liu K, Liu F, et al. Tubular p53 regulates multiple genes to mediate AKI. Journal of the American Society of Nephrology : JASN. 2014;25(10):2278-89.
243. Laorodphun P, Cherngwelling R, Panya A, Arjinajarn P. Curcumin protects rats against gentamicin-induced nephrotoxicity by amelioration of oxidative stress, endoplasmic reticulum stress and apoptosis. Pharmaceutical Biology. 2022;60(1):491-500.
244. Zhou L, Fu P, Huang XR, Liu F, Lai KN, Lan HY. Activation of p53 promotes renal injury in acute aristolochic acid nephropathy. Journal of the American Society of Nephrology : JASN. 2010;21(1):31-41.
245. Wei MC, Zong WX, Cheng EH, Lindsten T, Panoutsakopoulou V, Ross AJ, et al. Proapoptotic BAX and BAK: a requisite gateway to mitochondrial dysfunction and death. Science. 2001;292(5517):727-30.
246. Nakano K, Vousden KH. PUMA, a novel proapoptotic gene, is induced by p53. Molecular cell. 2001;7(3):683-94.

247. Mihara M, Erster S, Zaika A, Petrenko O, Chittenden T, Pancoska P, et al. p53 has a direct apoptogenic role at the mitochondria. Molecular cell. 2003;11(3):577-90.
248. Buqué A, Muhialdin JS, Muñoz A, Calvo B, Carrera S, Aresti U, et al. Molecular mechanism implicated in Pemetrexed-induced apoptosis in human melanoma cells. Molecular Cancer. 2012;11(1):25.
249. Jelaković B, Karanović S, Vuković-Lela I, Miller F, Edwards KL, Nikolić J, et al. Aristolactam-DNA adducts are a biomarker of environmental exposure to aristolochic acid. Kidney Int. 2012;81(6):559-67.
250. Lakhani SA, Masud A, Kuida K, Porter GA, Jr., Booth CJ, Mehal WZ, et al. Caspases 3 and 7: key mediators of mitochondrial events of apoptosis. Science. 2006;311(5762):847-51.
251. Tsuruya K, Ninomiya T, Tokumoto M, Hirakawa M, Masutani K, Taniguchi M, et al. Direct involvement of the receptor-mediated apoptotic pathways in cisplatin-induced renal tubular cell death. Kidney international. 2003;63(1):72-82.
252. Taguchi S, Azushima K, Yamaji T, Urate S, Suzuki T, Abe E, et al. Effects of tumor necrosis factor-α inhibition on kidney fibrosis and inflammation in a mouse model of aristolochic acid nephropathy. Scientific Reports. 2021;11(1):23587.
253. Anger EE, Yu F, Li J. Aristolochic Acid-Induced Nephrotoxicity: Molecular Mechanisms and Potential Protective Approaches. Int J Mol Sci. 2020;21(3):1157.
254. Li F, Sun A, Cheng G, Liu D, Xiao J, Zhao Z, et al. Compound C Protects Against Cisplatin-Induced Nephrotoxicity Through Pleiotropic Effects. Frontiers in physiology. 2020;11:614244.
255. Huang Z, Guo F, Xia Z, Liang Y, Lei S, Tan Z, et al. Activation of GPR120 by TUG891 ameliorated cisplatin-induced acute kidney injury via repressing ER stress and apoptosis. Biomedicine & pharmacotherapy = Biomedecine & pharmacotherapie. 2020;126:110056.
256. Jaikumkao K, Pongchaidecha A, Thongnak L-o, Wanchai K, Arjinajarn P, Chatsudthipong V, et al. Amelioration of Renal Inflammation, Endoplasmic Reticulum Stress and Apoptosis Underlies the Protective Effect of Low Dosage of Atorvastatin in Gentamicin-Induced Nephrotoxicity. PLOS ONE. 2016;11(10):e0164528.
257. Zhu S, Wang Y, Jin J, Guan C, Li M, Xi C, et al. Endoplasmic reticulum stress mediates aristolochic acid I-induced apoptosis in human renal proximal tubular epithelial cells. Toxicology in vitro : an international journal published in association with BIBRA. 2012;26(5):663-71.
258. Xu Y, Ma H, Shao J, Wu J, Zhou L, Zhang Z, et al. A Role for Tubular Necroptosis in Cisplatin-Induced AKI. Journal of the American Society of Nephrology. 2015;26(11).
259. Hu BF, Gong Q, Chen SQ, Yue L, Ma WX, Wang F, et al. Protective effect of inhibiting necroptosis on gentamicin-induced nephrotoxicity. FASEB journal : official publication of the Federation of American Societies for Experimental Biology. 2022;36(9):e22487.
260. Huang H, Jin WW, Huang M, Ji H, Capen DE, Xia Y, et al. Gentamicin-Induced Acute Kidney Injury in an Animal Model Involves Programmed Necrosis of the Collecting Duct. Journal of the American Society of Nephrology : JASN. 2020;31(9):2097-115.
261. Zhang Y, Su SS, Zhao S, Yang Z, Zhong CQ, Chen X, et al. RIP1 autophosphorylation is promoted by mitochondrial ROS and is essential for RIP3 recruitment into necrosome. Nature communications. 2017;8:14329.

262. Matt S, Hofmann TG. The DNA damage-induced cell death response: a roadmap to kill cancer cells. Cellular and Molecular Life Sciences. 2016;73(15):2829-50.
263. Dhuriya YK, Sharma D. Necroptosis: a regulated inflammatory mode of cell death. J Neuroinflammation. 2018;15(1):199.
264. Zhang B, Ramesh G, Uematsu S, Akira S, Reeves WB. TLR4 signaling mediates inflammation and tissue injury in nephrotoxicity. Journal of the American Society of Nephrology : JASN. 2008;19(5):923-32.
265. Acloque H, Thiery JP, Nieto MA. The physiology and pathology of the EMT. Meeting on the epithelial-mesenchymal transition. EMBO reports. 2008;9(4):322-6.
266. Lee JM, Yoshida M, Kim MS, Lee JH, Baek AR, Jang AS, et al. Involvement of Alveolar Epithelial Cell Necroptosis in Idiopathic Pulmonary Fibrosis Pathogenesis. American journal of respiratory cell and molecular biology. 2018;59(2):215-24.
267. Mohammed S, Thadathil N, Selvarani R, Nicklas EH, Wang D, Miller BF, et al. Necroptosis contributes to chronic inflammation and fibrosis in aging liver. Aging Cell. 2021;20(12):e13512.
268. Anders HJ, Schaefer L. Beyond tissue injury-damage-associated molecular patterns, toll-like receptors, and inflammasomes also drive regeneration and fibrosis. Journal of the American Society of Nephrology : JASN. 2014;25(7):1387-400.
269. Kaczmarek A, Vandenabeele P, Krysko Dmitri V. Necroptosis: The Release of Damage-Associated Molecular Patterns and Its Physiological Relevance. Immunity. 2013;38(2):209-23.
270. Akira S, Takeda K. Toll-like receptor signalling. Nature reviews immunology. 2004;4(7):499-511.
271. Yu L, Wang L, Chen S. Endogenous toll-like receptor ligands and their biological significance. Journal of cellular and molecular medicine. 2010;14(11):2592-603.
272. He S, Liang Y, Shao F, Wang X. Toll-like receptors activate programmed necrosis in macrophages through a receptor-interacting kinase-3–mediated pathway. Proceedings of the National Academy of Sciences. 2011;108(50):20054-9.
273. He S, Liang Y, Shao F, Wang X. Toll-like receptors activate programmed necrosis in macrophages through a receptor-interacting kinase-3-mediated pathway. Proceedings of the National Academy of Sciences of the United States of America. 2011;108(50):20054-9.
274. Kaiser WJ, Sridharan H, Huang C, Mandal P, Upton JW, Gough PJ, et al. Toll-like receptor 3-mediated necrosis via TRIF, RIP3, and MLKL. Journal of Biological Chemistry. 2013;288(43):31268-79.
275. Maremonti F, Meyer C, Linkermann A. Mechanisms and Models of Kidney Tubular Necrosis and Nephron Loss. Journal of the American Society of Nephrology. 2022;33(3).
276. Gong Y, Fan Z, Luo G, Yang C, Huang Q, Fan K, et al. The role of necroptosis in cancer biology and therapy. Molecular Cancer. 2019;18(1):100.
277. Malek M, Nematbakhsh M. Renal ischemia/reperfusion injury; from pathophysiology to treatment. Journal of renal injury prevention. 2015;4(2):20-7.
278. Blantz RC, Singh P. Analysis of the prerenal contributions to acute kidney injury. Controversies in Acute Kidney Injury. 174: Karger Publishers; 2011. p. 4-11.

279. Schrier RW, Wang W, Poole B, Mitra A. Acute renal failure: definitions, diagnosis, pathogenesis, and therapy. The Journal of clinical investigation. 2004;114(1):5-14.
280. Basile DP, Anderson MD, Sutton TA. Pathophysiology of acute kidney injury. Compr Physiol. 2012;2(2):1303.
281. Dong Y, Zhang Q, Wen J, Chen T, He L, Wang Y, et al. Ischemic duration and frequency determines AKI-to-CKD progression monitored by dynamic changes of tubular biomarkers in IRI mice. Frontiers in physiology. 2019;10:153.
282. Dhuriya YK, Sharma D. Necroptosis: a regulated inflammatory mode of cell death. Journal of Neuroinflammation. 2018;15(1):199.
283. Linkermann A, Chen G, Dong G, Kunzendorf U, Krautwald S, Dong Z. Regulated Cell Death in AKI. Journal of the American Society of Nephrology. 2014;25(12):2689-701.
284. Linkermann A, Bräsen JH, Himmerkus N, Liu S, Huber TB, Kunzendorf U, et al. Rip1 (receptor-interacting protein kinase 1) mediates necroptosis and contributes to renal ischemia/reperfusion injury. Kidney Int. 2012;81(8):751-61.
285. Liu W, Chen B, Wang Y, Meng C, Huang H, Huang XR, et al. RGMb protects against acute kidney injury by inhibiting tubular cell necroptosis via an MLKL-dependent mechanism. Proceedings of the National Academy of Sciences of the United States of America. 2018;115(7):E1475-e84.
286. Chen H, Fang Y, Wu J, Chen H, Zou Z, Zhang X, et al. RIPK3-MLKL-mediated necroinflammation contributes to AKI progression to CKD. Cell Death & Disease. 2018;9(9):878.
287. Landau SI, Guo X, Velazquez H, Torres R, Olson E, Garcia-Milian R, et al. Regulated necrosis and failed repair in cisplatin-induced chronic kidney disease. Kidney International. 2019;95(4):797-814.
288. Xiao X, Du C, Yan Z, Shi Y, Duan H, Ren Y. Inhibition of Necroptosis Attenuates Kidney Inflammation and Interstitial Fibrosis Induced By Unilateral Ureteral Obstruction. American journal of nephrology. 2017;46(2):131-8.
289. Rosin DL, Okusa MD. Dangers within: DAMP responses to damage and cell death in kidney disease. Journal of the American Society of Nephrology : JASN. 2011;22(3):416-25.
290. Land WG. The Role of Damage-Associated Molecular Patterns in Human Diseases: Part I - Promoting inflammation and immunity. Sultan Qaboos University medical journal. 2015;15(1):e9-e21.
291. Wyczanska M, Lange-Sperandio B. DAMPs in Unilateral Ureteral Obstruction. Front Immunol. 2020;11:581300.
292. Campos EI, Reinberg D. Histones: annotating chromatin. Annual review of genetics. 2009;43:559-99.
293. Silvestre-Roig C, Braster Q, Wichapong K, Lee EY, Teulon JM, Berrebeh N, et al. Externalized histone H4 orchestrates chronic inflammation by inducing lytic cell death. Nature. 2019;569(7755):236-40.
294. Andersson U, Erlandsson-Harris H, Yang H, Tracey KJ. HMGB1 as a DNA-binding cytokine. Journal of leukocyte biology. 2002;72(6):1084-91.

295. Wu H, Ma J, Wang P, Corpuz TM, Panchapakesan U, Wyburn KR, et al. HMGB1 contributes to kidney ischemia reperfusion injury. Journal of the American Society of Nephrology : JASN. 2010;21(11):1878-90.
296. Bruchfeld A, Qureshi AR, Lindholm B, Barany P, Yang L, Stenvinkel P, et al. High mobility group box protein-1 correlates with renal function in chronic kidney disease (CKD). Molecular medicine. 2008;14:109-15.
297. Neal MD, Jia H, Eyer B, Good M, Guerriero CJ, Sodhi CP, et al. Discovery and validation of a new class of small molecule Toll-like receptor 4 (TLR4) inhibitors. PLoS One. 2013;8(6):e65779.
298. Zhao X-C, Livingston MJ, Liang X-L, Dong Z. Cell Apoptosis and Autophagy in Renal Fibrosis. In: Liu B-C, Lan H-Y, Lv L-L, editors. Renal Fibrosis: Mechanisms and Therapies. Singapore: Springer Singapore; 2019. p. 557-84.
299. Priante G, Gianesello L, Ceol M, Del Prete D, Anglani F. Cell Death in the Kidney. Int J Mol Sci. 2019;20(14):3598.
300. Shen S, Ji C, Wei K. Cellular Senescence and Regulated Cell Death of Tubular Epithelial Cells in Diabetic Kidney Disease. Front Endocrinol (Lausanne). 2022;13:924299.
301. Kim-Campbell N, Gomez H, Bayir H. Cell death pathways: apoptosis and regulated necrosis. Critical care nephrology: Elsevier; 2019. p. 113-21. e2.
302. Priante G, Gianesello L, Ceol M, Del Prete D, Anglani F. Cell Death in the Kidney. Int J Mol Sci. 2019;20(14).
303. Kennedy II WA, Buttyan R, Garcia-Montes E, Olsson CA, Sawczuk IS. Epidermal growth factor suppresses renal tubular apoptosis following ureteral obstruction. Urology. 1997;49(6):973-80.
304. Thomas GL, Yang B, Wagner BE, Savill J, El Nahas AM. Cellular apoptosis and proliferation in experimental renal fibrosis. Nephrology, dialysis, transplantation: official publication of the European Dialysis and Transplant Association-European Renal Association. 1998;13(9):2216-26.
305. Schelling JR, Nkemere N, Kopp JB, Cleveland RP. Fas-dependent fratricidal apoptosis is a mechanism of tubular epithelial cell deletion in chronic renal failure. Laboratory investigation; a journal of technical methods and pathology. 1998;78(7):813-24.
306. Choi Y-J, Baranowska-Daca E, Nguyen V, Koji T, Ballantyne CM, Sheikh-Hamad D, et al. Mechanism of chronic obstructive uropathy: increased expression of apoptosis-promoting molecules. Kidney international. 2000;58(4):1481-91.
307. Dai Q, Zhang Y, Liao X, Jiang Y, Lv X, Yuan X, et al. Fluorofenidone alleviates renal fibrosis by inhibiting necroptosis through RIPK3/MLKL pathway. Front Pharmacol. 2020;11:534775.
308. Piao SG, Ding J, Lin XJ, Nan QY, Xuan MY, Jiang YJ, et al. Inhibition of RIP1-RIP3-mediated necroptosis attenuates renal fibrosis via Wnt3α/β-catenin/GSK-3β signaling in unilateral ureteral obstruction. Plos one. 2022;17(10):e0274116.
309. Lin Z, Chen A, Cui H, Shang R, Su T, Li X, et al. Renal tubular epithelial cell necroptosis promotes tubulointerstitial fibrosis in patients with chronic kidney disease. The FASEB Journal. 2022;36(12):e22625.
310. Zhou Y, Zhang J, Guan Q, Tao X, Wang J, Li W. The role of ferroptosis in the development of acute and chronic kidney diseases. Journal of cellular physiology. 2022.

311. Zhou L, Xue X, Hou Q, Dai C. Targeting Ferroptosis Attenuates Interstitial Inflammation and Kidney Fibrosis. Kidney Diseases. 2022;8(1):57-71.
312. Wang Y, Zhu X, Yuan S, Wen S, Liu X, Wang C, et al. TLR4/NF-κB signaling induces GSDMD-related pyroptosis in tubular cells in diabetic kidney disease. Frontiers in endocrinology. 2019;10:603.
313. Maślińska D. [Apoptosis: physiological cell death and its role in pathogenesis of diseases]. Neurologia i neurochirurgia polska. 2003;37(2):315-26.
314. Ma T, Li H, Liu H, Peng Y, Lin T, Deng Z, et al. Neat1 promotes acute kidney injury to chronic kidney disease by facilitating tubular epithelial cells apoptosis via sequestering miR-129-5p. Molecular Therapy. 2022;30(10):3313-32.
315. Ho J. The regulation of apoptosis in kidney development: implications for nephron number and pattern? Frontiers in pediatrics. 2014;2:128.
316. Zhuo WQ, Wen Y, Luo HJ, Luo ZL, Wang L. Mechanisms of ferroptosis in chronic kidney disease. Frontiers in molecular biosciences. 2022;9:975582.
317. Guan Y, Liang X, Ma Z, Hu H, Liu H, Miao Z, et al. A single genetic locus controls both expression of DPEP1/CHMP1A and kidney disease development via ferroptosis. Nature communications. 2021;12(1):5078.
318. Wu M, Xia W, Jin Q, Zhou A, Wang Q, Li S, et al. Gasdermin E Deletion Attenuates Ureteral Obstruction- and 5/6 Nephrectomy-Induced Renal Fibrosis and Kidney Dysfunction. Front Cell Dev Biol. 2021;9:754134.
319. Peerapornratana S, Manrique-Caballero CL, Gómez H, Kellum JA. Acute kidney injury from sepsis: current concepts, epidemiology, pathophysiology, prevention and treatment. Kidney Int. 2019;96(5):1083-99.
320. Kim JS, Kim YJ, Ryoo SM, Sohn CH, Seo DW, Ahn S, et al. One--Year Progression and Risk Factors for the Development of Chronic Kidney Disease in Septic Shock Patients with Acute Kidney Injury: A Single-Centre Retrospective Cohort Study. Journal of clinical medicine. 2018;7(12).
321. Carollo DS, Nossaman BD, Ramadhyani U. Dexmedetomidine: a review of clinical applications. Current opinion in anaesthesiology. 2008;21(4):457-61.
322. Sun Y-B, Zhao H, Mu D-L, Zhang W, Cui J, Wu L, et al. Dexmedetomidine inhibits astrocyte pyroptosis and subsequently protects the brain in in vitro and in vivo models of sepsis. Cell Death & Disease. 2019;10(3):167.
323. Chen J, Jiang Z, Zhou X, Sun X, Cao J, Liu Y, et al. Dexmedetomidine Preconditioning Protects Cardiomyocytes Against Hypoxia/Reoxygenation-Induced Necroptosis by Inhibiting HMGB1-Mediated Inflammation. Cardiovascular Drugs and Therapy. 2019;33(1):45-54.
324. Zhong Y, Li Y-P, Yin Y-Q, Hu B-L, Gao H. Dexmedetomidine inhibits pyroptosis by down-regulating miR-29b in myocardial ischemia reperfusion injury in rats. International Immunopharmacology. 2020;86:106768.
325. Meng L, Li L, Lu S, Li K, Su Z, Wang Y, et al. The protective effect of dexmedetomidine on LPS-induced acute lung injury through the HMGB1-mediated TLR4/NF-κB and PI3K/Akt/mTOR pathways. Molecular Immunology. 2018;94:7-17.

326. Chang Y, Huang X, Liu Z, Han G, Huang L, Xiong Y-C, et al. Dexmedetomidine inhibits the secretion of high mobility group box 1 from lipopolysaccharide-activated macrophages In vitro. Journal of Surgical Research. 2013;181(2):308-14.
327. Bülow RD, Boor P. Extracellular Matrix in Kidney Fibrosis: More Than Just a Scaffold. Journal of Histochemistry & Cytochemistry. 2019;67(9):643-61.
328. Boor P, Floege J. Renal Allograft Fibrosis: Biology and Therapeutic Targets. American Journal of Transplantation. 2015;15(4):863-86.
329. He L, Wei Q, Liu J, Yi M, Liu Y, Liu H, et al. AKI on CKD: heightened injury, suppressed repair, and the underlying mechanisms. Kidney Int. 2017;92(5):1071-83.
330. Chawla LS, Eggers PW, Star RA, Kimmel PL. Acute Kidney Injury and Chronic Kidney Disease as Interconnected Syndromes. New England Journal of Medicine. 2014;371(1):58-66.
331. Rapa SF, Di Iorio BR, Campiglia P, Heidland A, Marzocco S. Inflammation and Oxidative Stress in Chronic Kidney Disease-Potential Therapeutic Role of Minerals, Vitamins and Plant-Derived Metabolites. Int J Mol Sci. 2019;21(1).
332. Akchurin OM, Kaskel F. Update on inflammation in chronic kidney disease. Blood purification. 2015;39(1-3):84-92.
333. Ruiz S, Pergola PE, Zager RA, Vaziri ND. Targeting the transcription factor Nrf2 to ameliorate oxidative stress and inflammation in chronic kidney disease. Kidney International. 2013;83(6):1029-41.
334. Schupp N, Stopper H, Heidland A. DNA Damage in Chronic Kidney Disease: Evaluation of Clinical Biomarkers. Oxid Med Cell Longev. 2016;2016:3592042.
335. Hayashi K, Hishikawa A, Itoh H. DNA Damage Repair and DNA Methylation in the Kidney. American journal of nephrology. 2019;50(2):81-91.
336. Rodrigues CE, Capcha JMC, de Bragança AC, Sanches TR, Gouveia PQ, de Oliveira PAF, et al. Human umbilical cord-derived mesenchymal stromal cells protect against premature renal senescence resulting from oxidative stress in rats with acute kidney injury. Stem Cell Research & Therapy. 2017;8(1):19.
337. Patschan D, Schwarze K, Henze E, Patschan S, Müller GA. Endothelial autophagy and Endothelial-to-Mesenchymal Transition (EndoMT) in eEPC treatment of ischemic AKI. Journal of nephrology. 2016;29(5):637-44.
338. Galvan DL, Green NH, Danesh FR. The hallmarks of mitochondrial dysfunction in chronic kidney disease. Kidney Int. 2017;92(5):1051-7.
339. Ayanga BA, Badal SS, Wang Y, Galvan DL, Chang BH, Schumacker PT, et al. Dynamin-Related Protein 1 Deficiency Improves Mitochondrial Fitness and Protects against Progression of Diabetic Nephropathy. Journal of the American Society of Nephrology : JASN. 2016;27(9):2733-47.
340. Lee SB, Kalluri R. Mechanistic connection between inflammation and fibrosis. Kidney Int Suppl. 2010(119):S22-6.
341. Baldassarre G, Nicoloso MS, Schiappacassi M, Chimienti E, Belletti B. Linking inflammation to cell cycle progression. Current pharmaceutical design. 2004;10(14):1653-66.
342. Saki M, Prakash A. DNA damage related crosstalk between the nucleus and mitochondria. Free radical biology & medicine. 2017;107:216-27.

343. Bruchfeld A, Qureshi AR, Lindholm B, Barany P, Yang L, Stenvinkel P, et al. High Mobility Group Box Protein-1 correlates with renal function in chronic kidney disease (CKD). Molecular medicine (Cambridge, Mass). 2008;14(3-4):109-15.
344. Musial K, Szprynger K, Szczepańska M, Zwolińska D. The heat shock protein profile in children with chronic kidney disease. Peritoneal dialysis international : journal of the International Society for Peritoneal Dialysis. 2010;30(2):227-32.
345. Vidyasagar A, Reese S, Acun Z, Hullett D, Djamali A. HSP27 is involved in the pathogenesis of kidney tubulointerstitial fibrosis. American journal of physiology Renal physiology. 2008;295(3):F707-16.
346. Lange-Sperandio B, Schimpgen K, Rodenbeck B, Chavakis T, Bierhaus A, Nawroth P, et al. Distinct roles of Mac-1 and its counter-receptors in neonatal obstructive nephropathy. Kidney Int. 2006;69(1):81-8.
347. Kypreou KP, Kavvadas P, Karamessinis P, Peroulis M, Alberti A, Sideras P, et al. Altered expression of calreticulin during the development of fibrosis. Proteomics. 2008;8(12):2407-19.
348. Jiang YJ, Jin J, Nan QY, Ding J, Cui S, Xuan MY, et al. Coenzyme Q10 attenuates renal fibrosis by inhibiting RIP1-RIP3-MLKL-mediated necroinflammation via Wnt3α/β-catenin/GSK-3β signaling in unilateral ureteral obstruction. International Immunopharmacology. 2022;108:108868.
349. Giovannitti JA, Jr., Thoms SM, Crawford JJ. Alpha-2 adrenergic receptor agonists: a review of current clinical applications. Anesth Prog. 2015;62(1):31-9.
350. Yao Y, Hu X, Feng X, Zhao Y, Song M, Wang C, et al. Dexmedetomidine alleviates lipopolysaccharide-induced acute kidney injury by inhibiting the NLRP3 inflammasome activation via regulating the TLR4/NOX4/NF-κB pathway. Journal of cellular biochemistry. 2019;120(10):18509-23.
351. Gu J, Sun P, Zhao H, Watts HR, Sanders RD, Terrando N, et al. Dexmedetomidine provides renoprotection against ischemia-reperfusion injury in mice. Critical care (London, England). 2011;15(3):R153.
352. LeBleu VS, Taduri G, O'Connell J, Teng Y, Cooke VG, Woda C, et al. Origin and function of myofibroblasts in kidney fibrosis. Nat Med. 2013;19(8):1047-53.
353. Lovisa S, Zeisberg M, Kalluri R. Partial Epithelial-to-Mesenchymal Transition and Other New Mechanisms of Kidney Fibrosis. Trends in Endocrinology & Metabolism. 2016;27(10):681-95.
354. Lovisa S, LeBleu VS, Tampe B, Sugimoto H, Vadnagara K, Carstens JL, et al. Epithelial-to-mesenchymal transition induces cell cycle arrest and parenchymal damage in renal fibrosis. Nature Medicine. 2015;21(9):998-1009.
355. Li Q, Chen C, Chen X, Han M, Li J. Dexmedetomidine attenuates renal fibrosis via α2-adrenergic receptor-dependent inhibition of cellular senescence after renal ischemia/reperfusion. Life Sciences. 2018;207:1-8.
356. Zhou R, Chen X. Dexmedetomidine represses TGF-β1-induced extracellular matrix production and proliferation of airway smooth muscle cells by inhibiting MAPK signaling pathway. Allergologia et immunopathologia. 2022;50(2):16-22.
357. Dhillon AS, Hagan S, Rath O, Kolch W. MAP kinase signalling pathways in cancer. Oncogene. 2007;26(22):3279-90.

358. Kim EK, Choi E-J. Pathological roles of MAPK signaling pathways in human diseases. Biochimica et Biophysica Acta (BBA) - Molecular Basis of Disease. 2010;1802(4):396-405.
359. Matsuguchi T, Masuda A, Sugimoto K, Nagai Y, Yoshikai Y. JNK-interacting protein 3 associates with Toll-like receptor 4 and is involved in LPS-mediated JNK activation. The EMBO journal. 2003;22(17):4455-64.
360. Grynberg K, Ma FY, Nikolic-Paterson DJ. The JNK Signaling Pathway in Renal Fibrosis. Frontiers in physiology. 2017;8:829.
361. Velden JL, Alcorn JF, Guala AS, Badura EC, Janssen-Heininger YM. c-Jun N-terminal kinase 1 promotes transforming growth factor-β1-induced epithelial-to-mesenchymal transition via control of linker phosphorylation and transcriptional activity of Smad3. American journal of respiratory cell and molecular biology. 2011;44(4):571-81.
362. Liao Z, Cao D, Han X, Liu C, Peng J, Zuo Z, et al. Both JNK and P38 MAPK pathways participate in the protection by dexmedetomidine against isoflurane-induced neuroapoptosis in the hippocampus of neonatal rats. Brain Research Bulletin. 2014;107:69-78.
363. Zhu Y, Li S, Liu J, Wen Q, Yu J, Yu L, et al. Role of JNK Signaling Pathway in Dexmedetomidine Post-Conditioning-Induced Reduction of the Inflammatory Response and Autophagy Effect of Focal Cerebral Ischemia Reperfusion Injury in Rats. Inflammation. 2019;42(6):2181-91.
364. Chen Y, Feng X, Hu X, Sha J, Li B, Zhang H, et al. Dexmedetomidine Ameliorates Acute Stress-Induced Kidney Injury by Attenuating Oxidative Stress and Apoptosis through Inhibition of the ROS/JNK Signaling Pathway. Oxidative Medicine and Cellular Longevity. 2018;2018:4035310.
365. Kong Q, Wu X, Qiu Z, Huang Q, Xia Z, Song X. Protective Effect of Dexmedetomidine on Acute Lung Injury via the Upregulation of Tumour Necrosis Factor-α-Induced Protein-8-like 2 in Septic Mice. Inflammation. 2020;43(3):833-46.
366. Bikbov B, Purcell CA, Levey AS, Smith M, Abdoli A, Abebe M, et al. Global, regional, and national burden of chronic kidney disease, 1990–2017: a systematic analysis for the Global Burden of Disease Study 2017. The Lancet. 2020;395(10225):709-33.
367. Wu W, Liu P, Li J. Necroptosis: an emerging form of programmed cell death. Critical reviews in oncology/hematology. 2012;82(3):249-58.
368. Kadigamuwa C, Choksi S, Xu Q, Cataisson C, Greenbaum SS, Yuspa SH, et al. Role of Retinoic Acid Receptor-γ in DNA Damage-Induced Necroptosis. iScience. 2019;17:74-86.
369. Aki T, Uemura K. Cell Death and Survival Pathways Involving ATM Protein Kinase. Genes. 2021;12(10).
370. Tenev T, Bianchi K, Darding M, Broemer M, Langlais C, Wallberg F, et al. The Ripoptosome, a signaling platform that assembles in response to genotoxic stress and loss of IAPs. Molecular cell. 2011;43(3):432-48.
371. Xu Q, Jitkaew S, Choksi S, Kadigamuwa C, Qu J, Choe M, et al. The cytoplasmic nuclear receptor RARγ controls RIP1 initiated cell death when cIAP activity is inhibited. Nature communications. 2017;8(1):425.
372. Yang H, Wang H, Andersson U. Targeting Inflammation Driven by HMGB1. Front Immunol. 2020;11:484.

373. Harris HE, Andersson U, Pisetsky DS. HMGB1: A multifunctional alarmin driving autoimmune and inflammatory disease. Nature Reviews Rheumatology. 2012;8(4):195-202.
374. Lynch J, Nolan S, Slattery C, Feighery R, Ryan MP, McMorrow T. High-mobility group box protein 1: a novel mediator of inflammatory-induced renal epithelial-mesenchymal transition. American journal of nephrology. 2010;32(6):590-602.
375. He M, Kubo H, Ishizawa K, Hegab AE, Yamamoto Y, Yamamoto H, et al. The role of the receptor for advanced glycation end-products in lung fibrosis. American Journal of Physiology-Lung Cellular and Molecular Physiology. 2007.
376. Ma J, Xu Y, Li W, Zhou Y, Wang D, Yang M, et al. High-mobility group box 1 promotes epithelial-to-mesenchymal transition in crystalline silica induced pulmonary inflammation and fibrosis. Toxicology Letters. 2020;330:134-43.
377. Yuan S, Liu Z, Xu Z, Liu J, Zhang J. High mobility group box 1 (HMGB1): a pivotal regulator of hematopoietic malignancies. Journal of Hematology & Oncology. 2020;13(1):91.
378. Ma FY, Flanc RS, Tesch GH, Han Y, Atkins RC, Bennett BL, et al. A pathogenic role for c-Jun amino-terminal kinase signaling in renal fibrosis and tubular cell apoptosis. Journal of the American Society of Nephrology. 2007;18(2):472-84.
379. Mariasegaram M, Tesch GH, Verhardt S, Hurst L, Lan HY, Nikolic-Paterson DJ. Lefty antagonises TGF-β1 induced epithelial–mesenchymal transition in tubular epithelial cells. Biochemical and biophysical research communications. 2010;393(4):855-9.
380. Lan R, Geng H, Polichnowski AJ, Singha PK, Saikumar P, McEwen DG, et al. PTEN loss defines a TGF-β-induced tubule phenotype of failed differentiation and JNK signaling during renal fibrosis. American journal of physiology-renal physiology. 2012;302(9):F1210-F23.
381. De Borst MH, Prakash J, Sandovici M, Klok PA, Hamming I, Kok RJ, et al. c-Jun NH2-terminal kinase is crucially involved in renal tubulo-interstitial inflammation. Journal of Pharmacology and Experimental Therapeutics. 2009;331(3):896-905.

Appendix

Publication list during the course of my PhD study

1. Saito J, Zhao H, Wu L, Iwasaki M, **Sun Q**, Hu C, Ishikawa M, Hirota K, Ma D, ESA-IC Onco-Anaesthesiology Research Group. “Anti-cancer” effect of ketamine in comparison with MK801 on neuroglioma and lung cancer cells. European Journal of Pharmacology. 2023 Feb 8:175580.

2. Liu L, **Sun Q**, Davis F, Mao J, Zhao H, Ma D. Epithelial–mesenchymal transition in organ fibrosis development: current understanding and treatment strategies. Burns & Trauma. 2022 Jan 1;10.

3. Chen Q, Qin Z, Sun Y, Liu X, Pac Soo A, Chang E, **Sun Q**, Yi B, Wang DX, Zhao H, Ma D. Dexmedetomidine Activates Akt, STAT6 and IRF4 Modulating Cytoprotection and Macrophage Anti-Inflammatory Phenotype Against Acute Lung Injury in vivo and in vitro. Journal of Inflammation Research. 2022 Jan 1:2707-20.

4. Ishikawa M, Iwasaki M, Zhao H, Saito J, Hu C, **Sun Q**, Sakamoto A, Ma D. Inhalational anaesthetics inhibit neuroglioma cell proliferation and migration via miR-138, -210 and-335. International Journal of Molecular Sciences. 2021 Apr 21;22(9):4355.

5. Wen J, **Sun Q**, Cheng Z, Liao X, Wang L, Yuan Y, Li J, Hou L, Gao W, Wang W, Soh W. Extracorporeal membrane oxygenation for coronavirus disease 2019-associated acute respiratory distress syndrome: Report of two cases and review of the literature. World Journal of Clinical Cases. 2021 Mar 3;9(8):1953.

6. Ishikawa M, Iwasaki M, Zhao H, Saito J, Hu C, **Sun Q**, Sakamoto A, Ma D. Sevoflurane and desflurane exposure enhanced cell proliferation and migration in ovarian cancer cells via miR-210 and miR-138 downregulation. International Journal of Molecular Sciences. 2021 Feb 12;22(4):1826.

7. Saito J, Zhao H, Iwasaki M, Wu L, Hu C, **Sun Q**, Hirota K, Ma D. Potential anti-cancer effects of N-methyl-d-aspartate receptor antagonists in vitro. British Journal of Anaesthesia. 2019 Oct 1;123(4): e498-9.